

## **General Disclaimer**

### **One or more of the Following Statements may affect this Document**

- This document has been reproduced from the best copy furnished by the organizational source. It is being released in the interest of making available as much information as possible.
- This document may contain data, which exceeds the sheet parameters. It was furnished in this condition by the organizational source and is the best copy available.
- This document may contain tone-on-tone or color graphs, charts and/or pictures, which have been reproduced in black and white.
- This document is paginated as submitted by the original source.
- Portions of this document are not fully legible due to the historical nature of some of the material. However, it is the best reproduction available from the original submission.



# **The Asteroid Rendezvous Spacecraft**

## **An Adaptation Study Of TIROS/DMSP Technology**

### **Final Report**

Contract No. 956219  
December 1, 1982

Prepared for:  
Jet Propulsion Laboratory  
California Institute of Technology  
Pasadena, California

Prepared by:  
RCA Government Systems Division  
Astro-Electronics  
Princeton, New Jersey



## ABSTRACT

This report summarizes the results of a study done by RCA Astro-Electronics for JPL to determine the feasibility of using the TIROS/DMSP Earth-orbiting meteorological satellite in application to a near-Earth asteroid rendezvous mission. During the course of the study, system and subsystems analysis was carried out to develop a configuration of the spacecraft suitable for this mission. Mission analysis studies were also done and maneuver/rendezvous scenarios developed for baseline missions to both Anteros and Eros. The fact that the Asteroid mission is the most complex of the Pioneer class missions currently under consideration notwithstanding, the basic conclusion very strongly supports the suitability of the basic TIROS bus for this mission in all systems and subsystems areas, including science accommodation. Further, the modifications which are required due to the unique mission are very low risk and can be accomplished readily. The key issue is that in virtually every key subsystem, the demands of the Asteroid mission are a subset of the basic meteorological satellite mission. This allows a relatively simple reconfiguration to be accomplished without a major system redesign.

## TABLE OF CONTENTS

<u>Section</u>	<u>Page</u>
1.0 OVERVIEW AND SUMMARY	1-1
2.0 SCIENCE ACCOMMODATION	2-1
2.1 Instrument Requirements	2-1
2.2 Payload Accommodation	2-1
3.0 MISSION ANALYSIS	3-1
3.1 Asteroid Rendezvous Opportunities	3-1
3.2 Mission Selection	3-1
3.3 Near-Term Candidate Missions to Anteros or EROS	3-12
3.4 Launch Phase	3-17
3.5 Earth to Asteroid Transfer	3-18
3.6 Rendezvous and Orbit Initialization	3-24
3.6.1 Anteros Rendezvous and Orbit Initialization	3-25
3.6.2 EROS Rendezvous - Strawman Low Energy Profile	3-26
3.7 On-Orbit Operations	3-29
4.0 ASTEROID SPACECRAFT SYSTEM	4-1
4.1 Introduction	4-1
4.2 TIROS Technical Summary	4-2
4.3 Applicability of Earth Orbiter Spacecraft to Deep Space Missions	4-4
4.4 Asteroid Spacecraft System Overview	4-8
4.5 Reliability and Autonomy	4-8
4.6 New Technology Tools	4-14
5.0 SPACECRAFT SUBSYSTEM DESIGN	5-1
5.1 Mechanical Design	5-1
5.1.1 Heritage and Commonality	5-1
5.1.2 General Spacecraft Description	5-1
5.1.3 Asteroid Configuration	5-4
5.1.4 Weight Summary	5-4
5.1.5 Deployables	5-4
5.2 Propulsion Subsystem	5-15
5.2.1 Introduction	5-15
5.2.2 Detailed Subsystem Design	5-17
5.2.3 Propulsion Subsystem Operation	5-18
5.3 Attitude Control Subsystem	5-22
5.3.1 Attitude Control System (ACS) Overview	5-22
5.3.2 Base Line Design Summary	5-23
5.3.3 Attitude Control Subsystem Base Line Design	5-25
5.3.4 Safe-Hold Control System	5-27
5.4 Power Subsystem	5-27
5.5 Telecommunications	5-34
5.6 Thermal Design Considerations	5-50
5.7 Data Handling and Command	5-52
5.7.1 Command	5-52
5.7.2 Data Handling	5-56



## TABLE OF CONTENTS (Continued)

<u>Section</u>		<u>Page</u>
6.0	AEROSPACE GROUND EQUIPMENT AND GROUND DATA SYSTEM	6-1
6.1	Airborne Support Equipment (ASE)	6-1
6.2	Asteroid Aerospace Ground Equipment (AAGE)	6-2
6.2.1	System Configuration	6-2
6.2.2	Hardware Configuration	6-3
6.2.3	Special Tools and Fixtures	6-6
7.0	PROGRAM MANAGEMENT	7-1
7.1	Asteroid Program Philosophy	7-1
7.2	PMO Organization	7-1
7.3	Cost Schedule Management	7-1
7.4	Quality Control Plan	7-3
7.5	Reliability and Quality Assurance Laboratory Facilities	7-4
7.6	Use of Existing Hardware	7-4
8.0	REFERENCES	8-1

## LIST OF ILLUSTRATIONS

<u>Figure</u>		<u>Page</u>
1-1	Low Cost Planetary Spacecraft Options	1-3
1-2	Limits of Design Applicability	1-4
3.2-1	STS Launch Geometry	3-4
3.2-2.	Rendezvous with Near-Earth Asteroids with Launch Dates in 1988-1990, plus Anteros 1987 Launch (Integrated Hydrazine Propulsion System)	3-5
3.2-3	Rendezvous with Near-Earth Asteroids with Launch Dates in 1991-1996 (Integrated Hydrazine Propulsion System)	3-6
3.2-4	Rendezvous with Near-Earth Asteroids with Launch Dates in 1988-1990, plus Anteros 1987 Launch (Integrated MMH-NTO Propulsion System)	3-7
3.2-5	Rendezvous with Near-Earth Asteroids with Launch Dates in 1991-1996 (Integrated MMH-NTO Propulsion System)	3-8
3.2-6	Rendezvous with Near-Earth Asteroids with Launch Dates in 1988-1990, plus Anteros 1987 Launch (Solid Rocket for Rendezvous Maneuver, Hydrazine System for Navigation and Orbit Sustenance)	3-9
3.2-7	Rendezvous with Near-Earth Asteroids with Launch Dates in 1991-1996 (Solid Rocket for Rendezvous Maneuver, Hydrazine System for Navigation and Orbit Sustenance)	3-10
3.2-8	IUS Planetary Performance	3-12
3.3-1	Match of STS Upper Stages with Throwmasses for Four Near-Term Candidate Asteroid Rendezvous Missions (for a 500-kg Class TIROS-Based Spacecraft Using Available Titanium Hydrazine Tanks and Kevlar Pressurant Tanks)	3-16
3.3-2	Change in $C_3$ for $ DLA  > \text{Parking Orbit Inclination}$ for 240-280 km Altitude Circular Parking Orbit	3-18
3.5-1	EROS Transfer Geometry - 1989 Launch	3-20
3.5-2	Anteros Transfer Geometry - 1987 Launch	3-21
3.5-3	Anteros Transfer Geometry - 1990 Launch	3-22
3.5-4	Anteros Transfer Geometry - 1992 Launch	3-23
3.6-1	Rendezvous Drift Trajectory	3-26
3.6-2	Rendezvous Final Approach Trajectories	3-27
3.6-3	Geometry at Rendezvous Impulse for Mission to EROS, Launching 1989	3-28
3.7-1	EROS Mission Phase Geometry - 1989 Launch	3-30
3.7-2	Anteros Mission Phase Geometry - 1987 Launch	3-31
3.7-3	Anteros Mission Phase Geometry - 1990 Launch	3-32
3.7-4	Anteros Mission Phase Geometry - 1992 Launch	3-33
4-1	Advanced TIROS-N Spacecraft, NOAA-G Configuration	4-3
4-2	TIROS-N/NOAA Series	4-5
4-3	Array Power Maximum Power Point Tracker	4-7
4-4	Science Channel Capacity	4-7
4-5	Tradeoffs - Cruise and Injection Phase	4-12
5.1-1	Asteroid Spacecraft	5-2
5.1-2	Configuration 1 - Stowed	5-5

# LIST OF ILLUSTRATIONS (Continued)

<u>Figure</u>		<u>Page</u>
5.1-3	Configuration 1 - Deployed	5-6
5.1-4	Configuration 2 - Stowed	5-7
5.1-5	Configuration 2 - Deployed	5-8
5.1-6	Configuration 1 - Cruise Mode	5-16
5.1-7	Fully Deployed On-Orbit Configuration	5-16
5.2-1	STS Propulsion Subsystem Configuration Schematic	5-18
5.3-1	Simplified Block Diagram of the Attitude Determination and Control Subsystem (ADACS)	5-23
5.3-2	Primary ADACS Functional Block Diagram	5-26
5.4-1	SAATN Power Subsystem Block Diagram	5-28
5.4-2	Asteroid Load Profile for Cruise and Mission Phases	5-32
5.4-3	Power Available for DET Power Subsystem	5-33
5.4-4	Solar Array Output Power for DET Power Subsystem	5-33
5.4-5	Maximum Power Tracker (MPT) Block Diagram	5-34
5.4-6	Power Availability for MPT Power Subsystem	5-35
5.5-1	Communications Subsystem	5-36
5.5-2	Science Channel Capacity	5-37
5.5-3	Engineering Channel Capacity	5-37
5.5-4	Engineering Channel Capacity (S/C LGA)	5-38
5.5-5	Command Channel Capacity	5-38
5.6-1	Thermal Control Configuration	5-51
5.7-1	Command Subsystem Block Diagram	5-53
5.7-2	Cross Strapping Proposed for Asteroid	5-55
5.7-3	Data Handling Subsystem	5-56
6-1	TIROS-N Aerospace Ground Equipment	6-2
6-2	ATNAGE System Configuration with Asteroid Mission Modifications	6-4
6-3	ATNAGE Hardware Configuration	6-5
6-4	Satellite Support Rack and Remote Power Switch	6-7
6-5	RF Section of ATNAGE	6-8
6-6	Ordnance Device Simulator	6-8
7-1	RCA Management Tools	7-2
7-2	Dynamics Explorer Overall Program Schedule	7-3

## LIST OF TABLES

<u>Table</u>	<u>Page</u>
1-1 Comparison of Actual TIROS-N and Proposed TIROS-N/ Anteros Primary Sensors	1-6
2-1 Asteroid Mission Instrument Summary	2-2
2-2 Individual Instrument Requirements	2-3
2-3 Instrumentation Commonality (Missions Currently Under Consideration)	2-7
2-4 Summary of Asteroid Payload Requirements and TIROS Capabilities	2-8
3.1-1 Summary of Missions To Anteros, Launching 1987-1992	3-2
3.1-2 Summary of Missions to EROS, Launching 1987-1996	3-2
3.1-3 Summary of Missions to 1982 DB, Launching 1988-1998	3-3
3.3-1 Propulsion Mass Budget for Anteros Rendezvous Mission, Launching 5/27/87-6/6/87	3-14
3.3-2 Parametrically Derived Estimates of the On-Board Propulsion Subsystem Mass Budgets for Four Near-Term Candidate Asteroid Rendezvous Missions	3-15
3.6-1 Velocity Change Requirements	3-27
4-1 Power/Thermal Impact	4-6
4-2 Equipment Heritage and Description	4-9
4-3 Selected Operation Scenarios	4-13
4-4 Primary Results	4-14
5.1-1 NOAA-D Weight Report With Asteroid Version Option	5-9
5.2-1 STS Safety Requirements, NHB 1700.7	5-19
5.2-2 Asteroid Propulsion System Requirements	5-20
5.2-3 Base Line Feed System Components Summary	5-21
5.3-1 ADACS Requirements for Asteroid Mission	5-24
5.3-2 ADACS Design for Asteroid Mission as Compared to DMSP	5-24
5.4-1 EPS Component Characteristics (SAATN)	5-30
5.4-2 Asteroid Power Requirements	5-32
5.4-3 Advantages and Disadvantages of the DET and MPT Systems	5-35
5.5-1 Communications Link Assumptions	5-39
5.5-2 Science/Engineering X-Band Links with High Gain Antenna	5-40
5.5-3 Science/Engineering S-Band Links with High Gain	5-42
5.5-4 Engineering Data S-Band Links with Omni Antenna	5-44
5.5-5 Engineering Data K-Band Links with Omni Antenna	5-46
5.5-6 S-Band Command Link Summary	5-48
5.6-1 Asteroid Mission Equipment Temperature Requirements	5-50
5.6-2 Thermal Control Heater Requirements at 1.8 AU	5-52
5.7-1 Command and Data Handling	5-54

## SECTION 1.0

### OVERVIEW AND SUMMARY

Since the advent of space flight, very few missions have been more intriguing and enlightening than those to deep space -- first, the preliminary lunar missions, precursors to the Apollo program, followed by preliminary fly-by probes to Mars, Venus, and Mercury. Predicated on the technology and scientific return from these missions, we extended our study of the inner planets to include Mars landing and sample analysis, sophisticated multi-spacecraft missions to Venus, and fly-by missions to the outer planets Jupiter and Saturn. These outer planet fly-bys, first accomplished by Pioneers 10 and 11 and subsequently by the more sophisticated Voyager 1 and 2 spacecraft, provided spectacular data which have greatly expanded our understanding of these giants of the solar system. More importantly, these data, along with the more detailed data available from the inner planets, provide us with a far more enlightened view of our solar system and of our Earth as a planet. These data provide us with significant clues as to the evolution and, perhaps, the future of our own planet's atmosphere and topology by relating such seemingly varied topics as plate tectonics (continental drift), the evolution of the atmosphere, and the development of life on the Earth. This is done through a complex series of hypotheses, still very preliminary, involving data gained from these planetary missions.

The first look at Uranus and, if we are lucky, Neptune, will be provided by Voyager late in this decade, extending still further man's presence in the solar system. In addition, the Galileo orbiter/probe mission, also scheduled late in this decade, will provide our first in-depth study of Jupiter; it will include a probe that will, for the first time, sample the atmosphere of the largest planet. In the same time frame, the Venus mapper will make detailed maps of the surface of Venus by use of a synthetic aperture radar system. This will provide, for the first time, sufficient resolution of the surface details of that cloud-shrouded planet to allow a detailed geological comparison with the Earth.

Given the current state of our exploration of the solar system, the next set of targets is quite readily chosen; they are the minor bodies, asteroids and comets.

Asteroids and comets are extremely important to our understanding of the evolution of the solar system and the formation and evolution of the planets since they may provide us with unique samples of the primordial material from which the solar system evolved, uncomplicated by the geological evolution that has taken place on the inner planets. Because of this, asteroids and comets are prime candidates for exploration. The asteroids, aside from being keys to our understanding of the solar system, may also be important for other reasons. Since asteroids are suitable for manned missions, it is conceivable that they could be tapped in the future as a source of resources, such as exotic materials in short supply on Earth or, more likely, common materials for use in large scale space structures. This last option is potentially feasible since many asteroids are in orbits that are compatible with the transfer of material (either processed or for processing) to geosynchronous orbit with far less energy than would be necessary to bring the same mass up from the ground. This leads to speculation, for example, that aluminum smelting operations on a

manned base on the surface of an asteroid might be possible. Another possibility is a mine that is used to deliver raw material to a space manufacturing facility in Earth orbit. A manned asteroid base could also provide for a variety of other space research and manufacturing operations.

Currently, the fact remains that before any of these possibilities can be seriously considered, we must significantly expand our knowledge of the physical and chemical properties of the asteroids. Exactly what would be done with a preliminary scientific spacecraft mission to such a body could then be determined. The only data currently available are from ground-based observation. These data allow some crude classification (by spectral type), allow us to calculate spin rate, and, with some assumptions, allow us to estimate the size distribution of the asteroids. None of these observations are adequate for anything other than selection of a target for precursor missions required as preliminaries to the exploitation of the asteroids. Further, since asteroids exhibit such diverse properties, multiple asteroid rendezvous missions are required to many different types of targets. Several scientific working groups have addressed the question of what sample of asteroids would be adequate to understand their nature. In general, these recommendations include several sizes and a wide range of orbital parameters, between 1 and 5 astronomical units (AU). These recommendations include one group, the near-Earth asteroids, which can be studied using modified Earth orbiter spacecraft technology (the RCA TIROS spacecraft) and existing launch vehicles. This can be done at a very low cost, significantly less than any past planetary missions and, more importantly, consistent with present day fiscal realities and NASA budgetary policy.

The concept of the low cost planetary spacecraft has been evolving at RCA as an independent research and development (IR&D) program since 1980. In 1981 and 1982, NASA funded studies at RCA and elsewhere, through both the Jet Propulsion Laboratory (JPL) and the Ames Research Center, for low cost Mars missions. One of these concepts is shown in Figure 1-1. The concept of using a modified TIROS spacecraft for an asteroid rendezvous mission was first developed under the RCA IR&D program, and later development was subsequently funded by JPL by this contract. The initial work done at RCA established the limits of applicability of Earth-orbiter spacecraft to deep space missions, as shown in Figure 1-2. Closer to the Sun than Venus, for example, on Mercury, the thermal constraints are so significant that systems designed for Earth application are totally inadequate. Farther away from the Sun, Mars is an ideal candidate for the application of Earth-orbiter technology; in fact, the environment encountered by a spacecraft in orbit around Mars is surprisingly close to that of the Earth. Farther out, some designs may be applied to missions to the main asteroid belt, the major limitation being the amount of power that can be derived from the solar array. However, at Jupiter and beyond, it can be clearly demonstrated that Earth-orbiter technology does not apply without significant modification. At these distances, radio-thermal generators must replace solar arrays as the source of power, and the extremely cold temperatures preclude the use of Earth-orbiter thermal design. In addition, the environment near Jupiter and the planets beyond is characterized by intense radiation hazards, far past the nominal design limits of most spacecraft.

Once the range of applicability of Earth technology was established, it became clear that a wide range of missions of high scientific interest can be accomplished by the application of the Earth-orbiter technology, in a very cost-effective manner, with no scientific compromise. Near-Earth asteroid

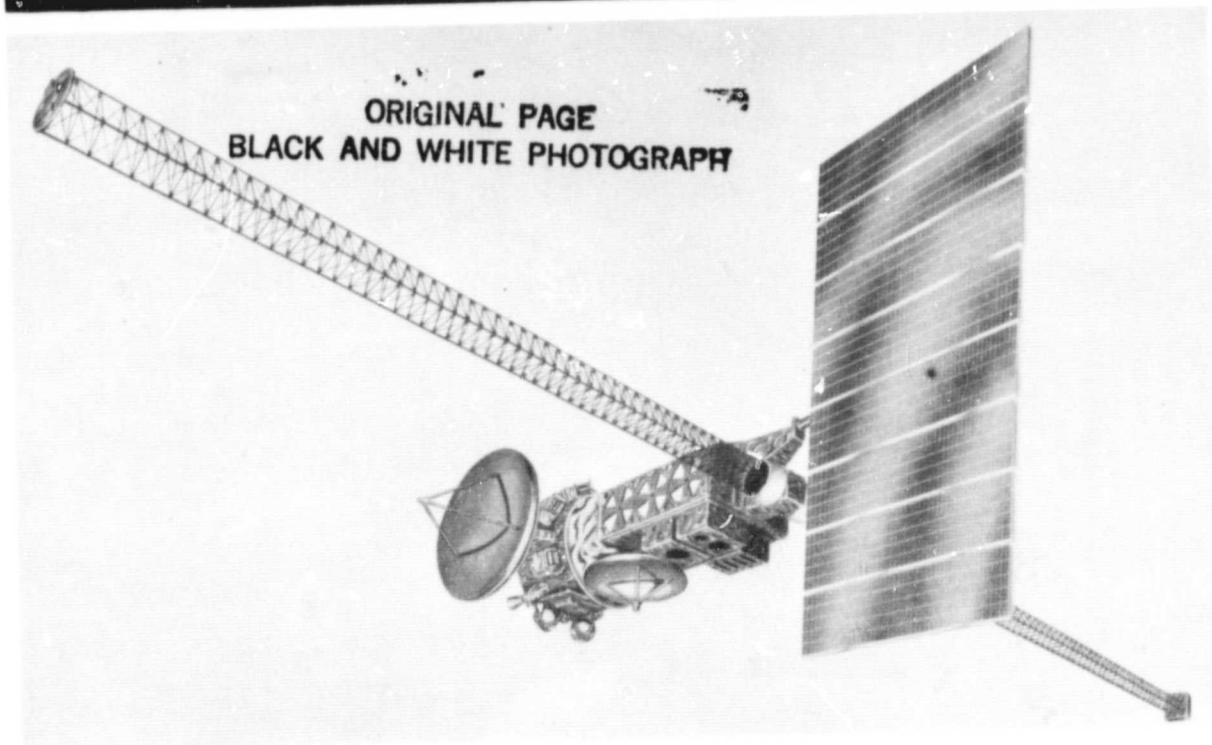
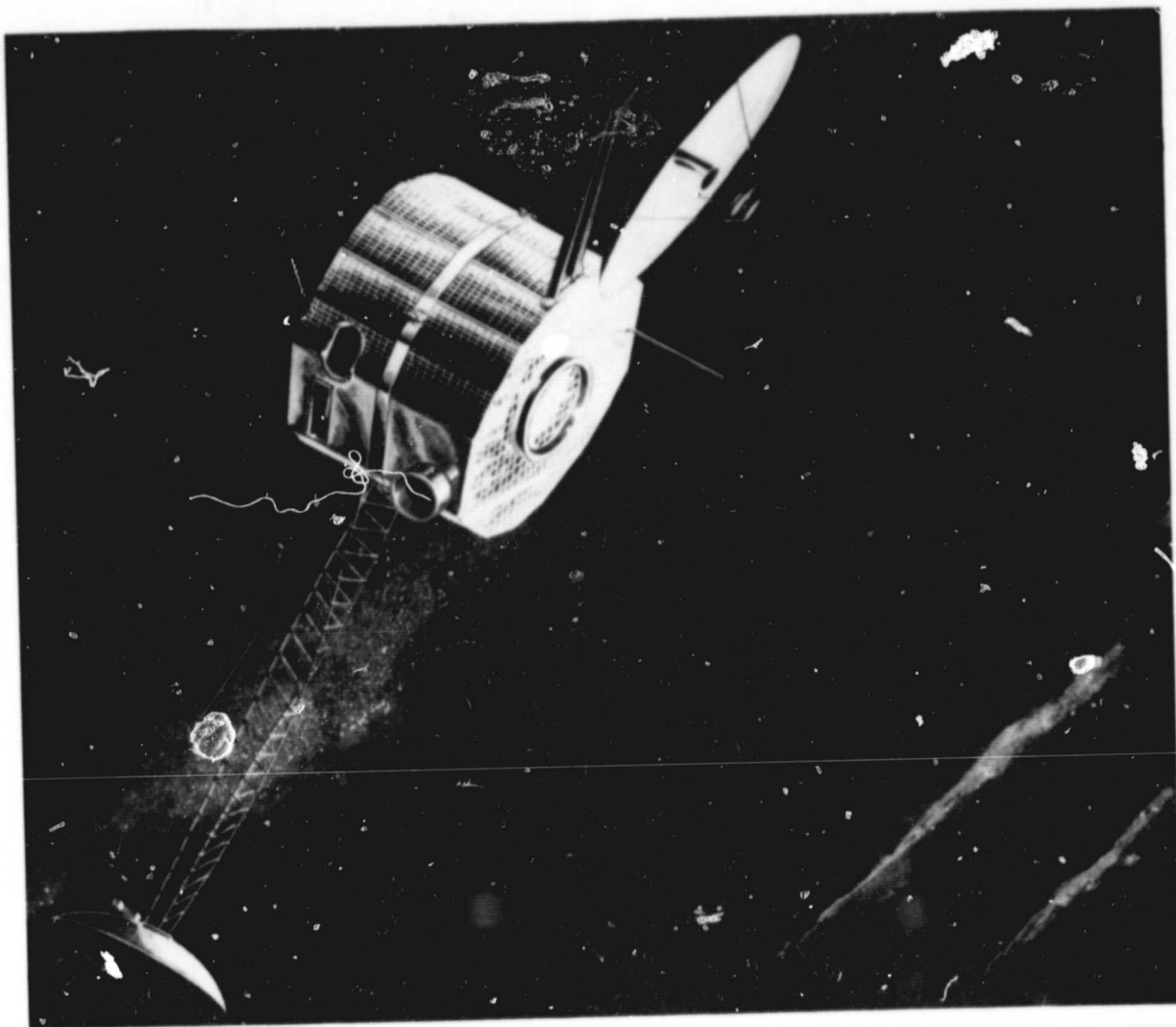


Figure 1-1. Low Cost Planetary Spacecraft Options

ORIGINAL PAGE IS  
OF POOR QUALITY

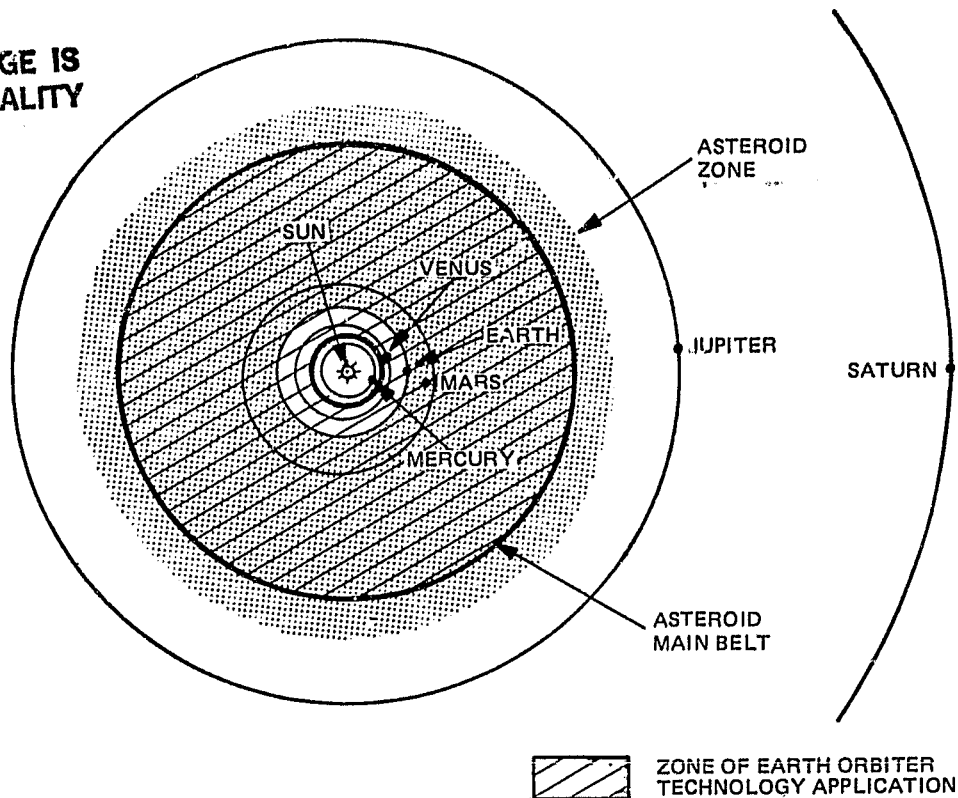


Figure 1-2. Limits of Design Applicability

rendezvous missions are among the most exciting prospects. To fully appreciate the rather astonishing conclusion that TIROS, a spacecraft designed to make meteorological observations from a low, Earth circular polar orbit, can fully support a mission as exotic as an asteroid rendezvous, it is necessary to understand in more detail the rationale (and therefore the instrument complement) behind the Asteroid mission. To do this, let us see what it is we hope to learn in the first such mission.

The first obvious question is, where do the asteroids come from? Are they remnants of an exploded planet? Perhaps a planet that never quite formed? Did they evolve in their present form because of the influence of Jupiter? Why are they mostly concentrated between Mars and Jupiter? We know that the great majority of asteroids fall in a region called the main belt (between Mars and Jupiter). We also know, however, that asteroids are not constrained to lie in the main belt. Hundreds, or perhaps thousands, of asteroids penetrate deep into the inner solar system, extending into and even across the orbit of the Earth. This set of asteroids, Earth-approaching and Earth-crossing, are taken together as near-Earth asteroids. To fully understand the nature of asteroids and their implication in the development and evolution of the solar system, it is important to study both main belt and near-Earth asteroids and to understand their relationship. Since we need to study both types, and since near-Earth asteroids are far more easily accessible than the main belt asteroids, it is logical to select the latter as the target for the first spacecraft mission. Given this selection, the questions that the first mission should address are readily defined. Specifically, where do the near-Earth asteroids come from? Are they merely asteroids from the inner edge of the main belt, asteroids whose orbits were perturbed, perhaps by a close approach to Mars, in a way that sent them on orbits into the inner solar



system? Are they extinct nuclei of short period comets, or are they in any way related to comets? Perhaps they have nothing to do with main belt asteroids or comets; if not, where do they come from? The next question concerns the relationship of Earth-approaching asteroids to meteorites and their classification. Meteorites fall into a highly structured classification scheme, and understanding the relationship between the asteroids and this classification scheme is potentially of great value to our understanding of the asteroids themselves. It may also provide a better understanding of the geologic and/or cosmogenic context in which the vast amount of existing meteorite data should be placed. The same can be said of the relationship of the asteroid data with the lunar data provided by Apollo. In addition to these major questions, there are many secondary questions related to the space environment, its variation, and the implications of a study of the asteroids.

To allow us to address these questions, the first asteroid mission will be required to: 1) determine the chemical and mineralogical composition, 2) observe the surface morphology, 3) determine the bulk density and density distribution, and 4) determine the magnetic properties. The definition of a straw man instrument complement that could be used to address these objectives was carried out at JPL and supplied to RCA. Instruments included are a gamma-ray spectrometer (objective 1), an x-ray spectrometer (objective 1), a multi-spectral infra-red mapper (objectives 1 and 2), an altimeter (objectives 2 and 3), an optical charge coupled device (CCD) imager (objective 2), and a magnetometer (objective 4).

A comparison between the existing TIROS instrumentation and the Asteroid mission instrumentation is shown in Table 1-1. This comparison clearly shows that the spacecraft requirements to support both sets of instruments are similar. The imagers and sounders that TIROS normally carries are nadir-pointing devices that must be held steady and properly pointed. The same is true of the imager, infra-red mapper, altimeter, and spectrometers on the Asteroid mission. The total weight and mounting area requirements of the Asteroid mission are significantly less than those of TIROS, thus allowing for simplification of the basic spacecraft. In addition, the power, thermal, command and control, and data systems of TIROS can be applied to this mission with little or no modification. The communications system requires extensive modification since, as is the case in any deep space mission, the distances from Earth to spacecraft are exceedingly large. This necessitates, among other things, a large high gain dish antenna. The attitude control system also requires a degree of modification because of the requirement to use a star reference for navigation guidance. Tracking, command, and data acquisition will be carried out via the deep space network.

One of the key elements of this mission is the ability to use an existing launch vehicle, thereby avoiding the programmatic and cost problems that arise when a launch vehicle development is required in parallel with a spacecraft development. Accordingly, it was decided at the outset of the study that the selected target asteroid must fall in a category accessible by existing vehicles. The launch system chosen is the Space Transportation System (STS) with the Two-Stage Inertial Upper Stage (IUS). All portions of this system have been developed, and the STS/IUS combination will fly early in 1983 to launch the first tracking and data relay satellite (TDRS).

TABLE 1-1. COMPARISON OF ACTUAL TIROS-N AND PROPOSED TIROS-N/ANTEROS  
PRIMARY SENSORS

	Asteroid SSI	TIROS AVHRR	Anteros NIMS	TIROS HIRS
Mass (kg)	28.0	30.4	18.0	33.1
Power (W)	25	30	16	22
Dimensions (cm)	30x24x88	51x30x65	66x47x81	51x30x65
Data Rate (kbps)	806.4	660.0	11.5	2.88

If we consider the known performance of the STS/IUS combination, the mass of the spacecraft, and the orbit of the target asteroid, we can determine if the mission is energetically feasible. In essence, we calculate the possibility of achieving the same orbit about the Sun as that of the target asteroid. In general, to rendezvous with the asteroid involves a five-phase mission. First, the STS lifts off and goes to a standard STS parking orbit with an acceptable inclination, as determined by the orbit of the target asteroid. Second, the IUS/spacecraft combination is separated from the STS and, after achieving proper inertial reference and a safe separation distance from the STS, the IUS fires and injects the spacecraft into the proper heliocentric transfer orbit. The remnants of the IUS and the separation adapter are then jettisoned, the array is partially deployed, the cruise-phase configuration is assumed, and the second phase of the mission begins. This phase of the mission will last between three and twelve months (depending on the target) and involves a cruise coast around the Sun, as shown in Figure 3.7-1 for the specific case of the asteroid Eros. During this mission phase, the spacecraft and instruments are essentially dormant, with periodic checkouts, health monitoring, and an occasional mid-course correction the only planned activities. During this period, detailed tracking of the spacecraft and the asteroid are ongoing, and the mid-course maneuvers are derived from this detailed tracking data. The target window for the spacecraft is an imaginary circle, centered on the asteroid, with a radius of about 6000 km.

As the spacecraft approaches the asteroid, the third phase of the mission begins. This is the crucial phase in which the on-board propulsion system (a large hydrazine system in the current system design concept) is used for a major velocity adjustment (on the order of 1-2 km/second) which changes the orbit of the spacecraft from the transfer orbit to the asteroid orbit. At this point, the spacecraft is flying along with the asteroid, in the same orbit but far enough away to be unaffected by its gravitational pull. The asteroid will appear as the brightest object in the sky to the spacecraft, somewhat like a full Moon appears on Earth, and will therefore be easily picked up by the on-board instruments. All instruments will be brought on-line, checked out, and begin operation. Images will start coming back from the asteroid, providing scientific data as well as a critical navigational tool for the fourth phase, the approach to the asteroid.

During this phase, the spacecraft is given a small push by its propulsion system in the direction of the asteroid. Over a period of several days, it slowly approaches the asteroid, imaging the target as it goes, on-board sensors carefully monitoring any perturbations to its trajectory as it enters the gravitational sphere of influence of the asteroid. When the sphere of influence of the asteroid is reached, the fifth mission phase begins. At this point, there are several mission options available. They include: 1) sequential drift arcs (repeated hyperbolic passes by the asteroid from long distances), 2) interrupted free fall (stopping the spacecraft, letting it fall into the asteroid, and interrupting the free fall before impact), 3) station-keeping (holding a fixed position over the asteroid), and 4) orbiting the asteroid.

The reason so many options are available and, for the most part, energetically feasible, is that the asteroids are small and their gravitational attraction is very weak. As a measure of this for a typical asteroid, a few kilometers in diameter, the escape velocity is so low that a man running across the surface would fly off into space and escape the body's gravitational pull. Another consequence is that, for our orbiting spacecraft, the altitudes would be on the order of 10 kilometers and the velocities less than one meter per second, far different than what we are used to dealing with.

Calculations have been made on the consequences of these four options, and the current mission scenario involves three of the four options. Stationkeeping has been eliminated because, even given the weak gravitational attraction of the asteroid, fuel requirements are excessive at the low altitudes we would like to achieve. The current base line goes something like the following. Near the end of phase four, we would target the spacecraft and adjust its velocity so that the first pass near the asteroid would result in an unbound hyperbolic trajectory (the sequential drift arc). We would then stop, reverse direction, and fly a series of such maneuvers at an ever decreasing distance of closest approach. After this series of maneuvers, we would have a fairly detailed map of the surface and would be able to safely define an optimum orbit into which we would then insert the spacecraft. From this orbit, detailed magnetic field and altimetry observations would be performed, surface maps would be improved, and the x-ray and gamma ray survey would be done. After detailed orbital coverage was accomplished, we would "stop" the spacecraft and do a series of interrupted free fall maneuvers to image the asteroid as closely as possible. The entire duration of the fifth mission phase would be between three and twelve months. At the end of the mission, we would most likely attempt as soft a landing (in reality a quasi-controlled crash) on the asteroid as possible. For this first mission, such a maneuver would not be mission-critical and should at most be construed as an engineering test for the next generation mission.

Thus far we have discussed target asteroids only in a generic sense. It is possible to quantitize the constraints caused by spacecraft size, IUS performance, and orbit injection velocity change requirements and relate this to the accessibility of specific asteroids. In Figure 3.2-2, we have plotted  $C_3$  (in essence, the launch energy achievable from the IUS) against the total velocity change requirements post injection. Several asteroids are plotted on this graph at the point where the  $C_3$  and  $\Delta V$  would allow an entry to their orbit (and a launch window for rendezvous). The line of the graph shows what is achievable for a 500-kg dry spacecraft, roughly the TIROS/Asteroid space-

craft mass, using an all-hydrazine propulsion system. Any asteroid that falls below this line is, therefore, a viable target.

One important consequence of looking at the problem this way is that it allows the project to begin even before the target is selected. As long as the ultimate target asteroid falls below this line, it is a feasible mission option. The working base lines for the study were the asteroids Anteros and Eros, both shown on the cross plot. The known asteroid easiest to get to, 1982 DB, was only recently discovered (and was a relatively near miss in its most recent pass by the Earth). New asteroids are being discovered periodically and the list is expanding.

In summary, the TIROS/Asteroid spacecraft mission has significance in two very important ways. First, as the first mission to a minor body, it will provide us with our first look at a very important class of bodies in the solar system and will therefore provide the opportunity for basic discoveries, in much the same way Voyager has done for the outer planets. It will also serve as a precursor, providing critical data required to plan more extensive asteroid missions and perhaps leading to manned missions. Second, and equally important in its own way, this mission could be the first of a series of low cost deep space missions which will allow us to expand significantly the number of missions flown consistent with the NASA budget for planetary programs. This will allow optimum use of the capability provided by the STS to expand our knowledge of the solar system. Other missions currently being considered for this series are several Mars missions (including climatology, geochemistry, and aeronomy) and a lunar polar orbiter (to survey the polar region of the Moon and ascertain the feasibility of using the Moon as a source of resources for space manufacturing). In fact, the TIROS spacecraft described here is also a candidate for several of these missions, opening the possibility of a spacecraft series that would further enhance the cost effectiveness of exploring the solar system and understanding the implications for our own planet.

## SECTION 2.0

### SCIENCE ACCOMMODATION

#### 2.1 INSTRUMENT REQUIREMENTS

Since asteroids and comets may provide unique samples of the primordial material of the solar system, they are prime candidates for exploration. Ground-based observation (primarily light curves and some spectroscopy) can classify spectral types, size distribution, and some morphology of asteroids, but direct observation by nearby spacecraft is required to satisfy the primary scientific objectives of the study of asteroids.

In addition, to completely understand the asteroids, missions to a variety of types, including Earth-approaching targets, are required. For example, it is important to determine the source of Earth-approaching asteroids. Do they come from the inner belt? Are they extinct comets? Are they perhaps related to neither of these? It is also important to determine the relationship, if any, between Earth-approaching asteroids and meteorites. Observation of near-Earth asteroids may provide a better understanding of the geologic and/or cosmogenic context in which the meteorite data should be placed. The same can be said for the Apollo lunar data. Study of the asteroid surface will also help us to understand the long term variation in the space environment.

To carry out these goals, we must:

- 1) Determine the chemical and mineralogical composition of the asteroid
- 2) Observe the surface morphology of the asteroid
- 3) Determine the bulk density and density distribution of the asteroid
- 4) Determine the magnetization state of the asteroid

As a basic payload to support these measurement requirements, JPL has specified a gamma ray spectrometer and an x-ray spectrometer (for requirement 1), a multi-spectral mapper (for 1 and 2), an altimeter (for 2 and 3), a CCD imager (for 2), and a magnetometer (for 4). All of these measurements must be repeated over as large a fraction of the asteroid surface as possible. A summary of the instruments and their physical accommodation parameters is shown in Table 2-1. Table 2-2 summarizes each of the instruments and its impact on the spacecraft. The most stringent requirements are due to the MSM attitude control. Some improvement over currently used TIROS capability is required to meet these specifications; however, it is readily within the capability of the DMSP system (see Section 5.3). It is important to note the similarity of the asteroid instruments with those of other missions currently of interest, as shown in Table 2-3. This is a key point since, as the table shows, there are several other missions of interest in the pioneer class that use virtual subsets of the Asteroid instrument complement. Even in those missions where the instrument complement differs, the mass, power, and data rate do not exceed those specified for the Asteroid rendezvous spacecraft (ARS). The ARS mission is clearly the most demanding of the group, in all respects.

#### 2.2 PAYLOAD ACCOMMODATION

Since the base line payload uses only a small fraction of the TIROS capability (see Figure 4-2), significant simplifications are possible. Specifically, the

TABLE 2-1. ASTEROID MISSION INSTRUMENT SUMMARY

Instrument	Weight (kg)	Power (W)	Data Rate (kbps)	Duty Cycle	Avg Data Rate	Mounting	FOV	Cooling
Gamma Ray Spec- trometer (GRS)	12	10	1.5	~100%	1.50	Extendable Boom	2 $\pi$ STR	Passive (~100°K)
X-Ray Spec- trometer (XRS)	11	10	0.3	~50%	0.15	Bus or Boom	2 $\pi$ STR	Passive (~170°K)
CCD Imager (CCD)	28	35	800.0	~10%	80.00	Bus	50X50 mR Cooler ~150°	Passive (~80°K)
Multispectral Mapper (MSM)	17	8	1.5-12	~50%	~3.00	Bus	4X . 2mR Cooler ~150°	Passive (~80°K)
Radar Altimeter (ALT)	10	18	0.6	100%	0.60	Bus	2° 30° Exclusion	Passive
(Laser Altimeter Option)*	(10)*	(18)*	(10.0)*	(100%)*	(10.00)*	Bus	5 mR 30° Exclusion	Passive
Magnetometer (MAG)	4	4	0.4	100%	0.40	Boom	N/A	N/A
Total	82	85	815.0	-	86.00	-	-	-
*Replaces ALT								

ORIGINAL PAGE IS  
OF POOR QUALITY

TABLE 2-2. INDIVIDUAL INSTRUMENT REQUIREMENTS

GRS	
<ul style="list-style-type: none"> <li>• Primary Data</li> <li>• Calibration</li> <li>• Constraints</li> <li>• Attitude Control</li> </ul>	<p>Gamma ray pulse height spectra from the Martian/lunar surface</p> <p>Spectra obtained prior to mid- and post-boom deployment mid-course boom deployment required</p> <p>Spectra should be obtained at various orientations with respect to the galactic background and at various levels of solar flare activity and periodically repeated as the mission progresses (special maneuvers may be desirable for this purpose)*</p> <p>Passive cooler pointed at deep space</p> <p>No strong EMI sources or susceptibility</p> <p>No radioisotopes of any kind carried and/or used by the spacecraft or other instruments</p> <p>Control <math>\sim \pm 50</math> mR</p> <p>Knowledge <math>\pm 50</math> mR</p> <p>Stability - not specified (Note: the better/longer the nadir pointing can be held, the better the S/N of a given pulse height spectra and therefore the more components which can be identified)</p>
XRS	
<ul style="list-style-type: none"> <li>• Primary data</li> <li>• Calibration</li> <li>• Constraints</li> </ul>	<p>X-ray pulse height spectra from the lunar surface</p> <p>Reference target solar pointing, continuously monitored</p> <p>Passive cooler pointed at deep space, reference target solar pointing</p> <p>No strong EMI sources or susceptibility</p> <p>Possibly boom, possibly body-mounted</p>
<p>*An on-board monitor such as an ionization chamber &amp; monitor total dose of galactic/solar cosmic rays would be helpful.</p>	

TABLE 2-2. INDIVIDUAL INSTRUMENT REQUIREMENTS (Continued)

XRS (Continued)	
● Attitude Control	Control $\sim \pm 50$ mR Knowledge $\sim \pm 50$ mR Stability $\sim \pm 100$ R/min Nadir pointing (see note on GRS)
CCD	
● Primary Data	Visible images of the surface (with or without color filters)
● Calibration	Internal, wide dynamic range proper settings iterated after encounter Cruise calibration internal
● Constraints	Keep optics away from Sun Cooler pointing at deep space required No strong EMI sources or susceptibility Thruster plume impingement excluded from optics/cooler Thermal input constraint to maintain optics at stable temperature (make-up heaters used when power off) Covers may be required
● Attitude Control	Control $\sim \pm 10$ mR Knowledge $\sim \pm 10$ mR Stability $\sim \pm 200$ $\mu$ R/second Pointed at the asteroid (essentially nadir)



TABLE 2-2. INDIVIDUAL INSTRUMENT REQUIREMENTS (Continued)

MSM	
<ul style="list-style-type: none"> <li>• Primary Data</li> <li>• Calibration</li> <li>• Constraints</li> <li>• Attitude Control</li> </ul>	<p>IR images (several bands) of the surface</p> <p>Two reference targets, one reflective and one active thermal</p> <p>Cruise calibration internal</p> <p>Keep optics away from Sun</p> <p>Cooler pointing at deep space required</p> <p>No strong EMI sources or susceptibility</p> <p>Thruster plume impingement excluded from optics/cooler</p> <p>Covers are required</p> <p>Control <math>\pm 2</math> mR</p> <p>Knowledge <math>\pm 1</math> mR</p> <p>Stability <math>\sim 20</math> <math>\mu</math>R/second</p> <p>Nadir pointing</p>
ALT	
<ul style="list-style-type: none"> <li>• Primary Data</li> <li>• Calibration</li> <li>• Constraints</li> <li>• Attitude Control</li> </ul>	<p>Surface roughness/height variations</p> <p>Internal, no spacecraft impact</p> <p>Possible EMI source</p> <p>Control <math>\sim \pm 30</math> mR</p> <p>Knowledge <math>\sim \pm 30</math> mR</p> <p>Stability <math>\sim \pm 100</math> <math>\mu</math>R/minute</p> <p>Nadir pointing</p>
<p>Note: Replacing the nadir altimeter by a laser altimeter is an option that has yet to be fully assessed; however, to the first order, no substantial additional problems are apparent.</p>	

TABLE 2-2. INDIVIDUAL INSTRUMENT REQUIREMENTS (Continued)

MAG	
<ul style="list-style-type: none"> <li>● Primary Data</li> <li>● Calibration</li> <li>● Constraints</li> <li>● Attitude Control</li> </ul>	<p>Magnetic field measurements near Mars or the Moon (to determine the magnetization state of the body and the nature of the body/solar wind interaction)</p> <p>Internal, no spacecraft impact</p> <p>Boom mounted</p> <p>No spacecraft magnetic fields (ac or dc) &gt;0.01 gamma at sensor</p> <p>EMI susceptibility concerns</p> <p>Control - N/A</p> <p>Knowledge - <math>\sim \pm 20</math> mR (<math>1.2^\circ</math>)</p> <p>Stability N/A</p>

TABLE 2-3. INSTRUMENTATION COMMONALITY (MISSIONS CURRENTLY UNDER CONSIDERATION)

Asteroid Rendezvous	Lunar Geochemical	Mars Geochemical	Mars Climatology	Mars Aeronomy
Gamma Ray Spectrometer (GRS)	GRS	GRS	GRS	Neutral Mass Spectrometer
Multispectral Mapper (MSM)	MSM	MSM	Pressure Modulated Radiometer	Ion Mass Spectrometer
Magnetometer (MAG)	MAG	MAG	Frost Detector	Langmuir Probe
Radar Altimeter (ALT)	ALT	ALT	Ultraviolet Detector	Retarding Potential Analyzer
X-Ray Spectrometer (XRS)	XRS		ALT	MAG
Charge Coupled Device (CCD) Imager	Electron Reflectometer			Electric Fields
				Solar Wind Plasma
				UV Spectrometer
				Fabry-Perot
Total Mass ~82 kg	~59 kg	~43 kg	~50 kg	~53 kg
Total Power* ~90W	~59W	~44W	~70W	~46W
Data Rate ~17.0 kbps*	~9.1 kbps	~8.5 kbps	~3.0 kbps	~2.5 kbps
Payload Accommodation	TIROS Capabilities	AE/DE Capabilities	SATCOM Capabilities	
Mass	360 kg	200 kg	200 kg	
Power**	1060W	110W	1225W	
Data Rate	2 Mbps	16 kbps	1 kbps	Housekeeping + Communications Payload
*Assuming 8 kbps Average for imager				
**All up, available for instruments (Note: Power capabilities speed at 1 AU, at Mars divide by X2)				

instrument mounting platform (IMP) which holds the primary instruments in the METSAT (meteorological satellite) configuration can be deleted. The primary mounting surface used for the Asteroid application is on the nadir-facing portion of the equipment support module (ESM). Several instruments and antennas are mounted on this surface in the case of METSATS, and it is easily capable of holding the Asteroid instruments. An adapter bracket will replace the IMP, and the brooms for the gamma ray spectrometer (GRS) and magnetometer (MAG) will be located in this area. There is ample room for all of the instruments and for growth, even with the TIROS-N (not to mention the Advanced TIROS-N). This can be done easily, even given the cooler accommodation requirements. Table 2-4 shows a direct comparison of the Asteroid mission requirements with TIROS capabilities.

TABLE 2-4. SUMMARY OF ASTEROID PAYLOAD REQUIREMENTS AND TIROS CAPABILITIES

Parameters	ARS Requirements	TIROS Capabilities
Instrument Mass	82 kg	344 kg
Instrument Power	85W	290W
Instrument Pointing	Nadir $\pm 0.8^\circ$	Nadir $\pm 0.20$ (spec 3)
Pointing Knowledge	Nadir $\pm 0.6^\circ$	Nadir $\pm 0.10$ (spec 3)
Data Rate	$\sim 17$ kbps*	665.4 kbps
Uplink Rate	$\sim 1$ kbps	1 kbps
On-Board Storage	$\sim 10^9$ bit	$4.5 \times 10^8$ bit/ transport (10 transports)
Oscillator Stability	TBD	1 part in $10^8$ /day
*See Table 2-1		

## SECTION 3.0

### MISSION ANALYSIS

#### 3.1 ASTEROID RENDEZVOUS OPPORTUNITIES

On grounds of mission energetics, frequency of opportunity, and low rendezvous velocity, as well as scientific interest, the near-Earth asteroids are the most likely targets for asteroid rendezvous missions in the near future.<sup>1</sup> Within this class of asteroids are the Aten/Apollo/Amor (AAA) objects.

Computer searches for low energy, two- and three-impulse transfers have been made by astrodynamacists. Lists containing 72 opportunities for delivering a 600-kg class spacecraft to near-Earth asteroids between 1988 and 1996, using the STS/IUS Two-Stage or STS/IUS Two-Stage/Star 48, have been presented by Hulkower.<sup>2,3</sup>

The most easily accessible of these bodies is the recently discovered 1982 DB. There is a hesitancy, however, among planetary scientists and astronomers over the orbit elements of any asteroid until observations have been made on at least two passes of the Earth; after that, the asteroid is named. Unnamed asteroids, therefore, were excluded from the list of candidate base line targets in the current study. Of the remaining easily accessible named asteroids, Alinda, Amor, Anteros, Anza, Bacchus, Beltrovata, Eros, and Ivar emerge as candidates for minimal-propulsion missions (see Section 3.2).

Summary characteristics of these low energy transfers to Anteros and Eros, with launches between 1987 and 1992, are presented in Tables 3.1-1 and 3.1-2. The 1987 launch opportunity to Anteros has been described by Hulkower and Ross.<sup>4</sup> Summary characteristics of the transfers to 1982 DB<sup>5</sup> are shown in Table 3.1-3 in order to indicate other easier opportunities, the details of which will be refined on the next passage of the Earth by this asteroid.

The present study was restricted to the examination of one-way missions to asteroids. Multiple, asteroid rendezvous missions using ballistic propulsion and solar electric propulsion strategies as well as sample-return missions are quite feasible, but more complex. At the present time, it is more appropriate to plan one-way missions for spacecraft that remain as close as possible to the forms of the current Earth orbiters from which they could be derived.

#### 3.2 MISSION SELECTION

The STS will be the only available launch system capable of providing the required launch energy for asteroid rendezvous missions in the frame of reference of the current study.

The launch geometry for STS-launched missions to asteroids is illustrated in Figure 3.2-1. The Earth departure energy,  $C_3$ , is the same as the square of the departure hyperbolic excess velocity, which vector lies along the launch asymptote. It may be seen from Figure 3.2-1, that for any coplanar injection, the declination of the launch asymptote, DLA, and the inclination of the Shuttle park orbit,  $I$ , satisfy the relationship:

$$-I \leq DLA \leq I$$

TABLE 3.1-1. SUMMARY OF MISSIONS TO ANTEROS, LAUNCHING 1987-1992\*

Launch Date	6/1/87	5/22/90	5/25/92
Flight Time (days)	430	699	513
Arrival Date	8/4/88	4/19/92	10/20/93
$C_3$ ( $\text{km}^2/\text{s}^2$ )	29.2	35.1	31.9
DLA ( $^\circ$ )	50.6	25.8	38.8
Total Post-Launch $\Delta V^{**}$ (m/s)	1588	1225	1012
<p>*Within capability of 600-kg class spacecraft injected by IUS Two-Stage or IUS Two Stage/STAR 48 upper stage</p> <p>**Excluding <math>\Delta V</math> allowance for navigation and orbit sustenance</p>			

TABLE 3.1-2. SUMMARY OF MISSIONS TO EROS, LAUNCHING 1987-1996\*

Launch Date	1/25/89	1/26/96
Flight Time (days)	681	696
Arrival Date	12/7/90	12/22/97
C <sub>3</sub> (km <sup>2</sup> /s <sup>2</sup> )	40.3	40.9
DLA (°)	-56.8	-55.9
Total Post-Launch ΔV (m/s)	1636	1771

\*Within capability of 600-kg class spacecraft injected by IUS Two-Stage or IUS Two Stage/STAR 48 upper stage

\*\*Excluding ΔV allowance for navigation and orbit sustenance

TABLE 3.1-3. SUMMARY OF MISSIONS TO 1982 DB, LAUNCHING 1988-1998

Launch Date	2/5/88	1/9/89	1/26/91	1/21/91	1/25/93	1/31/95	1/7/96	1/26/96	2/4/97	1/9/98
Flight Time (days)	420	662	282	471	570	498	761	860	426	670
Mid-Course Date	8/2/88	None	None	8/8/91	8/19/93	9/18/95	None	None	8/4/97	None
Arrival Date	4/1/89	11/2/90	11/5/91	5/6/92	8/19/94	6/11/96	2/6/98	6/4/98	4/6/98	11/10/99
C <sub>3</sub> (km <sup>2</sup> /s <sup>2</sup> )	5.3	26.6	24.8	22.3	17.3	11.5	32.2	31.4	5.7	27.0
DIA (°)	-20.6	-13.2	-16.3	-16.1	-19.9	-20.7	-12.8	-19.5	-21.0	-13.2
Total Post-Launch $\Delta V^*$ (m/s)	2869	803	249	266	871	1695	1315	1252	2774	843
*Excluding $\Delta V$ allowance for navigation and orbit sustenance										

ORIGINAL PAGE 18  
OF POOR QUALITY

ORIGINAL PAGE IS  
OF POOR QUALITY

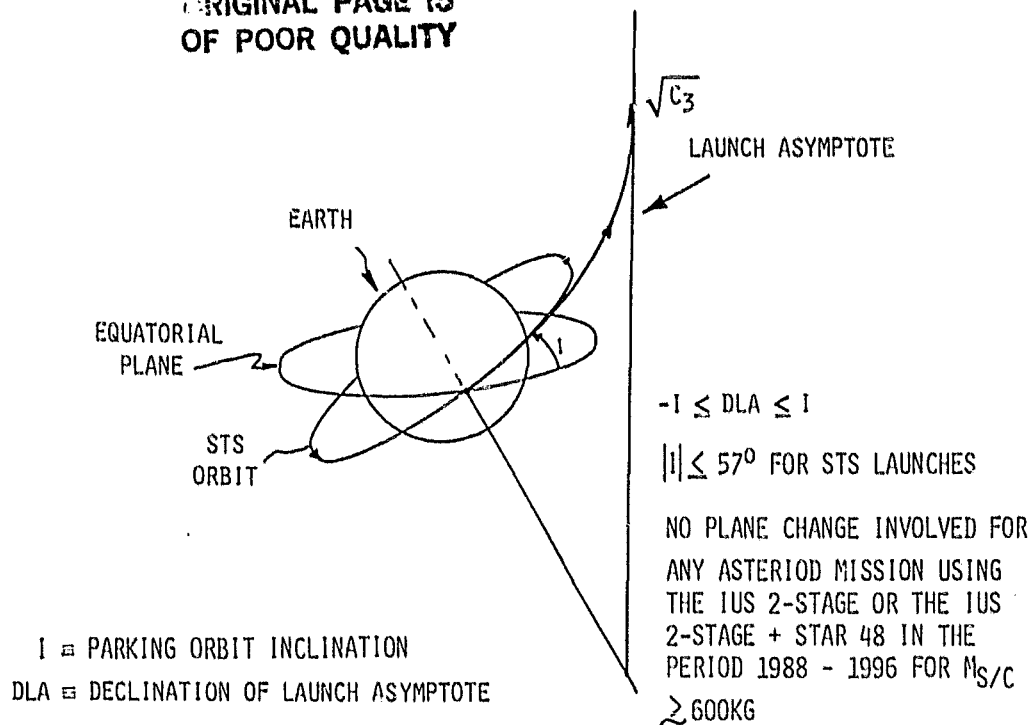


Figure 3.2-1. STS Launch Geometry

In this study it is assumed that the Shuttle will be capable of achieving an orbit inclination as high as  $57^\circ$ , i.e., that  $I \leq 57^\circ$ , which implies  $-57^\circ \leq DLA \leq 57^\circ$ . It is found, accordingly, that all known potential missions to the near-Earth asteroids during the period 1988-1996 using the STS/IUS Two-Stage or STS/IUS Two-Stage/Star 48 launch systems with a 600-kg class spacecraft could be accomplished using co-planar STS park orbits and upper stage injections.

The selection of feasible missions, together with their respective launch systems and post-launch propulsion systems, may be performed simultaneously through inspection of Figures 3.2-2 through 3.2-7. These figures are plots of the individual rendezvous  $\Delta V$  requirements for each of the missions listed by Hulkower,<sup>2,3</sup> and Hulkower and Ross,<sup>4</sup> together with curves of the rendezvous  $\Delta V$  capability of spacecraft whose mass is in the range of 400-750 kg (excluding propulsion system), all versus the launch energy,  $C_3$ .

There are three pairs of figures, corresponding to:

- 1) An integrated hydrazine on-board propulsion system
- 2) An integrated bipropellant on-board propulsion system
- 3) A hybrid (solid rendezvous motor plus on-board hydrazine) system

The first one of each pair of figures covers the years 1988-1990 and also includes the 1987 launch to Anteros. The second of each pair covers the years 1991-1996.

On each of Figures 3.2-2 through 3.2-7, there are two families of three curves. The higher triplet corresponds to the IUS Two-Stage/Injection Module (IM), the lower triplet to just the IUS Two-Stage. Within each triplet, the higher



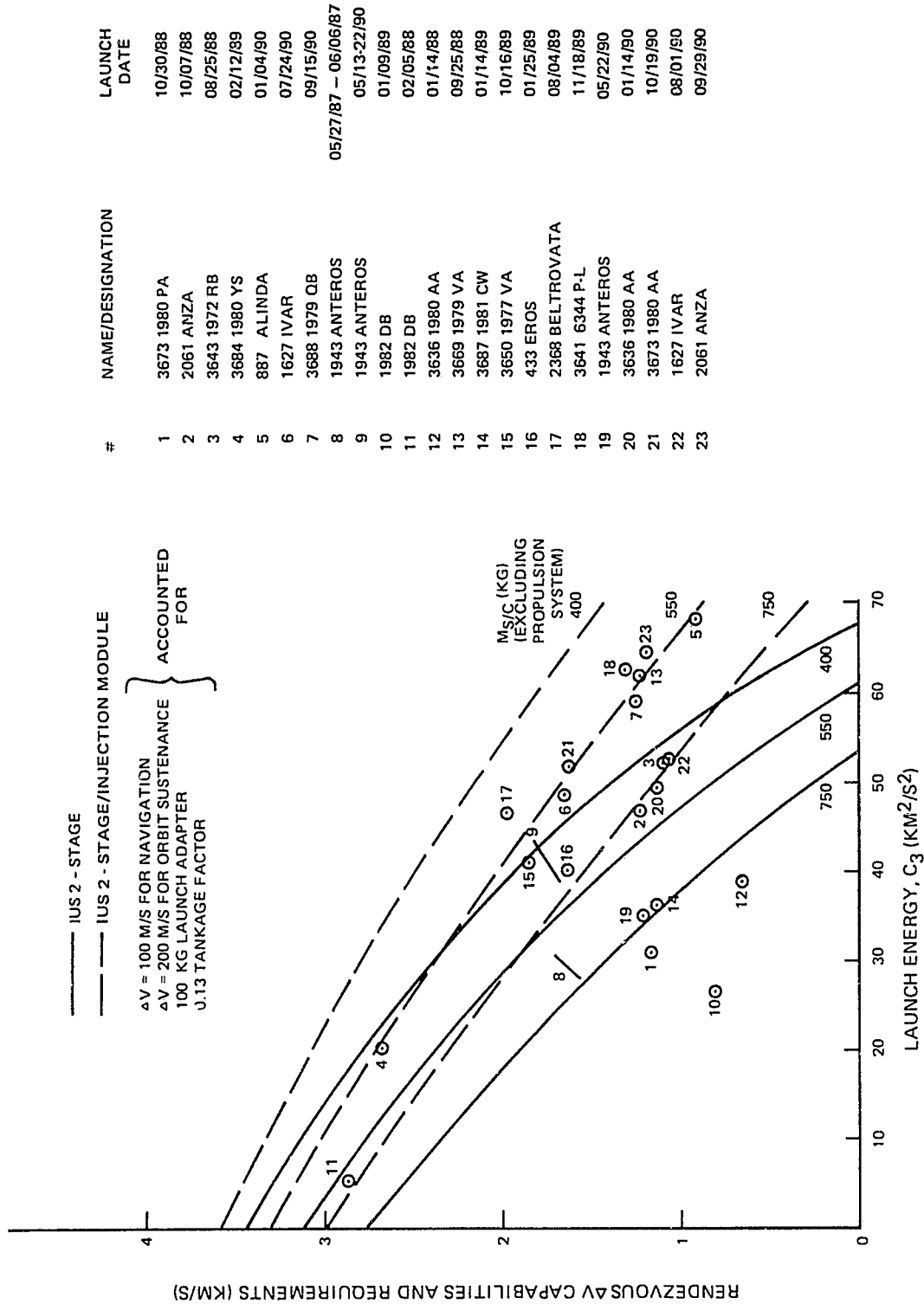


Figure 3.2-2. Rendezvous with Near-Earth Asteroids with Launch Dates in 1988-1990, plus Anteros 1987 Launch (Integrated Hydrazine Propulsion System)

ORIGINAL PAGE IS  
OF POOR QUALITY

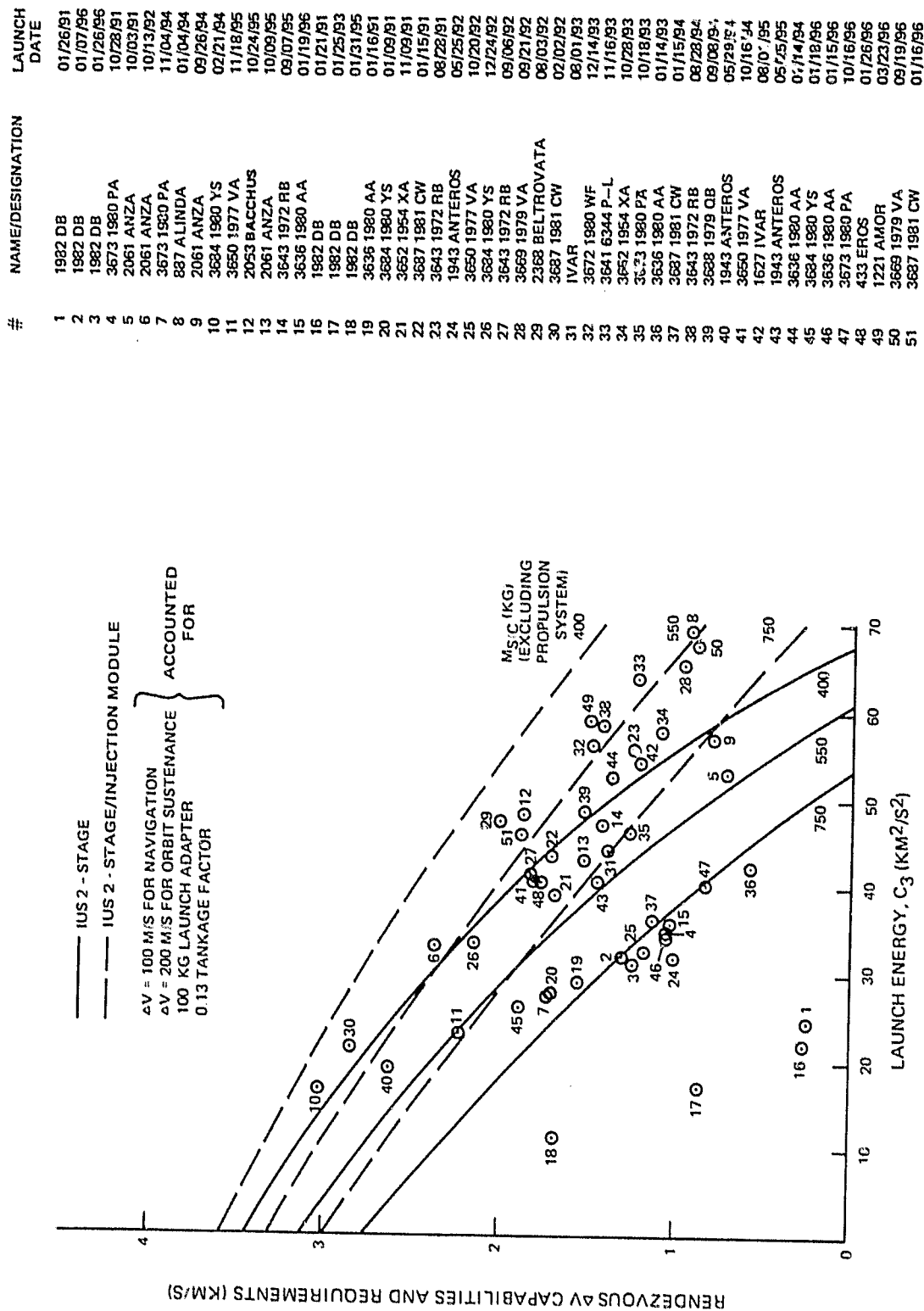


Figure 3.2-3. Rendezvous with Near-Earth Asteroids with Launch Dates in 1991-1996 (Integrated Hydrazine Propulsion System)

ORIGINAL PAGE IS  
OF POOR QUALITY

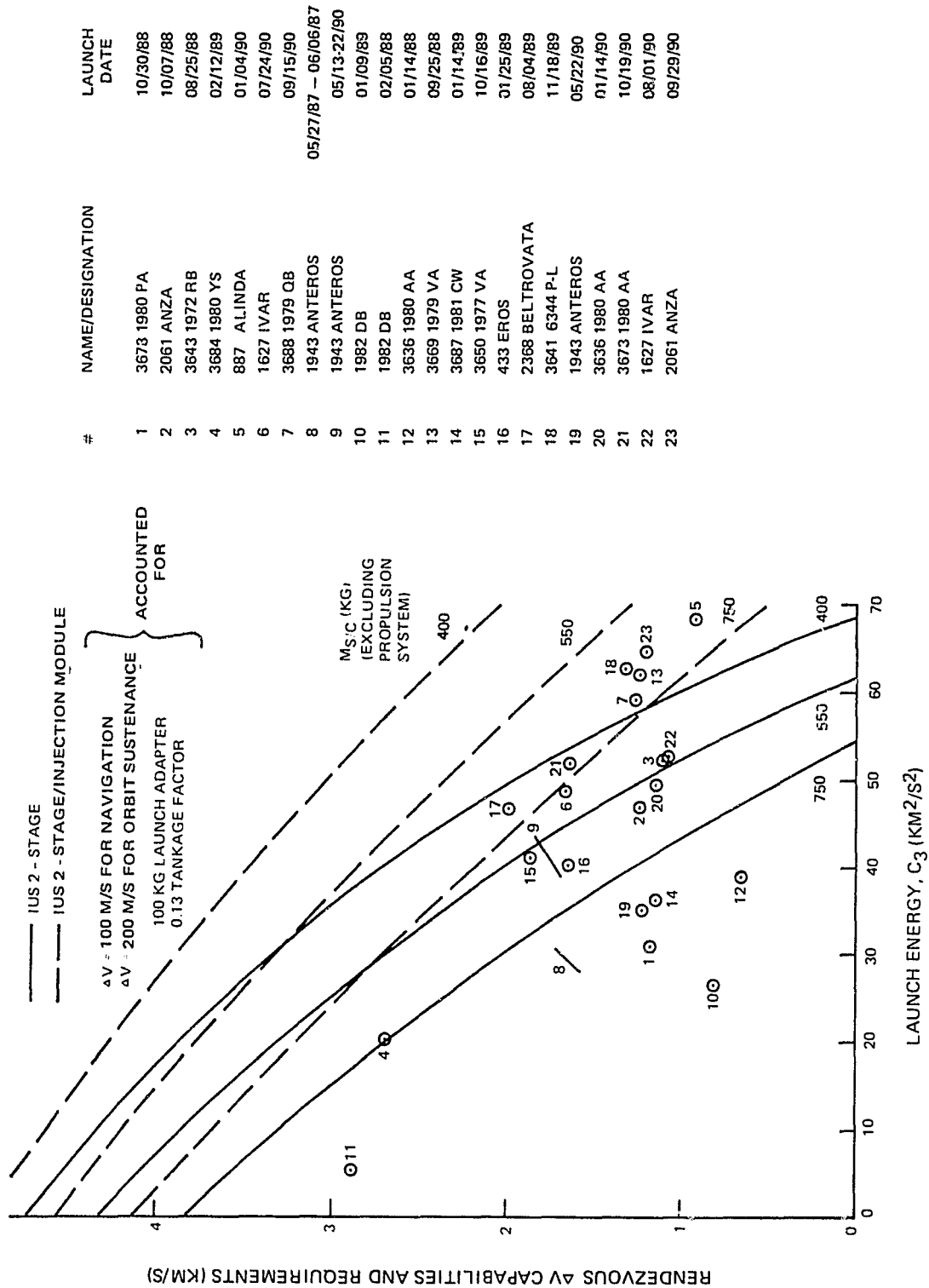


Figure 3.2-4. Rendezvous with Near-Earth Asteroids with Launch Dates in 1988-1990, plus Anteros 1987 Launch (Integrated MMH-NTD Propulsion System)

ORIGINAL PAGE IS  
OF POOR QUALITY.

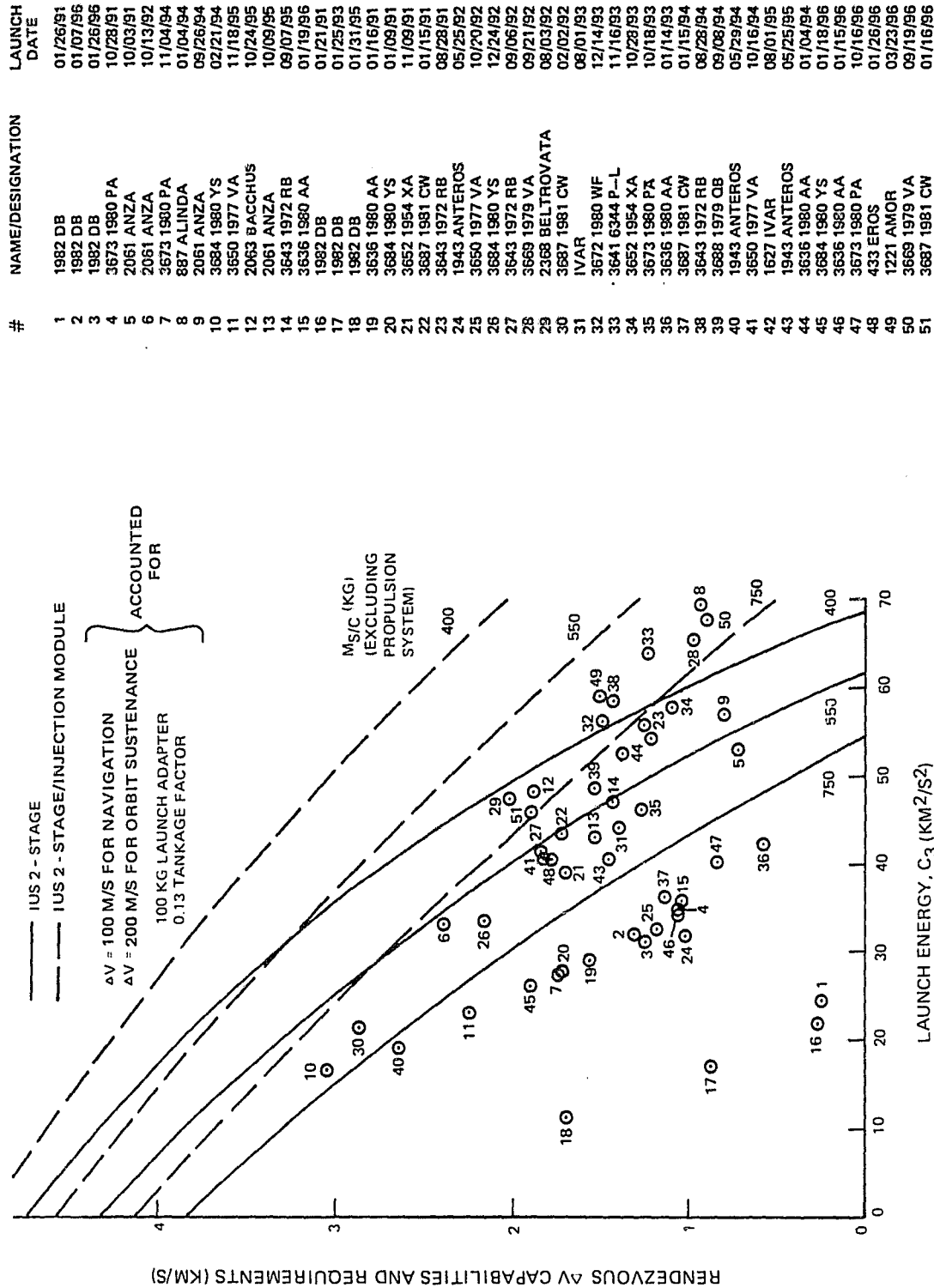


Figure 3.2-5. Rendezvous with Near-Earth Asteroids with Launch Dates in 1991-1996 (Integrated MMH-NTO Propulsion System)

ORIGINAL PAGE IS  
OF POOR QUALITY

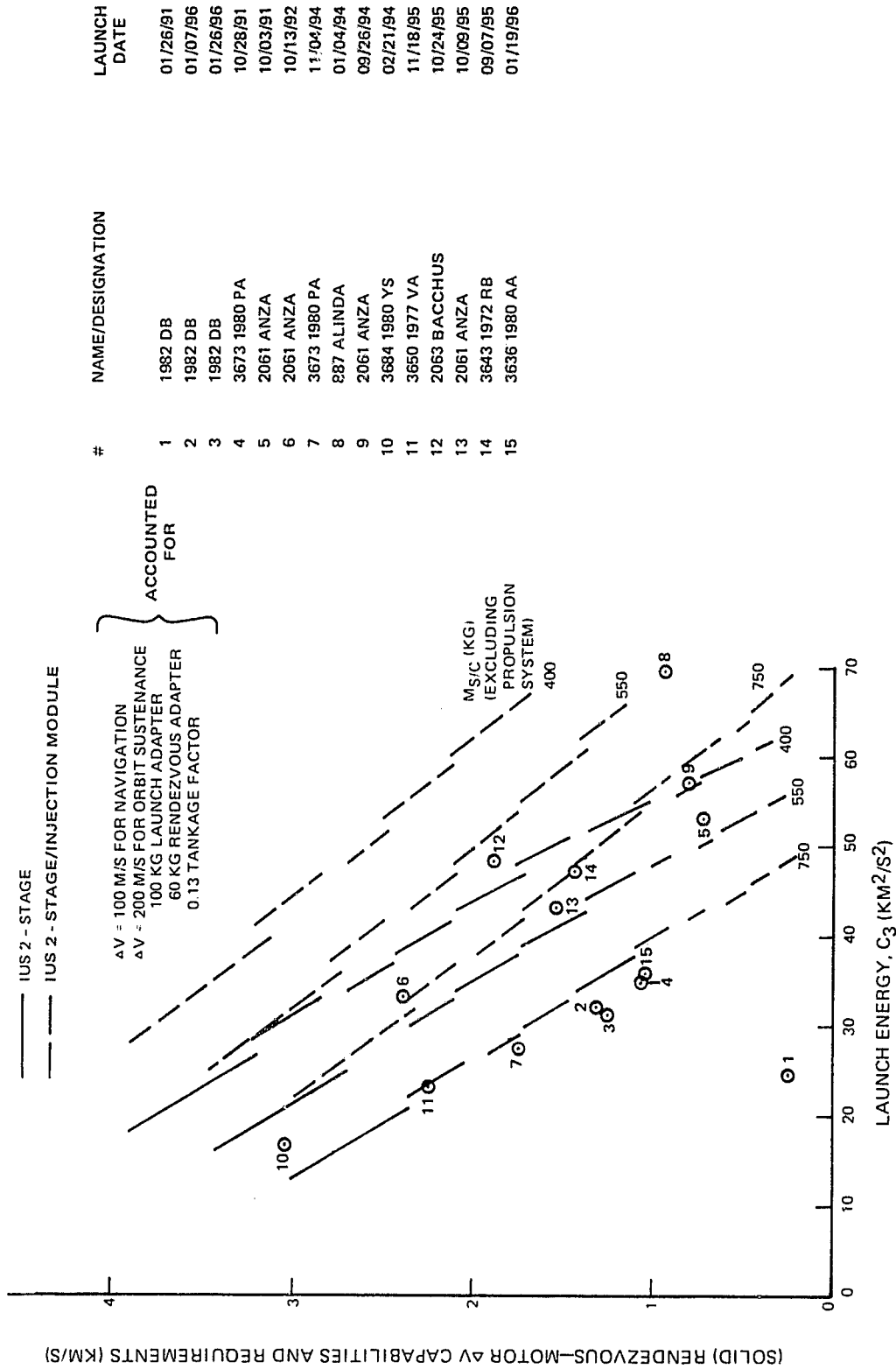


Figure 3.2-6. Rendezvous with Near-Earth Asteroids with Launch Dates in 1988-1990, plus Anteros 1987 Launch (Solid Rocket for Rendezvous Maneuver, Hydrazine System for Navigation and Orbit Sustenance)

ORIGINAL PAGE IS  
OF POOR QUALITY

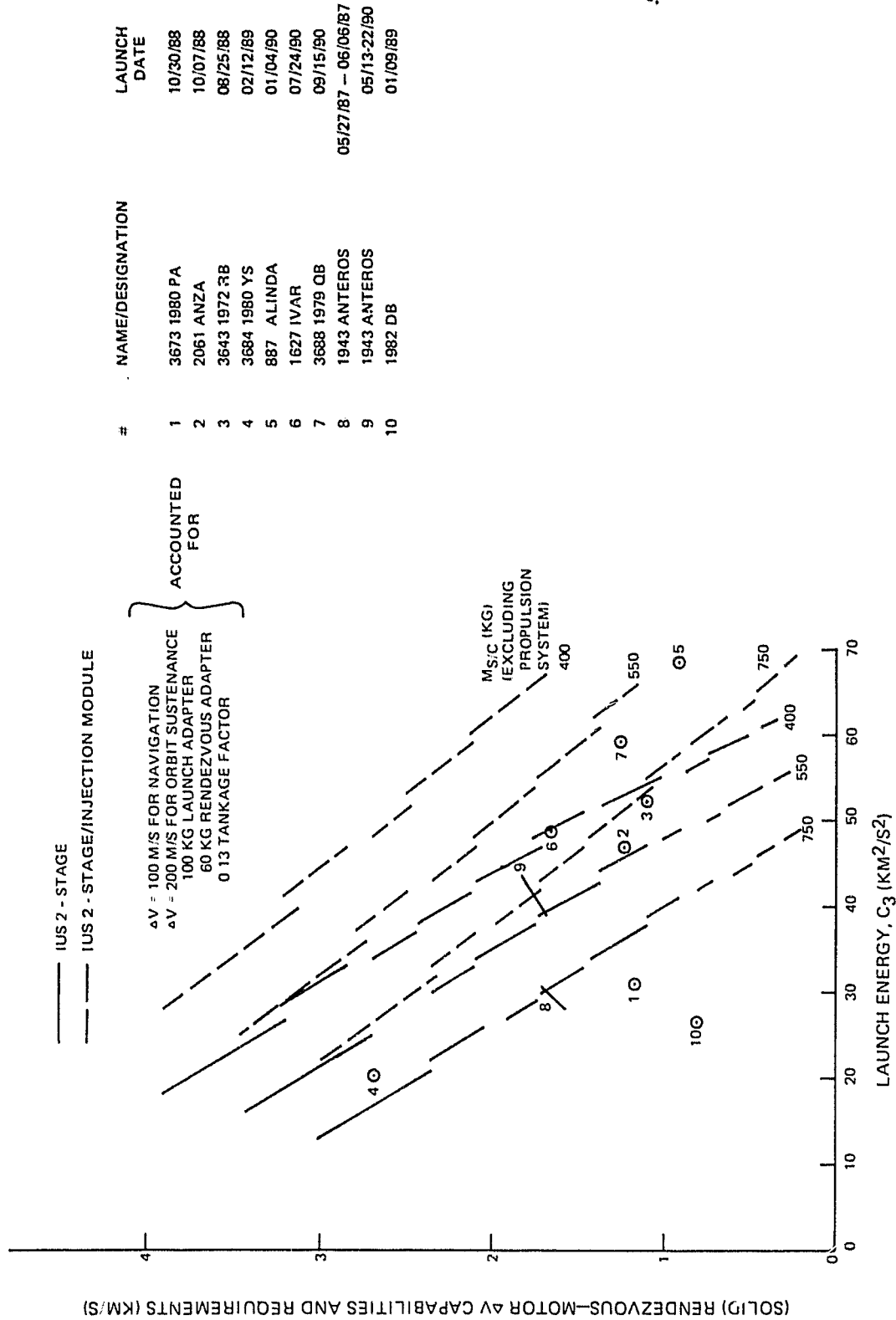


Figure 3.2-7. Rendezvous with Near-Earth Asteroids with Launch Dates in 1991-1996 (Solid Rocket for Rendezvous Maneuver, Hydrazine System for Navigation and Orbit Sustenance)

curve corresponds to a spacecraft mass of 400 kg, the median to 550 kg, and the lower to 750 kg.

The discontinuous nature of the curves in Figures 3.2-6 and 3.2-7 corresponds to the differences in characteristics within the family of available, or potentially available, Thiokol Star rocket motors. These are, in diminishing order, the Star 48, 37XE, 37E, 37F, 37S, 30B, 27, 26C, and 24.

In calculating each curve, very generous allowances were made when taking into account influencing factors. The on-board liquid propulsion system was assumed to provide a  $\Delta V$  of 100 m/s for purposes of trajectory corrections, i.e., navigation, and also 200 m/s for mission maneuvers and orbit sustenance following the rendezvous burn at the asteroid. In calculating the mass of the on-board liquid propulsion system, a tankage factor of 0.13 was allowed; this is considered realistic for pressure-regulated systems using Kevlar tanks and helium as pressurant. In addition, the launch adapter was very conservatively sized at 100 kg, which for spacecraft masses (excluding the propulsion system) of 400, 550, and 750 kg represents factors of 0.25, 0.18, and 0.13. For the hybrid propulsion system, the spacecraft-to-rendezvous motor adapter was sized at 60 kg.

The values given for total post-launch  $\Delta V$  by Hulkower<sup>2,3</sup> contained 0.115 km/s to cover navigation and orbital sustenance. This allowance was subtracted from Hulkower's values before they were plotted in Figures 3.2-2 through 3.2-7.

In these figures, the points representing the rendezvous  $\Delta V$  requirements for the individual missions are numbered in order to aid in identification.

The two two-impulse transfers to Anteros, one in 1987 and one in 1990, show up on the plots as spread lines rather than points since fuller data, covering a 10-day launch window, were available for these opportunities.

The all liquid, on-board propulsion systems allow multiple burn Earth-to-asteroid transfers. The plots for these propulsion systems, Figures 3.2-2 through 3.2-5, accordingly, show more mission opportunities, 74, than do the plots for hybrid propulsion systems, Figures 3.2-6 and 3.2-7. The latter are necessarily restricted to include only the 25 of these mission opportunities that feature two-burn transfer, since the solid rocket can obviously be fired only once, and the on-board liquid capability is generally too small for the performance of a significant mid-course maneuver.

The planetary performance capabilities of the IUS Two-Stage and the IUS Two-Stage/IM are shown in Figure 3.2-8. The term "throwmass", as used here, includes all mass above the IUS interface, i.e., includes the launch adapter mass. These two performance curves are also shown in Figure 3.3-1.

Since the mass of the base line spacecraft (excluding the propulsion system) is 500 kg, Figures 3.2-2 through 3.2-7 may be read easily to select feasible missions to the preferred named asteroids. It may be seen that, under the assumptions made using the IUS/Two-Stage and an integrated hydrazine system, launches with high margins to named asteroids are feasible to Anteros (1987, 1990, 1992, and 1995) and Anza (1991). Use of the IUS Two-Stage/IM would make additional missions with margins possible to Alinda (1990, 1994), Anteros (1994), Anza (1988, 1990, 1992, 1994, and 1995), Bacchus (1995), Eros (1989, 1996),

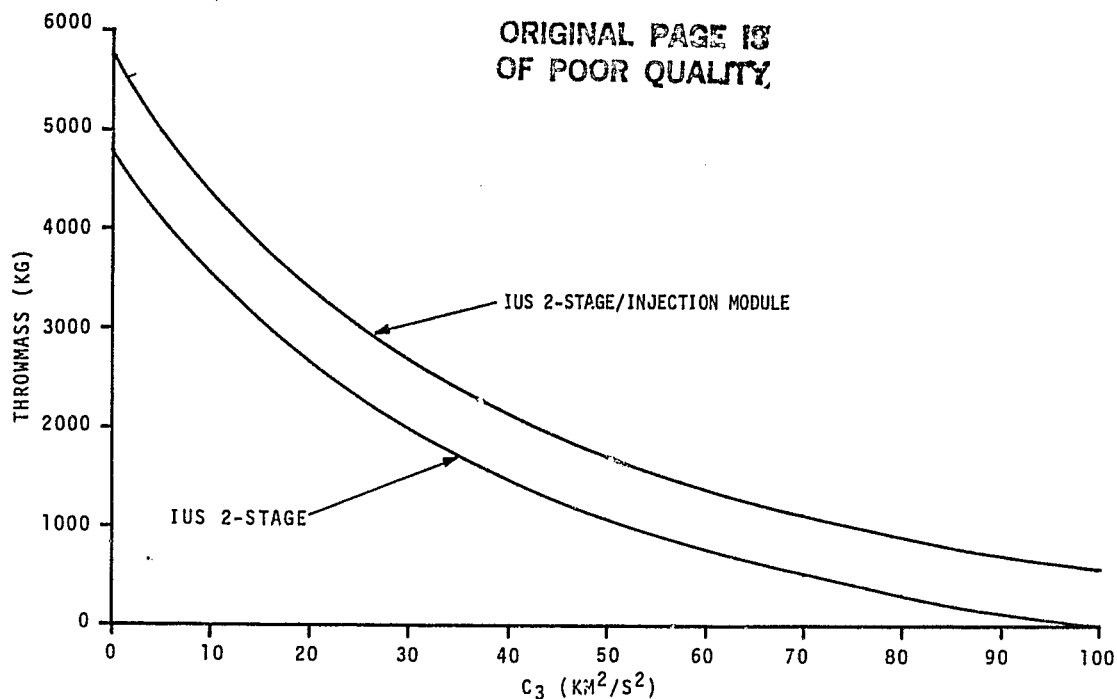


Figure 3.2-8. IUS Planetary Performance

and Ivar (1990, 1993). Only slight improvements or relaxations in the assumptions made are necessary to bring within reach Amor (1996) and Beltrovata (1989, 1992) while still maintaining good throw-mass margins.

Use of the IUS two-stage and an integrated bipropellant system (MMH plus NTO) would allow high margin missions to Anteros (1987, 1990, 1992, 1994, 1995), Anza (1988, 1991, 1992, 1994, and 1995), Eros (1989, 1996), and Ivar (1990, 1993). Use of the IUS Two-Stage/IM would give extremely high throw-mass margins for all of the listed opportunities.

The IUS Two-Stage used with a hybrid propulsion system allows high throw-mass margin missions to Anteros (1987, 1990) and Anza (1988, 1991, 1995), and use of the IUS Two-Stage/IM would allow additional high margin missions to Alinda (1990, 1994), Anza (1992, 1994), Bacchus (1995), and Ivar (1990).

If the unnamed asteroids shown in Figures 3.2-2 through 3.2-7 were considered suitable targets, then the list of potential candidate missions would clearly be doubled or tripled.

A further clear advantage of all-liquid propulsion systems is that they allow reallocation of the impulsive thrust budget within the total capability; one propulsion subsystem design may therefore be used for any one of several missions.

### 3.3 NEAR-TERM CANDIDATE MISSIONS TO ANTEROS OR EROS

Since Anteros is the most easily reached named asteroid, it is high on the list of candidates for the first mission. Eros is also relatively easily reached compared with most asteroids. It is also more interesting and larger (estimated at approximately 10 x 36 km) than Anteros, which is estimated to be about 2.3 km in diameter.



It is instructive to examine the propulsion mass breakdown for at least one of these missions. This is presented for Anteros, launching in 1987, in Table 3.3-1. The starting points for the table are the throwmasses of the IUS Two-Stage and of the IUS Two-Stage/IM, both for a launch energy,  $C_3$ , of  $30.5 \text{ km}^2/\text{s}^2$ , which corresponds to the last day, 6 June 1987, of a 10-day launch window to Anteros. The mass of the end-of-life spacecraft is then developed for hybrid (solid plus monopropellant), monopropellant, and bipropellant propulsion systems, taking into account the masses of the launch adapter and the propellant for mid-course corrections, for rendezvous, and for orbit sustenance. Information concerning the mass breakdown between the spacecraft payload and the on-board propulsion system has not been included in the table.

There is currently some preference towards basing the spacecraft on the TIROS/DMSF spacecraft and making as few changes as possible from the current flight designs of these spacecraft. An on-board propulsion system featuring hydrazine as propellant, nitrogen as pressurant, and existing tank designs has therefore been investigated further. Helium was also investigated as pressurant in order to estimate the potential for weight savings.

For the purposes of preliminary parametric sizing calculations, certain approximations concerning the propulsion system were made. These were:

- 1) Helium pressurant mass =  $0.012 \times$  hydrazine mass
- 2) Nitrogen pressurant mass =  $0.079 \times$  hydrazine mass
- 3) Propulsion system hardware mass =  $0.168 \times$  hydrazine mass  
(approximates to the use of existing Ti propellant tanks and existing Kevlar pressurant tanks)

Subsequent detailed propulsion system sizing has shown these assumptions to be conservative. In this way, preliminary estimates of the throwmass were calculated for the four near-term candidate opportunities to Eros and Anteros. The results are shown in Table 3.3-2. More accurate masses for the components of the propulsion systems for these opportunities, obtained from a reiteration, are presented in Table 5.2-2, and in certain cases the differences between the use of helium and nitrogen are not so profound. The results shown in Table 3.3-2 are accurate enough for preliminary planning purposes. Being mainly conservative, they may be used directly since any newfound margin will probably be used up in carrying a small amount of extra pressurant to compensate for leakage (especially with helium) and in allowing for growth of the payload.

In Figure 3.3-1, the throwmass results on the bottom line of Table 3.3-2 are shown plotted together with the planetary performance curves for existing and potential STS upper stages. As in Figures 3.2-2, 3.2-4, and 3.2-6, the 1987 launch opportunity to Anteros shows up as two spread lines rather than two points since data were available for conditions at the opening and closing of a 10-day launch window. It may be seen from Figures 3.3-1 and Table 5.2-2 that the IUS-1 is capable of all three Anteros missions and, at the high values of  $C_3$  involved ( $> 28 \text{ km}^2/\text{s}^2$ ), actually outperforms the IUS Two-Stage which is handicapped by the great mass of its avionics. For the Eros mission, however, it appears that one of the currently conceptual combinations of the IUS-1/PAM-D, IUS-1/IM, and IUS Two-Stage/IM would be necessary.

It is worthwhile stressing here that these results correspond to the greatest possible application of TIROS hardware and technology, substituting other cur-

TABLE 3.3-1. PROPULSION MASS BUDGET FOR ANTEROS RENDEZVOUS MISSION,  
LAUNCHING 5/27/87-6/6/87

Inertial Upper Stage	IUS Two-Stage			IUS Two-Stage/ Injection Module		
	N <sub>2</sub> H <sub>4</sub> Solid	N <sub>2</sub> H <sub>4</sub>	MMH + NTO	N <sub>2</sub> H <sub>4</sub> Solid	N <sub>2</sub> H <sub>4</sub>	MMH + NTO
Propulsion Sub-System Type						
IUS Throwmass (kg) For C <sub>3</sub> = 30.5 km <sup>2</sup> /s <sup>2</sup>	1970	1970	1970	2650	2650	2650
IUS-S/C Adapter (kg)	80	80	80	80	80	80
Heliocentric Transfer Assembly (kg)	1890	1890	1890	2570	2570	2570
Propellant for Trajectory Corrections (kg) ( $\Delta V$ = 100 m/s)	82	82	63	112	112	86
Asteroid Arrival Assembly (kg)	1808	1808	1827	2459	2459	2484
Propellant for Rendezvous Maneuver (kg) ( $\Delta V$ = 1711 m/s)	821*	961	805	1117**	1307	1095
Post-Rendezvous Assembly (kg)	987	847	1021	1342	1152	1389
Propellant for Mission Maneuvers (kg) ( $\Delta V$ = 200 m/s)	84	72	67	114	98	91
End-of-life Assembly*** (kg)	903	775	954	1228	1054	1298
*5% off-loaded Star 37F **16% off-loaded Star 37XE ***Includes propulsion hardware and solid motor adapter (where applicable)						
<ul style="list-style-type: none"> <li>• 10-Day launch window (5/27/87 - 6/6/87)</li> <li>• Correct DLA achieved without plane change by upper stage</li> <li>• Isp N<sub>2</sub>H<sub>4</sub> = 2256.3 m/s (230s)</li> <li>• Isp MMH + NTO = 2943 m/s (300s)</li> <li>• Propellant tanks made from Ti 6Al-4V. Safety factor of 1.5 on yield</li> <li>• Helium tanks made from Kevlar with metallic liner. Safety factor of 2.0 on yield</li> <li>• Nominal He tank temperature of 20°C</li> <li>• He tank operating pressure 3600 psia</li> <li>• Propellant tank operating pressure = 230 psia</li> <li>• For the all liquid propulsion subsystems, the current STAR 37 thrust tube will be used to accommodate new tankage.</li> <li>• All systems pressure regulated throughout entire life. Reduction in helium tankage mass feasible using more unusual pressurization methods, such as helium tank heating or limited pressure regulation cycles</li> </ul>						

TABLE 3.3-2. PARAMETRICALLY DERIVED ESTIMATES OF THE ON-BOARD  
PROPULSION SUBSYSTEM MASS BUDGETS FOR FOUR NEAR-TERM  
CANDIDATE ASTEROID RENDEZVOUS MISSIONS

Target	Anteros				Eros
Launch Date	5/27/87	6/6/87	5/22/90	5/25/92	1/25/89
Total Post-Launch $\Delta V$ (m/s)	1888	2011	1525	1312	1936
Pressurant Type	He N <sub>2</sub>	He N <sub>2</sub>	He N <sub>2</sub>	He N <sub>2</sub>	He N <sub>2</sub>
Propellant Mass (kg)	856 967	970 1115	585 634	460 490	899 1022
Propulsion Hardware Mass (kg)	144 163	163 187	98 107	77 82	151 172
Pressurant Mass (kg)	10.3 76.0	11.6 88.0	7.0 50.0	5.5 39.0	10.8 81.0
Charged Propulsion System Mass (kg)	1010.3 1206.0	1144.6 1390.0	690.0 791.0	542.5 611.0	1060.8 1275.0
EOL Spacecraft Mass (kg)	654 739	675 776	605 657	583 621	662 753
Launch Adapter Mass (kg)	100 100	100 100	100 100	100 100	100 100
Throw Mass (kg)	1610 1806	1745 1991	1290 1391	1142 1211	1661 1875
<ul style="list-style-type: none"> <li>• Mass of spacecraft (excluding propulsion subsystem) = 500 kg</li> <li>• Hydrazine propellant (Isp = 2256.3 m/s, i.e., 230s)</li> <li>• Helium mass = 0.012 x hydrazine mass</li> <li>• Nitrogen mass = 0.079 x hydrazine mass</li> <li>• Mass of available titanium propellant tanks plus Kevlar pressurant tanks = 0.216 x hydrazine mass</li> </ul>					

ORIGINAL PAGE 19  
OF POOR QUALITY

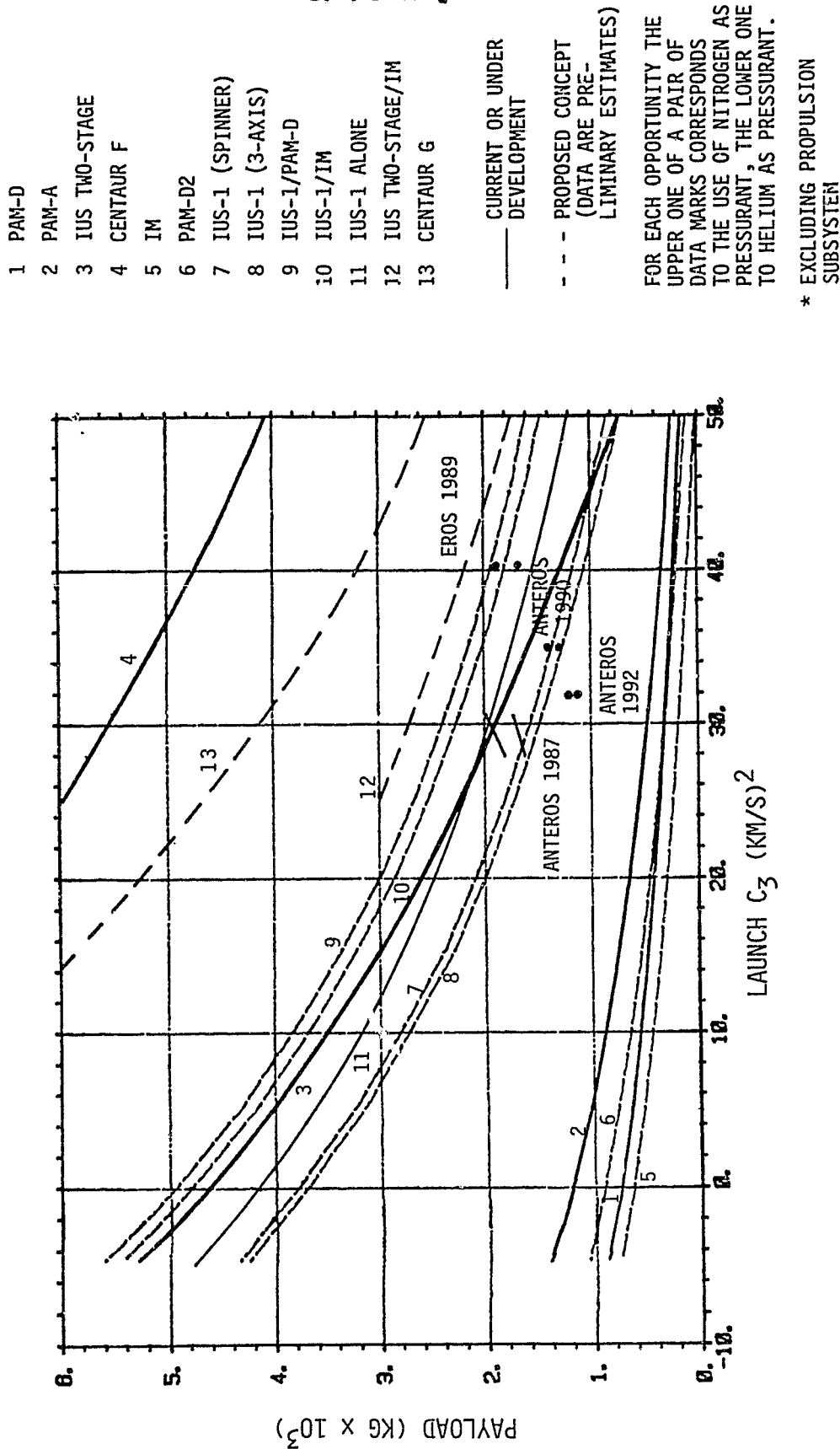


Figure 3.3-1. Match of STS Upper Stages with Throwmasses for Four Near-Term Candidate Asteroid Rendezvous Missions (for a 500-kg\* Class TIROS-Based Spacecraft Using Available Titanium Hydrazine Tanks and Kevlar Pressurant Tanks)

rently available hardware and currently practised technology only when necessary. The use of custom designed, Kevlar tanks throughout the propulsion system, would result in drastic reductions in the calculated throwmasses, with correspondingly improved margins in the matching of the throwmasses with the performance capabilities of STS upper stages.

The use of an unguided motor such as the IUS-1 is attractive for this base line mission since, by taking full advantage of the guidance and control avionics and thrusters of the TIROS spacecraft, the payload capability of the motor for any mission would be maximized. In that case, the IUS-1 would be held inertially in three axes, the TIROS thruster arms having been optimized for this purpose. A further benefit would be the minimizing of subsequent propellant requirements for launch vehicle error correction.

Of the four near-term candidate missions described here, only the 1990 launch to Anteros may be performed using the standard STS park-orbit inclination of  $28.6^\circ$  since the required DLA for this mission is lower, at  $25.8^\circ$ , whereas the range of DLA for the other three missions is from  $38.8^\circ$  to  $56.8^\circ$ . It is immediately clear, therefore, that the 1990 launch to Anteros could be achieved starting with a shared STS launch. Since the other three missions feature such high values of DLA, it seems unlikely that any other spacecraft would be found such that both missions could utilize a coplanar launch with the orbital inclination  $\geq$  DLA. However, if the likely STS upper stages (i.e., the IUS-1 for the 1990 and 1992 Anteros missions and the IUS Two-Stage/IM or IUS/Two-Stage/ PAM-D for the 1989 Eros launch) are used, the margin in  $C_3$  capability for the respective throwmasses, as shown in Figure 3.3-1, may be utilized to effect a plane change. By this means, a shared STS launch might be manifested more easily for the 1992 Anteros launch and the 1989 Eros launch. Figure 3.3-1 indicates that the  $C_3$  margins are  $\sim 10 \text{ km}^2/\text{s}^2$  and  $20 \text{ km}^2/\text{s}^2$ , respectively. This may be seen from Figure 3.3-2<sup>6</sup> to be translatable into plane changes of  $\sim 8^\circ$  for both launches. Thus the 1992 Anteros launch could be commenced from an STS park orbit at  $\sim 31^\circ$  inclination and the 1989 Eros launch from an STS park orbit at  $\sim 49^\circ$  inclination. These inclinations, unfortunately, are still not low enough to improve drastically the compatibility of the missions with shared STS launches, and it seems likely that these three missions would feature dedicated STS launches.

### 3.4 LAUNCH PHASE

Detailed designs of the STS ascent and park orbits will determine the flight sequence for the launch phase. The STS profile should be designed to enable adequate tracking coverage of the powered flight, to provide for suitable landing sites and contingency requirements, to allow injection through to a suitable launch asymptote and within the launch window, and possibly to satisfy constraints imposed by a shared STS launch.

The requirements on the inclination of the STS park orbit have already been discussed in Section 3.2. The orbit has been assumed to be circular at 296 km altitude.

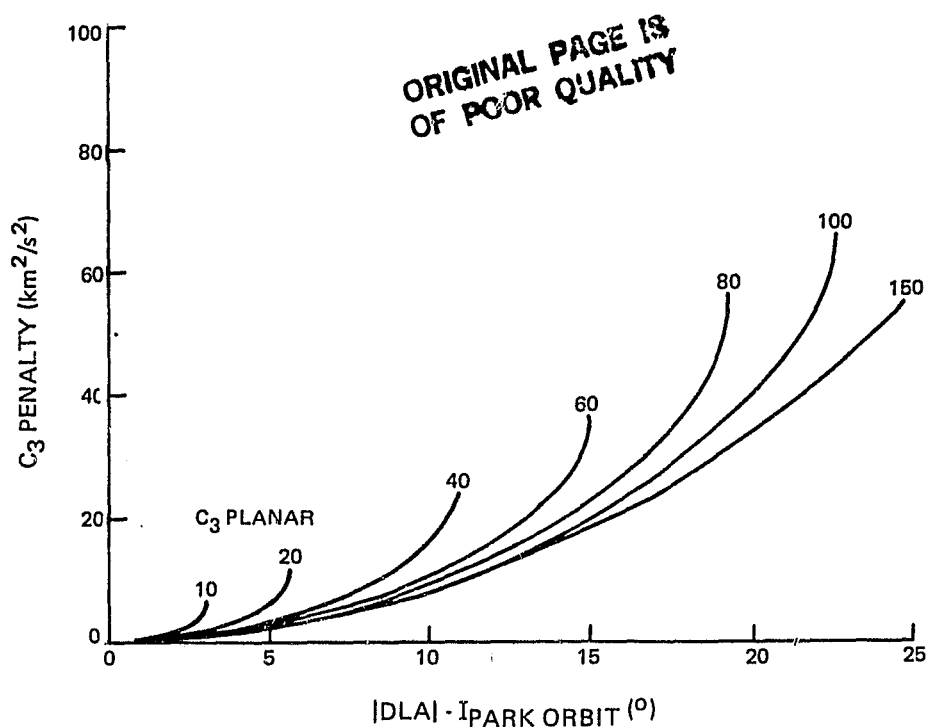


Figure 3.3-2. Change in  $C_3$  for  $|DLA| > \text{Parking Orbit Inclination}$  for 240-280 km Altitude Circular Parking Orbit

At the earliest opportunity, the stack of spacecraft and upper stage will be released from the Shuttle in an orientation as close as possible to that required at ignition.

The base line mission for this study is to Anteros, launching in 1987. As shown earlier, the launch vehicle for this mission is likely to be the IUS-1, and this will be three-axis controlled by the spacecraft. There will be a coast period following separation from the Shuttle in order to achieve safety clearance separation from the Shuttle, and during this time the spacecraft will accurately align the stack. Active control of the stack by the spacecraft will continue through to upper stage burnout and separation.

### 3.5 EARTH TO ASTEROID TRANSFER

During launch, the solar array will be stowed wrapped around the electronics support module (ESM), often called "the doghouse" because of its shape. After separation from the STS upper stage, the solar array will be partially deployed to lie in a plane along the apex of the doghouse. The spacecraft yaw axis will then be reoriented towards the Sun. In this way, adequate solar power generation through the transfer phase will be assured. The solar array will be held solidly enough to survive, fully intact and functional, the acceleration and vibration of the midcourse and rendezvous maneuvers performed by the four 100-lb<sub>f</sub> hydrazine thrusters.

The Sun-spacecraft range during the four near-term candidate transfers to Eros and Anteros, discussed in Section 3.3, is shown in Figures 3.5-1 through 3.5-4. These figures show several pertinent geometrical histories during the Earth-to-asteroid transfer phase. In the chase diagrams, the Earth's position is shown for only one year from the starting date of the launch.

It may be seen that during two of the three-burn transfers, those to Eros launching in 1989 and to Anteros launching in 1990, the spacecraft will actually travel farther away from the Sun than the aphelion of the target asteroid. The maximum Sun-spacecraft distance during these two transfers is approximately the same, at  $\sim 1.95$  AU.

Attitude control during the transfer phase is described in Section 5.3. Communications during the transfer phase is described in Section 5.5. Relevant geometries shown in 3.5-1 through 3.5-4 are the communications distance, the Sun-Earth spacecraft angle, the Sun-spacecraft-Earth angle, and the Sun-spacecraft-asteroid angle.

It may be seen from these figures that the maximum communications distance during transfer is  $< 3$  AU for all four near-term candidate missions. The central angles traveled around the Sun are in the range of approximately  $270$ - $370^\circ$ . Conjunction of the Sun and the spacecraft as seen from the Earth, and of the Sun and the Earth as seen from the spacecraft, either does not occur or occurs in the middle of the four transfers shown here. Therefore, there is no problematical interference with communications by the Sun for these four base line missions. Optical tracking of the asteroid by the CCD imager on board the spacecraft during the latter part of the transfer is also seen to be free from solar interference.

It has been calculated that  $\sim 4$  kg of gaseous nitrogen must be expelled by the attitude control system to keep the solar array facing the Sun during the transfer phase. This allocation has an insignificant effect on the gas-tankage requirements of the propulsion system. For example, as shown in Table 3.3-2, it has been estimated that approximately 88 kg of  $\text{GN}_2$  will be required for the mission to Anteros launching in 1987. An additional 4 kg of  $\text{GN}_2$  will have little impact on the pressurant tank size and on the launch throwmass, which is estimated at 1991 kg.

During the transfer phase, several targeting maneuvers will have to be made to correct for previous burn and navigation inaccuracies. In the preliminary propulsion sizing, a generous allowance of 100 m/s was allowed for these maneuvers. For the candidate Eros mission, and the Anteros missions launching in 1990 and 1992, there will also be a large propulsive maneuver carried out in mid-transfer. The spacecraft will be oriented to achieve the correct thrust vectors for large maneuvers and afterwards reoriented into the sunbathing orientation, with the yaw axis of the spacecraft pointing towards the Sun. Depending upon the actual location of the high gain antenna (HGA) on the spacecraft, temporary reorientations of the spacecraft might be necessary for communications at high data rates, e.g., for science instrument checkout. Communications are otherwise through the omni antenna.

The transfer times for the four near-term candidate missions range from 430 to 699 days, as shown in Tables 3.1-1 and 3.1-2.

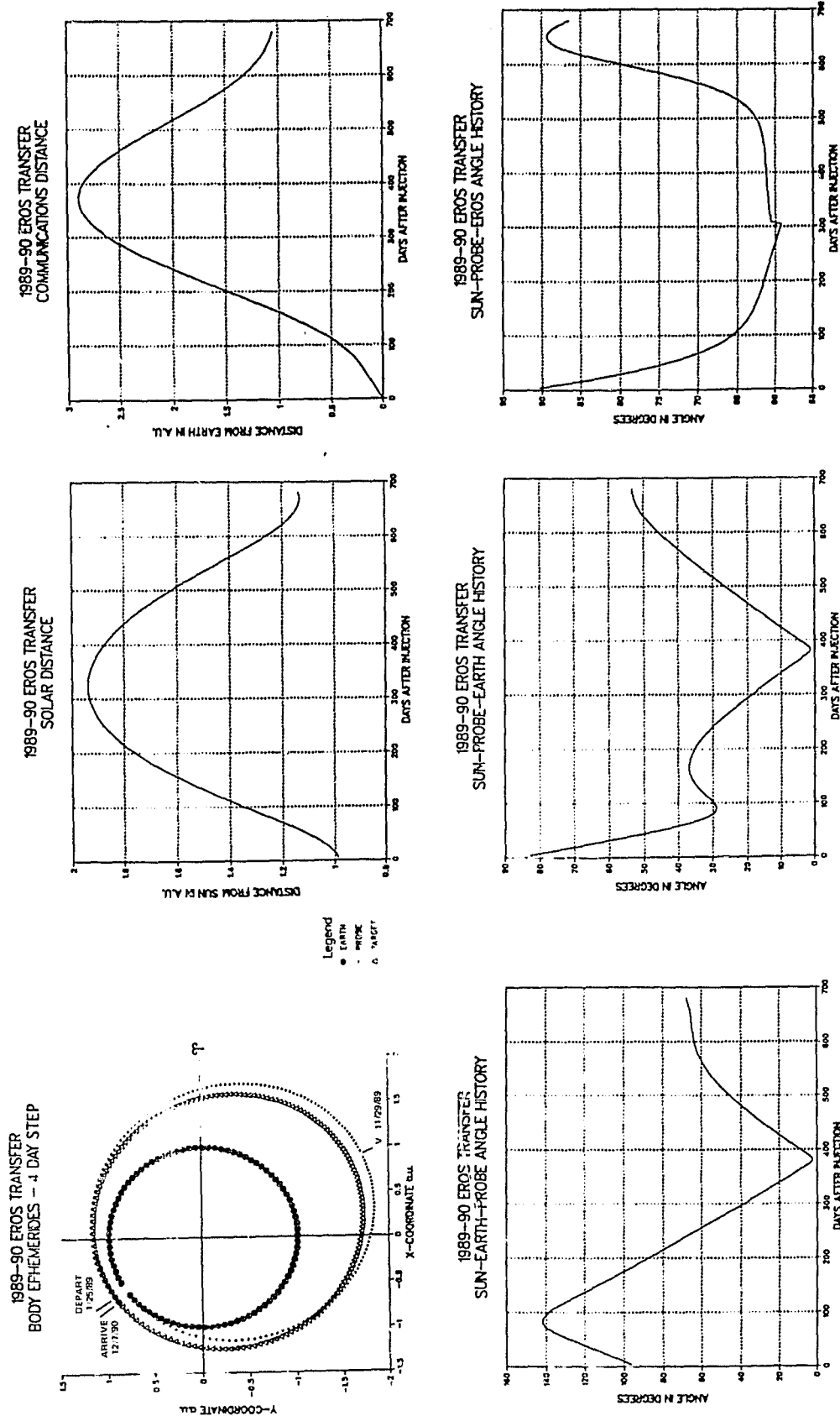


Figure 3.5-1. Eros Transfer Geometry - 1989 Launch



ORIGINAL PAGE NO  
OF POOR QUALITY

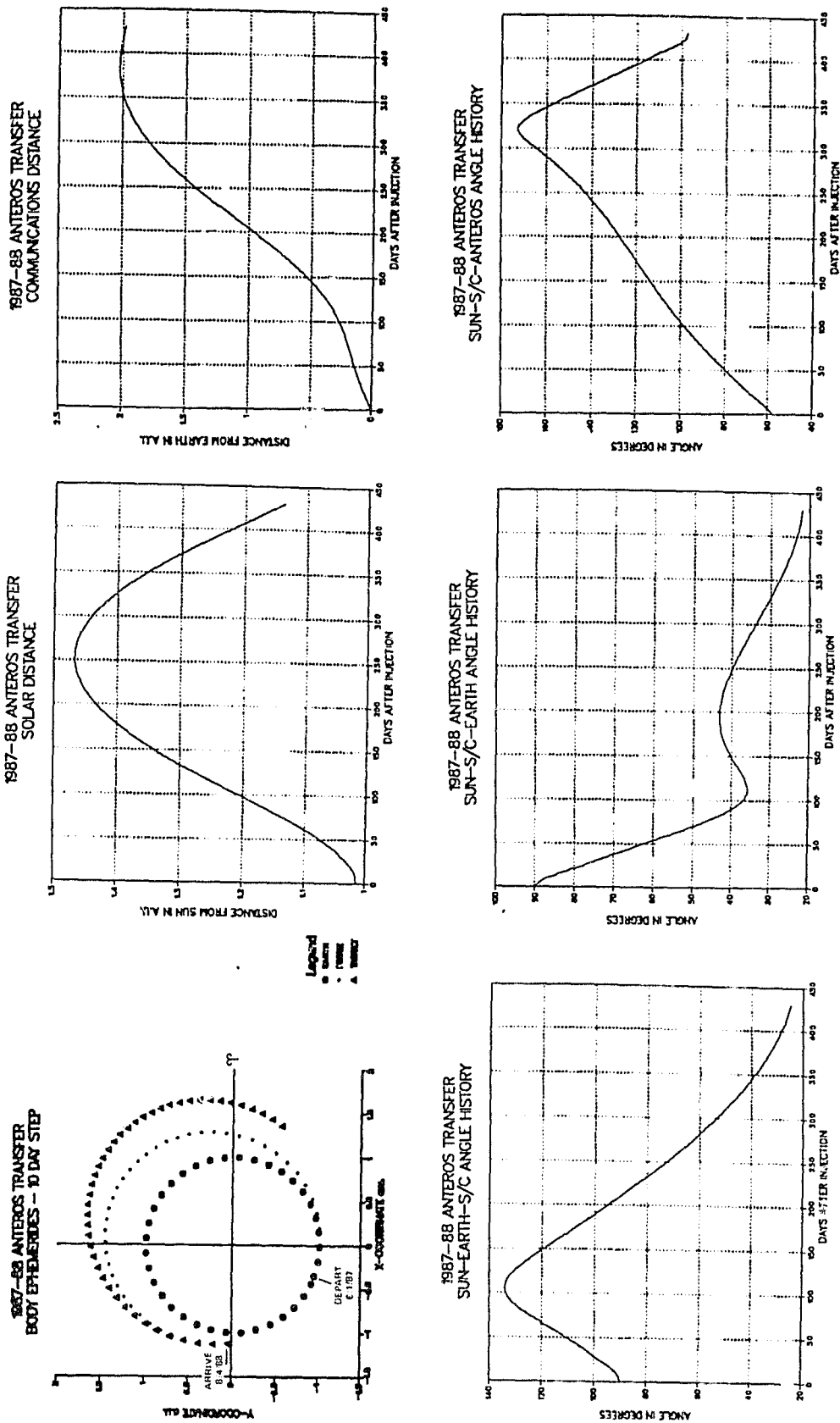


Figure 3.5-2. Anteros Transfer Geometry - 1987 Launch

ORIGINAL PAGE IS  
OF POOR QUALITY

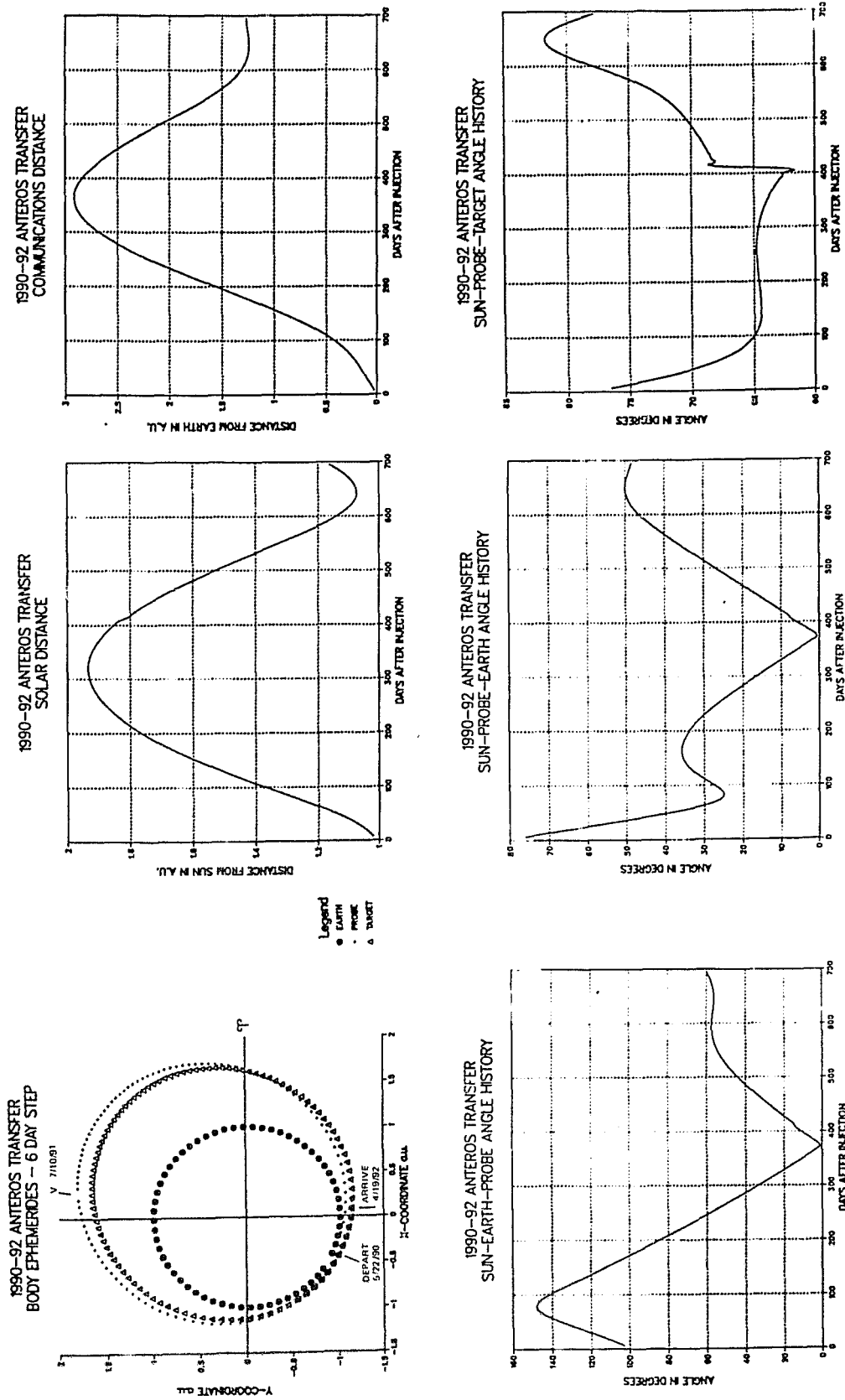


Figure 3.5-3. Anteros Transfer Geometry - 1990 Launch

ORIGINAL PAGE IS  
OF POOR QUALITY

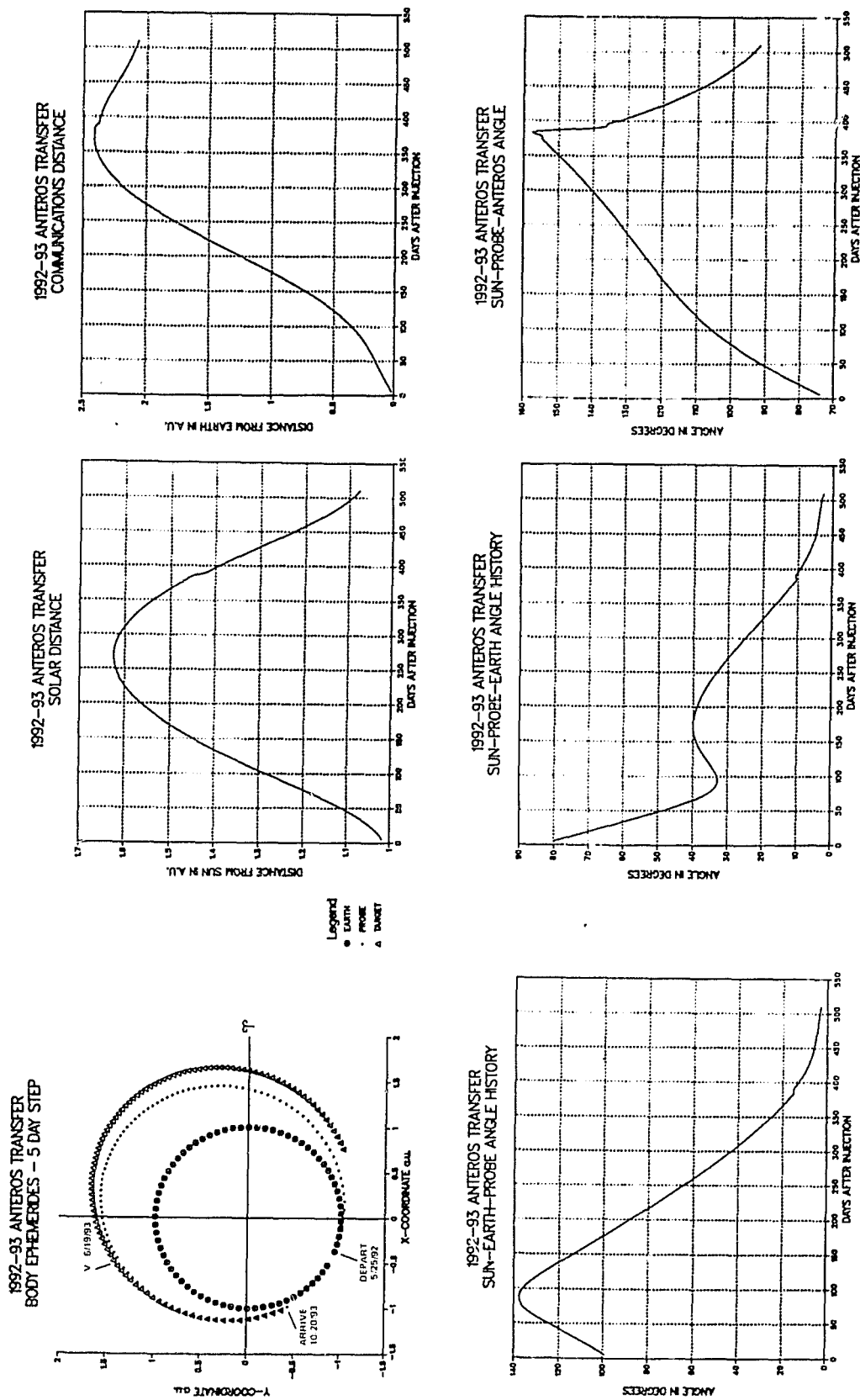


Figure 3.5-4. Anteros Transfer Geometry - 1992 Launch

It is interesting to note that for all four candidate missions the rendezvous occurs close to the asteroid perihelion. The spacecraft-Sun distance, therefore, generally increases from this minimum for the first year after rendezvous.

### 3.6 RENDEZVOUS AND ORBIT INITIALIZATION

Several hours before arrival at the nominal mid-course and/or rendezvous point(s), the spacecraft will be oriented so that the four 100-lb<sub>f</sub> hydrazine thrusters are aligned with the correct direction for the maneuver. Since these thrusters are mounted aligned with the roll axis, it will be possible to keep the partially deployed solar array pointed approximately towards the Sun even during these major-maneuver phases. Of the four near-term candidate missions presented here, the transfers to Anteros with launches in 1987 and 1992 will require boost rendezvous maneuvers, whereas, the remaining two transfers will require retro rendezvous maneuvers. The mid-course and rendezvous maneuvers will be performed on ground command. If a liquid propulsion system is used, these maneuvers may be performed very accurately by making incremental burns monitored on the Earth.

For the base line mission to Anteros launching in 1987, the size of the rendezvous maneuver is 1599 m/s. The other three of the four near-term candidate missions of Section 3.3 (to Anteros launching in 1990 and 1992, and to Eros launching in 1989) feature three-impulse transfers. The magnitudes of the mid-course and rendezvous maneuvers for these three missions are 615 and 610, 519 and 493, and 1094 and 542 m/s, respectively. It may be seen, therefore, that all of these burns are equally significant.

Since it is intended that the spacecraft will carry a CCD imager, the asteroid will have been located by this imager several weeks or months in advance of the rendezvous. By this means, a very close rendezvous indeed should be achievable. A worst case of 6000-km initial separation has been considered and presents no problems, while providing the benefit of a slow subsequent approach for the purposes of an observatory phase (see Section 3.6.1). At a distance of 6000 km, Anteros would be the brightest object visible apart from the Sun. Rendezvous at some such large separation will allow background measurements to be made by the gamma ray spectrometer (GRS) and the magnetometer (MAG), following the rendezvous maneuver and deployment of their booms but before close approach of the asteroid.

Two approach- and orbit-strategies have been investigated by computer numerical methods, one for Anteros and one for Eros. In these simulations, the motion of the spacecraft has been modeled as occurring in the planes of the orbits of these asteroids around the Sun. The equations of relative motion to be solved are:

$$\ddot{x} - 2n\dot{y} - 3n^2x = f_x \quad (1)$$

$$\ddot{y} + 2n\dot{x} = f_y \quad (2)$$

$$\ddot{z} + n^2z = f_z \quad (3)$$

ORIGINAL PAGE IS  
OF POOR QUALITY

**ORIGINAL PAGE IS  
OF POOR QUALITY**

where  $+x$  is in the direction from the Sun to the asteroid,  $+y$  is in the along-track direction,  $+z$  completes the right handed orthogonal set of axes,  $n$  is the angular rate of the asteroid around the Sun, and  $f$  is the acceleration of the spacecraft due to the asteroid (valid when  $f \ll$  solar gravity).

Generally, numerical integration must be employed to solve these equations, though when the gravitational pull of the asteroid is weak due to great distance or small size of the asteroid, the solutions for force-free drift are very nearly correct, i.e.:

$$x(t) = \frac{\dot{x}_0}{n} \sin nt - \left( \frac{2\dot{y}_0}{n} + 3x_0 \right) \cos nt + \frac{2\dot{y}_0}{n} + 4x_0 \quad (4)$$

$$y(t) = \frac{2\dot{x}_0}{n} \cos nt + \left( \frac{4\dot{y}_0}{n} + 6x_0 \right) \sin nt + \left( y_0 - \frac{2\dot{x}_0}{n} \right) - \left( 3\dot{y}_0 + 6nx_0 \right) t \quad (5)$$

$$z(t) = z_0 \cos nt + \frac{\dot{z}_0}{n} \sin nt \quad (6)$$

Summaries of the results of the two numerical simulations are presented below in Sections 3.6-1 and 3.6-2. The Anteros simulation is based on discussions with personnel at JPL. The Eros simulation is based on the strawman rendezvous scenario for the Mariner MK II mission. Both simulations involve orbital maneuvers about the asteroids. It will merely be stated now that non-orbital (e.g., stationkeeping) maneuvers in the close vicinity of asteroids of the size of Anteros ( $\sim 2.3$  km diameter) and Eros ( $\sim 10 \times 36$  km), and even orbital maneuvers near large asteroids such as Vesta, quickly exhaust the 200 m/s propulsive allowance assumed in this study for orbit sustenance and other post-rendezvous maneuvers and were considered impractical within the scope of this study.

### 3.6.1 ANTEROS RENDEZVOUS AND ORBIT INITIALIZATION

Rendezvous is initiated with the spacecraft nominally 6000 km ahead of the asteroid in its orbital path. For the base line mission to Anteros, this occurs on 4 August 1988, near asteroid perihelion, at a range of approximately 2 AU from the Earth. The spacecraft is reoriented, and the hydrazine engines are fired by ground command to cancel the relative velocity between the spacecraft and the asteroid. This requires a boost velocity increment of 1588 m/s for the base line 1988 Anteros rendezvous. A drift trajectory at 2.5 m/s towards the asteroid is commanded after the on-board imager data confirms that the relative velocity has been canceled. During the following 30 days of drift towards the asteroid, the imager provides: 1) navigational data, 2) identification of potential hazards, and 3) coarse mapping of the asteroid surface. The projection of the drift trajectory onto the orbit plane of Anteros is shown in Figure 3.6-1.

The initial drift trajectory is designed to have the spacecraft pass within 50 to 100 km of Anteros, either behind or in front of the asteroid as viewed from the Earth. The combination of Doppler, imager, and altimeter data will permit an accurate determination of the spacecraft trajectory and the mass of the asteroid during this initial fly-by. The drift trajectory is stopped at a range of approximately 200 km from the asteroid by firing the hydrazine thrusters to change the velocity by 4.38 m/s. This velocity is selected to start the spacecraft on the first leg of a sequence of zig-zag trajectories on the sun-

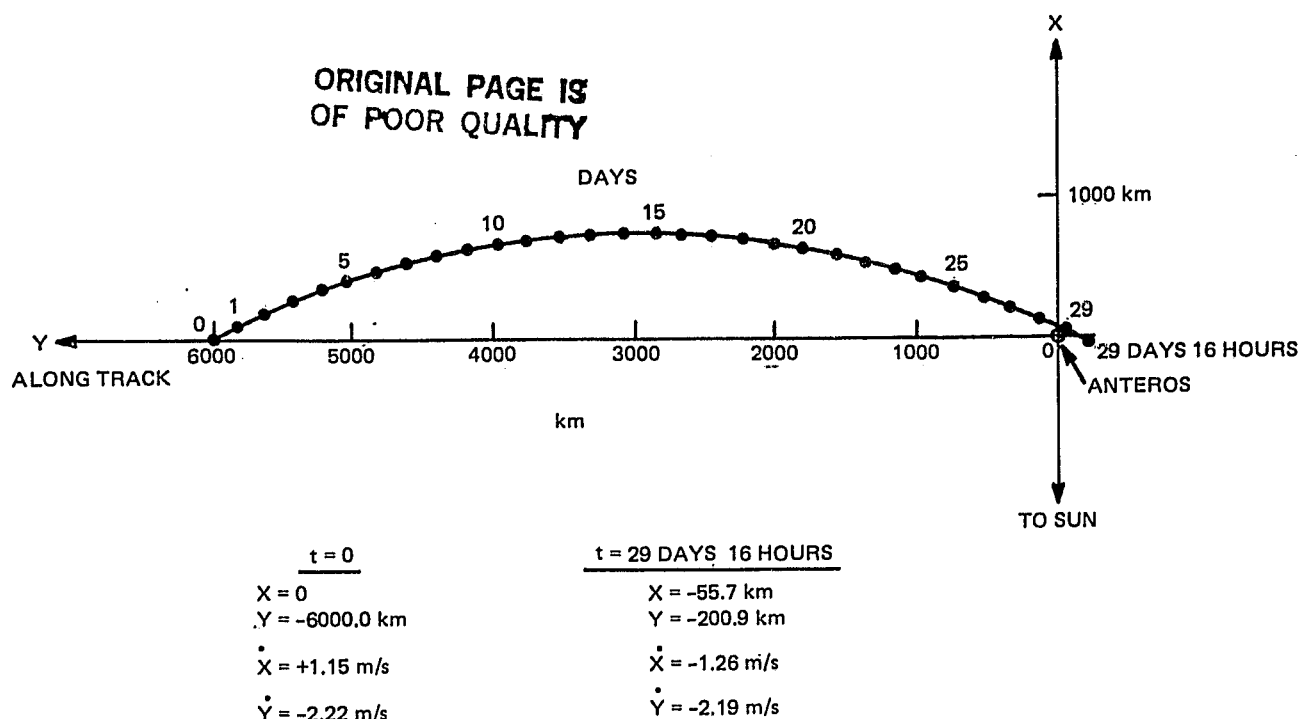


Figure 3.6-1. Rendezvous Drift Trajectory

ward side of the asteroid. Each succeeding trajectory leg lasts from one to two days and is initiated by a change in velocity of approximately 4 m/s. This series of maneuvers is designed to provide medium resolution mapping of the surface and final hazard evaluation so that the ground controllers can select the initial operational orbit. A sequence of three trajectory segments of this type are shown in Figure 3.6-2 although the actual number of such segments can be adjusted as required for mission safety.

At point D in Figure 3.6-2, a velocity change of 4.3 m/s is commanded as the first of a sequence of maneuvers to establish the initial operational orbit. Six hours later, at point E, a plane change maneuver of approximately 2 m/s is executed at a radius of 30 km. Final circularization at an operational radius of 10 km is achieved with a series of four thruster firings imparting a total  $\Delta V$  of 1.3 m/s. A summary of the  $\Delta V$  requirements, from rendezvous to the end of a one-year mission, is presented in Table 3.6-1. This includes 2 m/s for orbital precession to follow the Sun line. It also includes 3.4 m/s to permit one full revolution of the orbit plane for science accommodation. Correction of perturbations of a  $45^\circ$  inclined orbit for a 40 percent polar flattening of the asteroid would require 2.2 m/s.

### 3.6.2 EROS RENDEZVOUS STRAWMAN LOW ENERGY PROFILE

Rendezvous is initiated with the spacecraft nominally 23,740 km ahead of Eros along the orbital path. For the nominal mission, launching 25 January 1989, this occurs on 7 December 1990. The rendezvous  $\Delta V$  is 542 m/s, directed to slow the velocity around the Sun. The geometry of the situation is shown in Figure 3.6-3. The on-board CCD imager is used to confirm the cancellation of velocity relative to Eros.

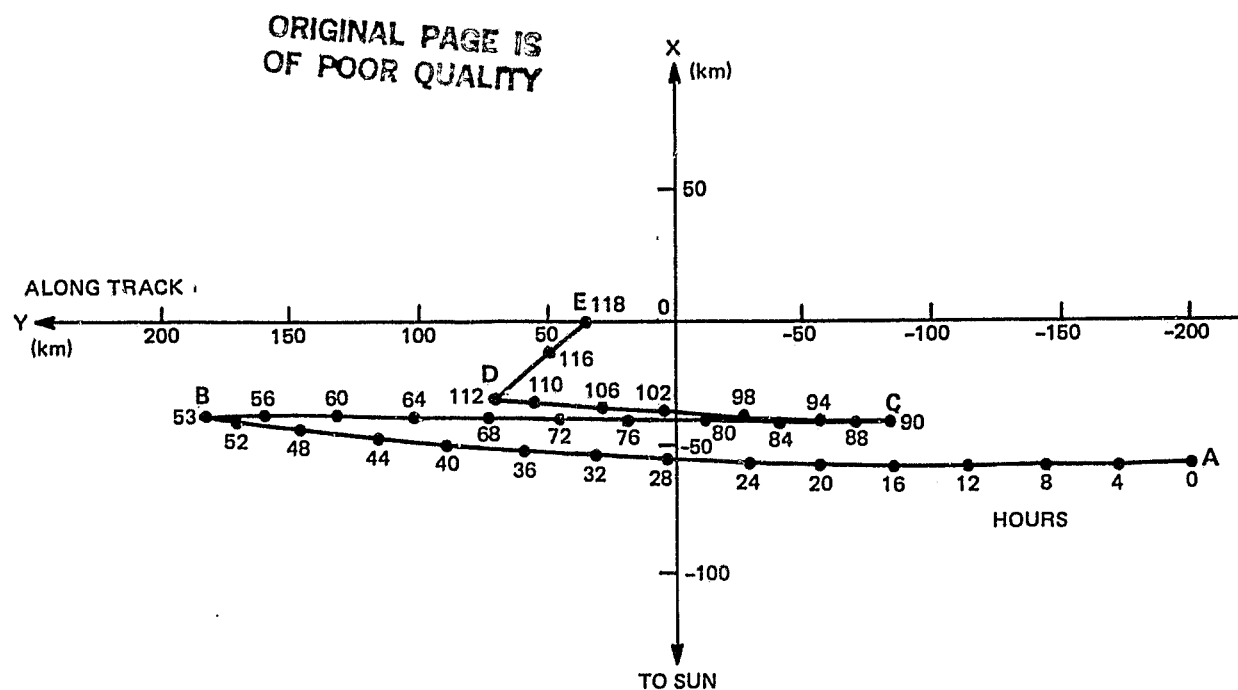


Figure 3.6-2. Rendezvous Final Approach Trajectories

TABLE 3.6-1. VELOCITY CHANGE REQUIREMENTS

Rendezvous	$\Delta V$ (m/s)
Initial Drift Velocity	2.5
Six Zig-Zag Maneuvers	24.0
Injection	4.3
Plane Change	2.0
Circularization	<u>1.3</u>
Subtotal	34.1
Operational Orbit	
Precession	2.0
Science Accommodation	3.4
Perturbations	<u>2.2</u>
Subtotal	<u>7.6</u>
Total	41.7

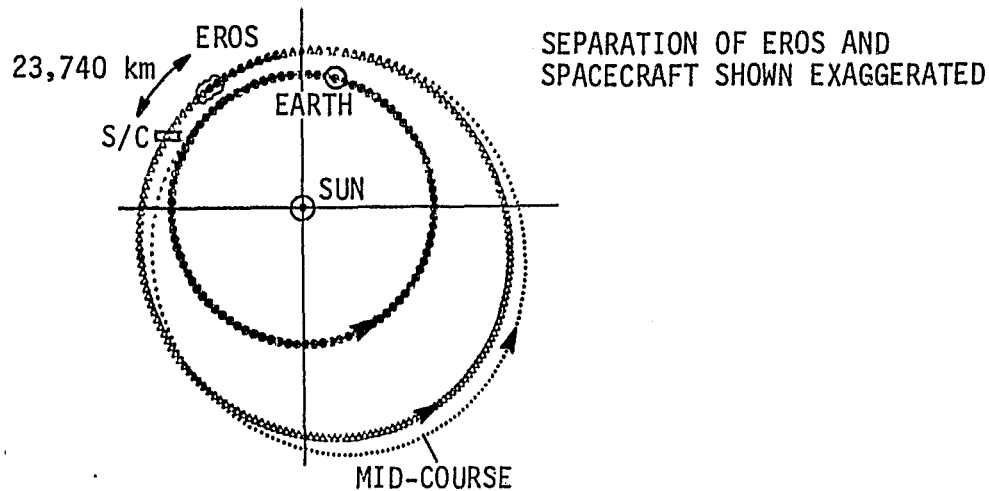


Figure 3.6-3. Geometry at Rendezvous Impulse for Mission to Eros, Launching 1989

A 90-day observatory phase is thus commenced. The spacecraft keeps station while long range observations of the asteroid are made. The optical data not only constitute sample imaging but also serve as optical navigation data to enable a close approach of the asteroid to be made. Magnetic fields, particles, and the gamma ray background are all measured during this stand-off phase. The  $\Delta V$  theoretically required to maintain this position against the gravitational pull of Eros is minute, at only  $\sim 6 \times 10^{-3}$  m/s. In fact, the spacecraft is then still well outside the sphere of influence of Eros, and solar pressure and gravity dominate.

At the end of the observatory phase, a drift of 6 m/s towards Eros is initiated in order to be 3000 km from Eros 40 days later. The  $\Delta V$  required to initiate the drift is 6 m/s. This is the start of the reconnaissance and exploration phase. Hazardous debris will be identified as early as possible. At 3000 km from Eros, a small velocity change of 0.89 m/s is made in order to initiate a trajectory resulting in a pass of Eros at 75-km radial distance. During this approach of Eros, the gross characteristics of the asteroid, such as mass, spin vector, etc., will be determined. A series of zig-zag maneuvers will ensue in order to obtain a good estimate of the mass of Eros, as in the Anteros simulation (Section 3.6.1).

On reaching 75-km radial separation, an insertion maneuver is made to achieve a circular orbit at the desired Sun angle for the purposes of mapping the surface of Eros. The  $\Delta V$  required is  $\sim 2.6$  m/s. To maintain a constant orbit-Sun angle, the orbit velocity must be precessed at the Eros orbit rate of  $\sim 1.16 \times 10^{-7}$  rad/s average. Thus the precession  $\Delta V$  for 100 days is 2.44 m/s; or for one year it is 8.89 m/s. During this phase, complete surface and geochemical mapping will be achieved.

The mission may be extended or terminated with close passes of Eros if it is safe to do so. A  $\Delta V$  of 2.42 m/s would cancel the orbit velocity at 75-km



radius. Free fall to the surface would then occur within  $\sim 5.5$  hours. A smaller  $\Delta V$  would result in close passes of Eros. Ultimately, a crash would follow unless an escape maneuver were made to terminate the mission. At 5 km from the center of Eros, the escape velocity is  $\sim 13.3$  m/s.

It may be quickly determined that the sum of all the post-rendezvous  $\Delta V$ s discussed in this subsection (Section 3.6.2) would be only  $\sim 34.1$  m/s for a one-year mission. The allowance of 200 m/s in the calculations for propulsion in Sections 3.2 and 3.3 is very generous.

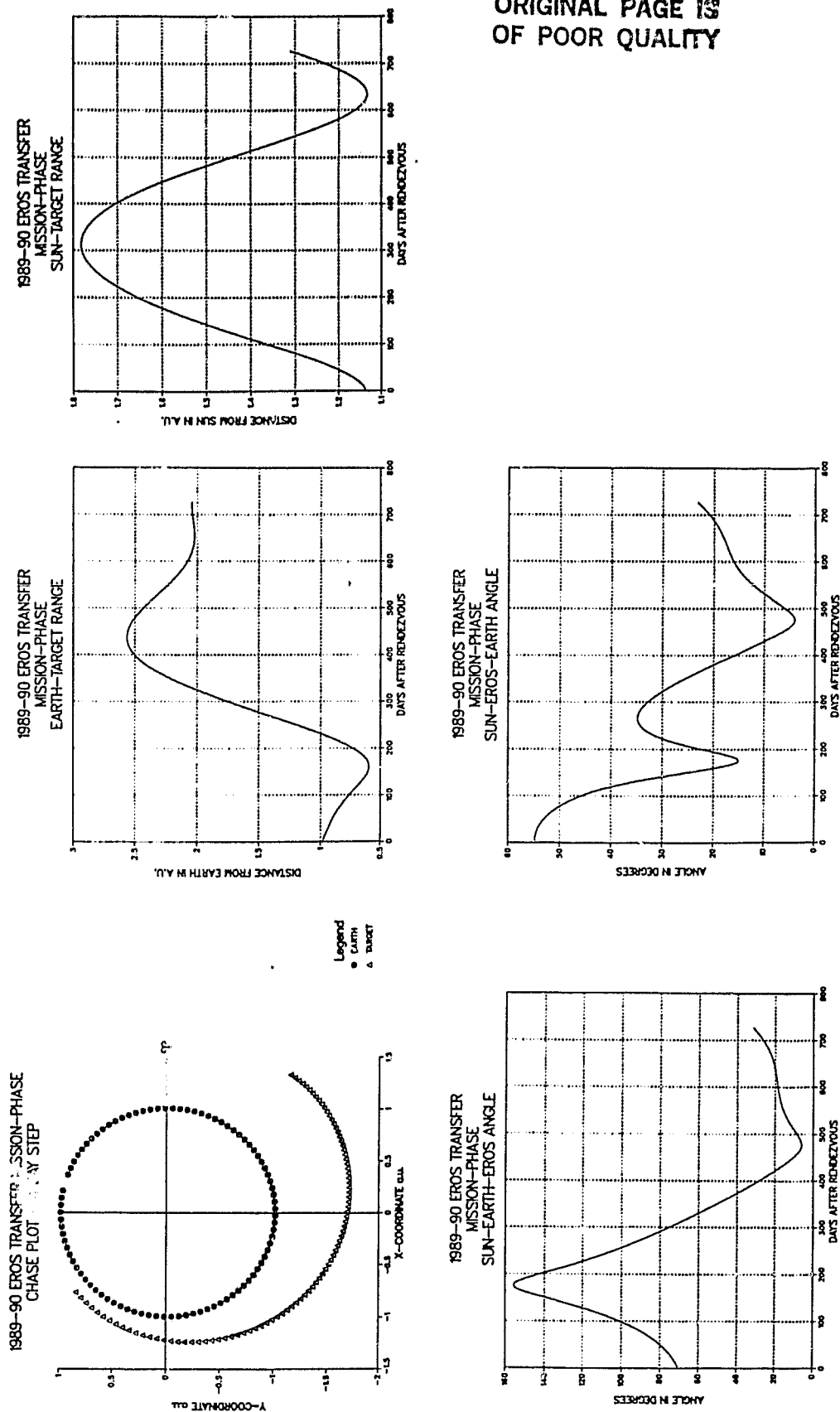
### 3.7 ON-ORBIT OPERATIONS

For the four base line missions discussed in detail here, the histories of several pertinent geometrical relationships between the spacecraft, the asteroid, the Earth, and the Sun for the two years following rendezvous are shown in Figures 3.7-1 through 3.7-4. The heliocentric diagram at the upper left is shown for only one year after rendezvous. The graphed geometrical histories are merely the relative properties of the ephemerides of the asteroids and the Earth.

As mentioned in Section 3.5, the asteroid-Sun distance increases from its minimum to its maximum over approximately the first year after rendezvous for all four near-term candidate missions. The communications distance develops quite differently for each case, though frequently not changing very significantly over the first 200 days and then changing drastically over the next 200 days. There are no problematical conjunctions of the Earth and Sun as seen from the spacecraft nor of the asteroid and the Sun as seen from the Earth.

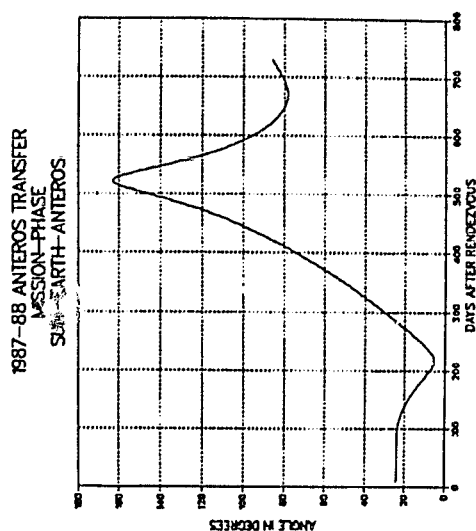
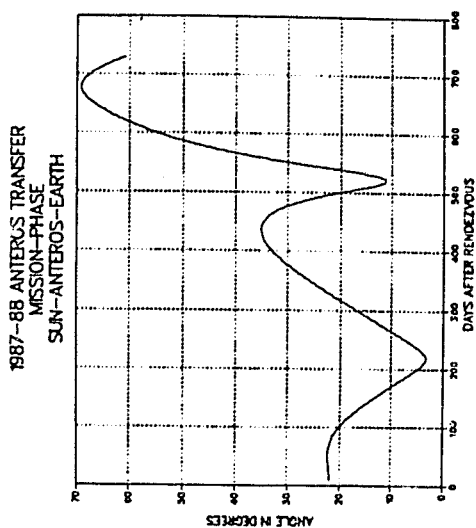
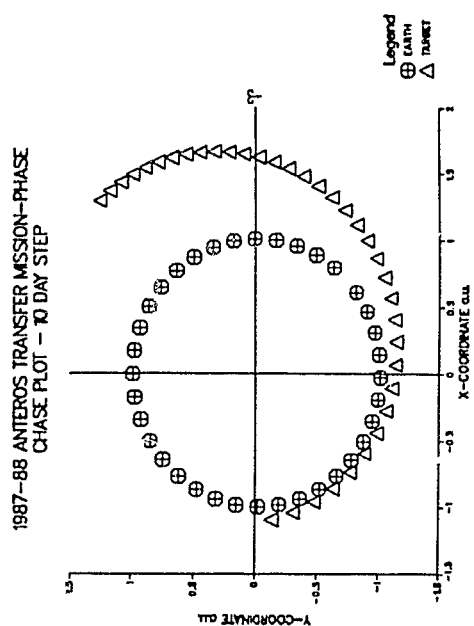
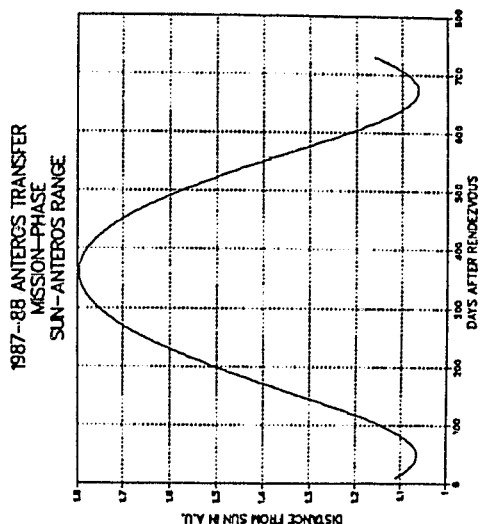
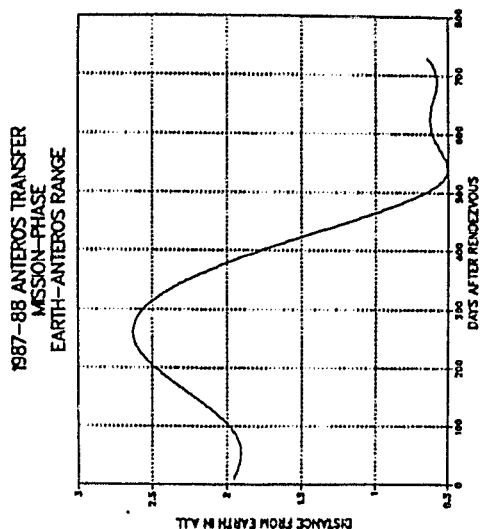
The base line spacecraft design presented in this report is intended for operation when the orbit normal is aligned with the Sun vector, i.e., in a dawn-dusk orbit. For the base line mission launching to Anteros in 1987, this would also mean that the Earth cone angle would not exceed  $35^\circ$ , measured from the pitch axis, over approximately the first year-and-one-half after rendezvous. To maintain the Sun angle constant, the orbit will be slowly precessed so as to exactly cancel the asteroid's orbital rate about the Sun. This integrated propulsive increment is approximately 1.84 m/s/year for a 10-km radius circular orbit at Anteros, and  $\sim 8.89$  m/s/year for a 75-km radius circular orbit at Eros, if the current estimates of asteroid mass are correct at  $4.4 \times 10^{13}$  kg and  $\sim 6.6 \times 10^{15}$  kg, respectively.

It is thought that Anteros is approximately spherical and that an orbit at 10-km radius will not behave very differently than if Anteros were truly spherical. Eros, however, is thought to be roughly cigar-shaped with dimensions of  $10 \times 36$  km, the spin axis being undoubtedly along the major principal axis. Furthermore, Eros is thought to be revolving about its own axis at several revolutions per day, and the orbit period of the spacecraft will typically be in the range 0.57 days (at 30-km radius) to 2.03 days (at 70-km radius). If this is the case, the asymmetrical gravity field will be rotating much faster than the spacecraft in its orbit. Thus, anomalies of an orbit would be attenuated considerably as compared to the case of a non-rotating asteroid. In any case, the orbital motion at low altitudes over Eros is expected to be highly irregular. Based on work by Friedlander, Wells, and Davis,<sup>7</sup> and Ottke,<sup>8</sup> it has been predicted that for a tri-axial ellipsoidal body approximately the size of Anteros, with axial radii of 1.75, 0.5, and 0.25 km, circular orbits at



ORIGINAL PAGE IS  
OF POOR QUALITY

Figure 3.7-1. Eros Mission Phase Geometry - 1989 Launch



ORIGINAL PAGE IS  
OF POOR QUALITY

Figure 3.7-2. Anteros Mission Phase Geometry - 1987 Launch

ORIGINAL PAGE 13  
OF. POOR QUALITY

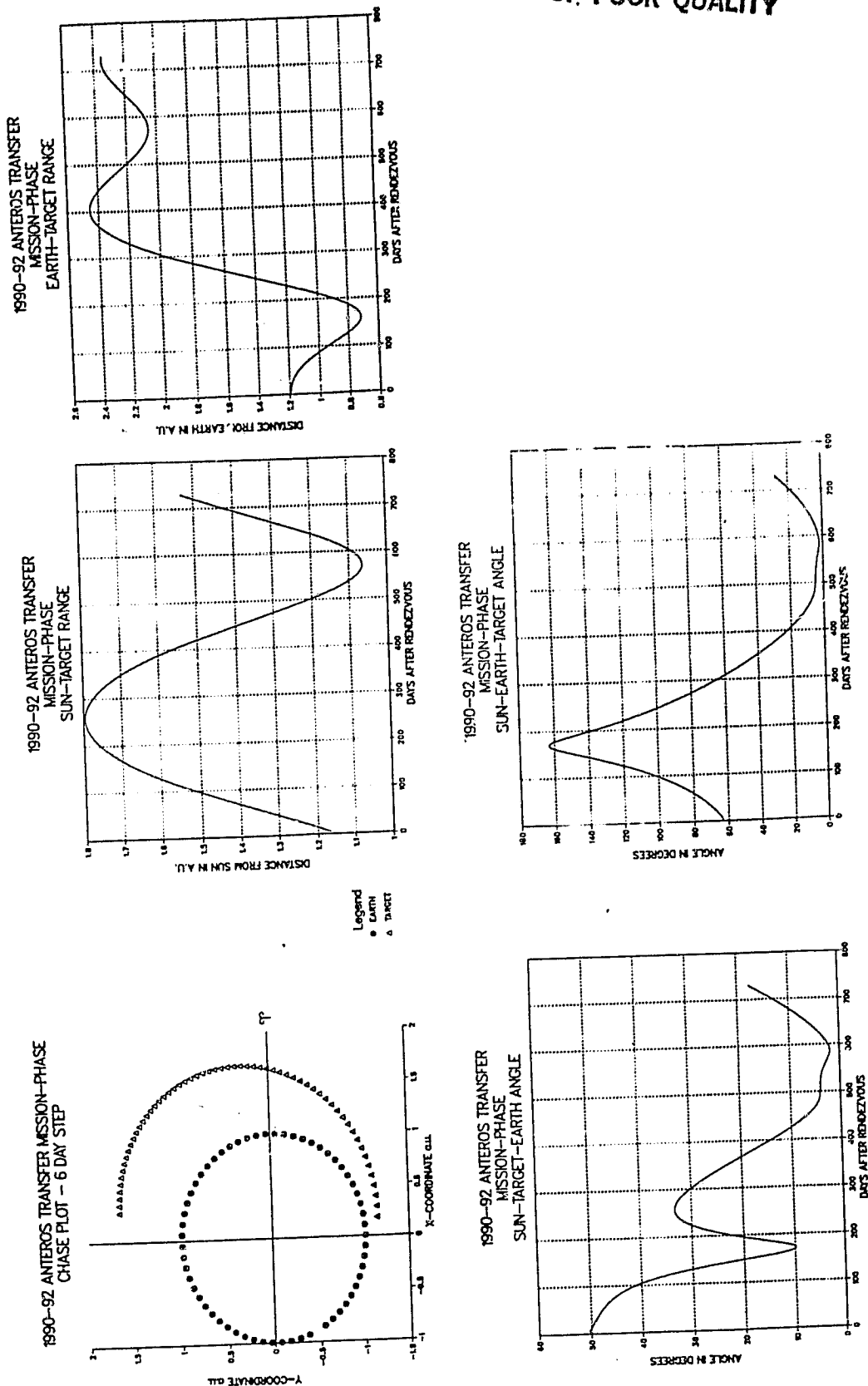
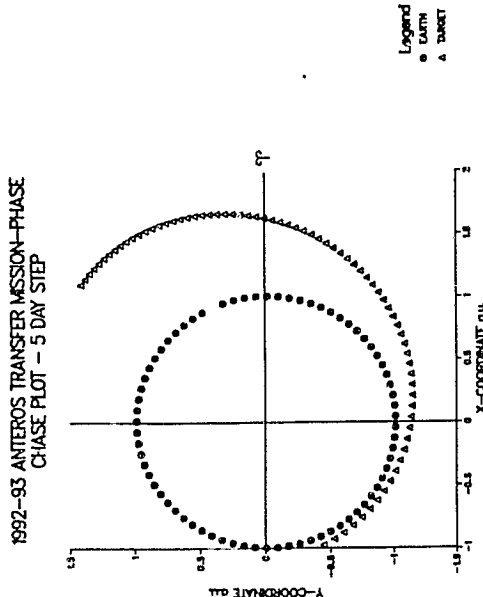
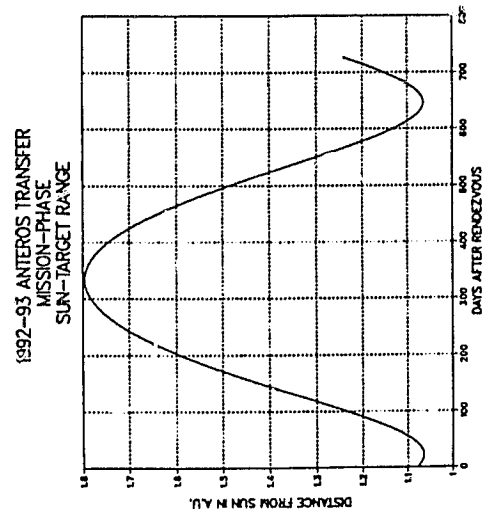
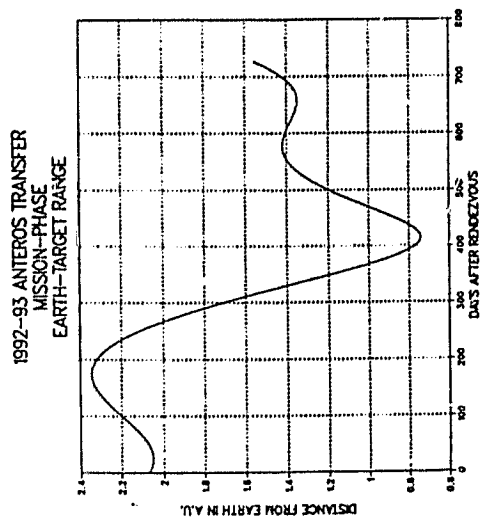


Figure 3.7-3. Anteros Mission Phase Geometry - 1990 Launch



ORIGINAL PAGE IS  
OF POOR QUALITY

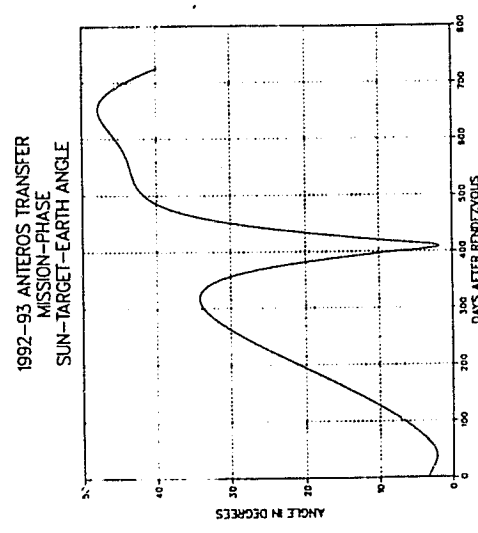
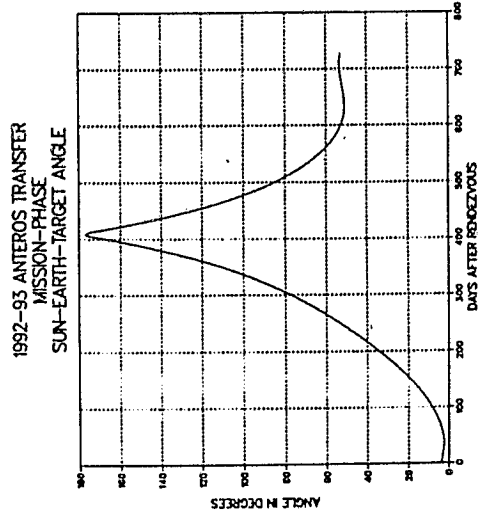


Figure 3.7-4. Anteros Mission Phase Geometry - 1992 Launch

10-km altitude will be fairly stable and need infrequent restoration. Circular orbits at 75-km radial distance from the center of Eros are expected to be similarly stable. Detailed predictions specific to a given mission would require further modeling and simulation.

Of course the gravitational potential of the asteroid will not be known in three dimensions until well into the orbital phase. Imagery will not suffice entirely for gravitational mapping since there will undoubtedly be mascons throughout the asteroid. At Anteros, for example, it is proposed that the spacecraft motion be monitored through ground-tracking and through sensor imagery while the spacecraft is in an orbit which has a period of approximately two days (12.8 km radial distance) and without any mass expulsion devices being employed. In this way, the gravitational potential of the asteroid may be mapped. Using the present base line configuration of the spacecraft, in a circular orbit with the orbit normal towards the Sun, there will be no secular torque build-up to the first order of analysis; therefore, desaturation thrusting may be done in that configuration once a week or less frequently. The ability to seal off components leaking gas will be dependent on the propulsion subsystem design. The base line design features redundant NEAs, sealable by solenoid valves, as described in Section 5.2.3.

The spacecraft will orbit the asteroid with the bottom face of the doghouse (ESM) pointing towards nadir. The zenith-nadir line will be the yaw axis. The orbital motion of the spacecraft, i.e., the roll axis, will be along the long dimension of the TIROS spacecraft. The pitch axis, therefore, will be along a line joining the two louvered faces of the ESM. Since, in the base line design, the spacecraft will operate in the terminator plane, the pitch axis and the Sun line will be coincident. In the base line design, the solar array will be fully deployed into the roll-yaw plane; therefore, no solar array drive will be necessary during the base line mission operation.

The sensors will be mounted nadir-pointing underneath the ESM, except for the GRS and the MAG which will be mounted on booms deployed parallel to the pitch axis. Orbital operation restricted to the terminator plane, as in the base line mission design, may limit sensor coverage of asteroid latitude zones if the spin axis of the asteroid is aligned closely with the Sun line. Polar orbits would offer full coverage at all latitudes, but the design of the spacecraft for polar orbits is more complex. For example, a one- or two-axis solar array drive would be necessary, and the gimbaled mount of the HGA would have to be much less restricted than in the base line design. In the base line design for the mission launched to Anteros in 1987, the angle between the Sun and Earth as seen from the spacecraft is  $<35^\circ$  for the first 1.5 years after rendezvous. A more flexible spacecraft design is feasible, however, and the task of performing this redesign could fall within the scope of a follow-on study of the application of the TIROS spacecraft to asteroid rendezvous missions. It should be noted, however, that the base line spacecraft design is tolerant of small changes in the orientation of the orbit plane away from the terminator. Further, since such plane changes are performed very economically at all but the largest asteroids, this technique affords a way of obtaining greater if not complete latitudinal coverage of the asteroid, using the base line design.

## SECTION 4.0

### ASTEROID SPACECRAFT SYSTEM

#### 4.1 INTRODUCTION

The purpose of the Asteroid mission study is to assess the applicability of an existing spacecraft bus and subsystems to the requirements of a near-Earth Asteroid mission. RCA's recommended candidate is the operational meteorological satellite family of TIROS and DMSP. Both are built by RCA, TIROS for a civilian agency, NOAA, and DMSP for a military agency, the United States Air Force. These programs utilize a common bus to satisfy their Earth-observation missions. It should be noted that, although the instrument complements, the pointing accuracies, and, initially, the boosters were different (DMSP used the Thor booster and TIROS used the Atlas), a high degree of commonality was achieved. This experience was used in developing the approach presented herein. During the 23 years RCA has conducted the TIROS and DMSP programs, we have developed procedures and techniques for interface control, integration, and testing of multiple payloads on Earth-observation satellites. This experience has led to low cost approaches resulting from evolutionary development and was used to prepare technical and programmatic concepts for deep space missions. In particular, we relied heavily on the heritage of the Advanced TIROS-N (ATN) program.

There have been other studies, relating to changes to TIROS and DMSP and relating to other applications of these buses, that were used in the Asteroid rendezvous spacecraft (ARS) study. Specifically, extensive use was made of the design effort funded by NASA to configure ATN to be Atlas- and Shuttle-compatible. This is referred to as the Shuttle/Atlas Advanced TIROS-N (SAATN) configuration.

Similar studies were conducted on DMSP and are currently funded by the Air Force to design F-15 for a Shuttle launch. Other programs that bear on the Asteroid study are:

- Maritime Applications Experiment (MAE), funded by NASA to incorporate a coastal zone color scanner (CZCS), a scatterometer (SCATT), and a microwave imager (SSM/I) on the NOAA-I\* and -J spacecraft. These would be piggy-backed with the meteorological and climate sensors already planned for these flights
- Navy Remote Oceanography Satellite System (NROSS), which RCA has studied under its own funds (and for which we are hopeful for Navy support) to refurbish the NOAA-D bus (which exists but is not scheduled for launch) to carry a SCATT, an SSM/I, and an advanced very high resolution radiometer (AVHRR)

RCA has also investigated applications of TIROS-N, ATN, and DMSP to earth resource missions, synthetic aperture radar missions, a Halley Comet imaging mission, and, most recently, under JPL direction, the TOPEX mission. In all cases, we and our prospective users were interested in low cost application

---

\*Each spacecraft in the current TIROS series is named NOAA-(letter).

to proven bus technology, i.e., a bus which, due to its use in an operational mission, must provide reliable, long life operation.

#### 4.2 TIROS TECHNICAL SUMMARY

The ATN spacecraft is shown in Figure 4-1. It represents an evolution from the original DMSP 5D-1, which led to TIROS N<sup>o</sup> and then to ATN. Briefly, it is a meteorological spacecraft which is continuously pointed at nadir as the satellite circles the earth at 450 nautical miles (nmi) in a Sun-synchronous orbit. The solar array is continuously oriented toward the Sun by a solar array drive that is controlled by a central processing unit (CPU). The major structural elements of the spacecraft are:

- Reaction Control Equipment Support Structure (RSS), which carries the reaction control equipment (RCE), batteries, and upper stage solid motor, as well as interfacing with the Atlas
- Equipment Support Module (ESM), which carries most of the support subsystem electronics, as well as payload elements
- Instrument Mounting Platform (IMP), which provides a common structure for instruments requiring coalignment

The spacecraft subsystems are as follows:

- Structure subsystem
- Thermal subsystem - passive control with active augmentation
- Attitude determination and control subsystem (ADACS) - a zero-momentum, four-reaction-wheel system using Earth sensors and gyro Sun sensors for measurement, and magnetics for external torquing. Designed on DMSP to provide 0.01° control and on TIROS to provide 0.2° control
- Command and data handling subsystem (CDHS) - a centralized computer (CPU) controlled system providing fault-tolerant performance, with special purpose processors for primary data and an array of five NASA standard DTRs for data storage
- Communications subsystem (CS) - includes downlinks at VHF, L-Band, and S-Band, and uplink commands at VHF
- Propulsion subsystem - the final stage of ascent and attitude control functions
- Power subsystem - the primary (solar array) and secondary (NiCd batteries) power sources and associated regulation electronics, characterized by self-checking automatic redundancy switching with ground-commanded override

The ATN spacecraft is designed with no single-point failures and with a significant level of automatic switching, as described in Section 5.4 (power subsystem). The central computer also performs a variety of health checks on various subsystems, and, should a major fault be detected, it will command the



ORIGINAL PAGE IS  
OF POOR QUALITY

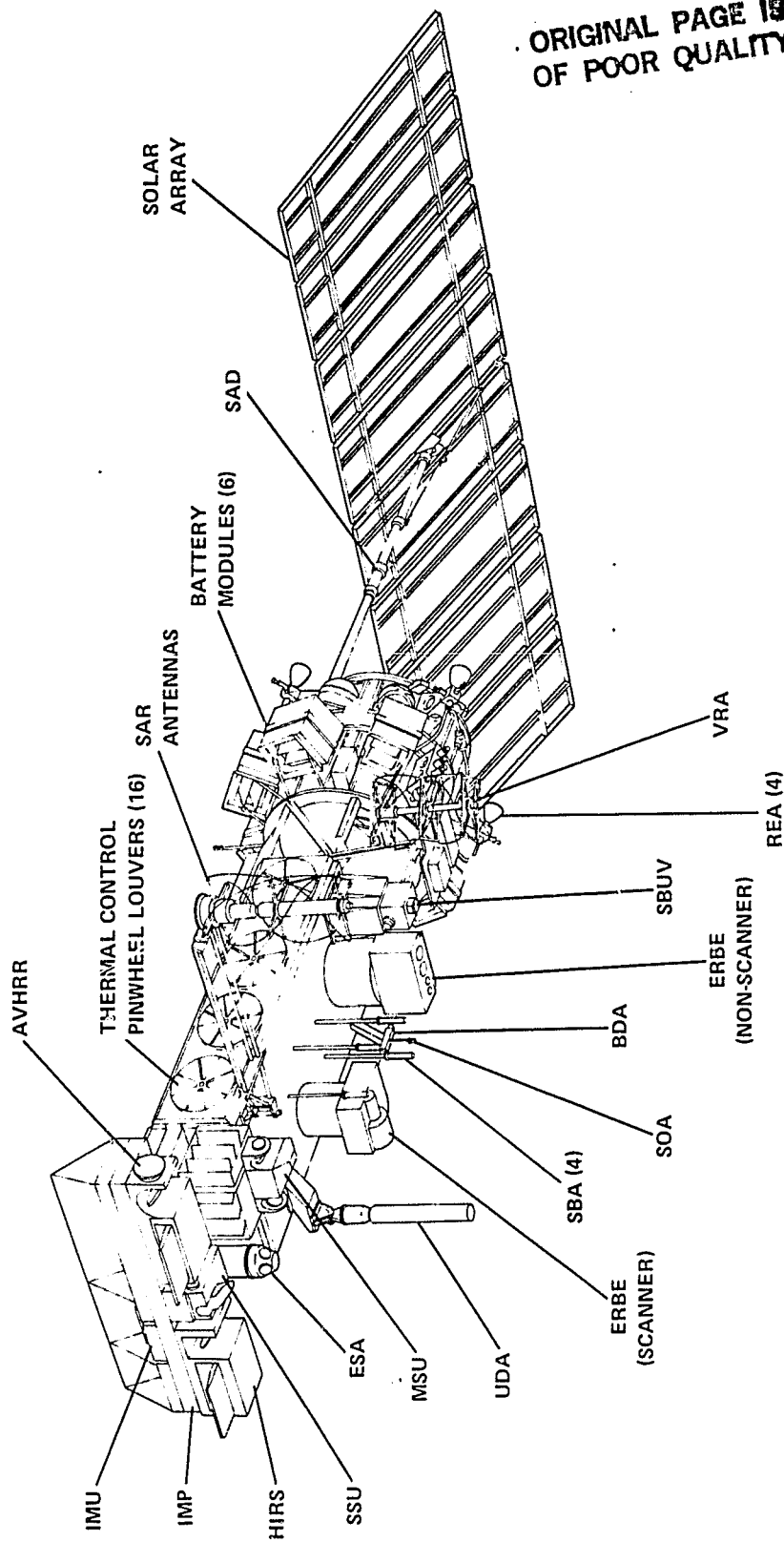


Figure 4-1. Advanced TIROS-N Spacecraft, NOAA-G Configuration

spacecraft to a "safe state." This high degree of autonomy minimizes ground control requirements. Tape recorder management and clock updates are the primary ground command functions.

During the course of the study, it was determined that the ATN structure was significantly larger than required to support the Asteroid mission instrument requirement, even with deletion of the IMP. While layouts and accommodation studies were done for both ATN and TIROS-N configurations, the TIROS-N structure was ultimately chosen as a base line to conserve weight. Most electrical subsystems, however, are based on ATN since it is the most recent in the series. The two spacecraft are virtually indistinguishable, with the exception that ATN is larger and has four thermal louvers on the ESM while TIROS-N has only three. Figure 4-2 shows the on-orbit configuration of TIROS-N as a weather satellite.

#### 4.3 APPLICABILITY OF EARTH ORBITER SPACECRAFT TO DEEP SPACE MISSIONS

RCA Astro-Electronics began an IR&D effort in 1980 to address this particular topic. The current study proposal was an outgrowth of that effort. The rationale behind trying to establish this capability is quite straightforward. Since the great majority of spacecraft technology development has been directed toward Earth orbiters, the amount of existing technology and the number of spacecraft designs available to planetary missions from this pool is large.

Calculations show that the spacecraft environment experienced between Venus and the inner edge of the asteroid belt is basically consistent with design margins on a large number of existing spacecraft designs. Mercury is a special case not accommodated easily by Earth-orbiter thermal systems, and beyond the asteroid belt, thermal/power considerations require a dedicated design.

Other subsystem modifications (e.g., communications, do not drive the fundamental system design (and are, in fact, typically modified from one Earth-orbiter mission to the next).

As examples of this, Table 4-1 shows the temperature and power differentials for a variety of spacecraft configurations over the range described above (1.8 AU is taken as a typical maximum solar distance for the Asteroid mission). Figure 4-3 shows the effect of the diminishing efficiency of the TIROS solar array as a function of distance from the Sun.

Also shown in this figure are the average power requirements for the mission; it is clear that, for a mission such as the one under consideration, the array is adequate even at the farthest distances from the sun.

Figure 4-4 shows the maximum data rate available from the base line 20-watt transmitter using a 1.5-m steerable dish antenna design for two ground antennas at both S- and X-band. We have assumed this system as a base line (S-band) for the current study; however, more work is needed to optimize this area. It is important to note that we have assumed that no technology would be developed for this mission. Should developments occur that apply to this mission, for example, a complete impact down link X-band system, we would certainly adopt them.

ORIGINAL PAGE  
BLACK AND WHITE PHOTOGRAPH



CUSTOMER	NASA/NOAA
MISSION	METEOROLOGICAL, OPERATIONAL
ORBIT	450 nmi
DESIGN LIFE	2 YEARS
BOOSTER	ATLAS F (CONTRACTOR LAUNCH)
WEIGHT, S/C TOTAL PAYLOAD	1634 LB 384 LB
AVERAGE POWER, TOTAL PAYLOAD	320 W 200 W MAX.
MAXIMUM ARRAY POWER	1200 W
ATTITUDE CONTROL	ZERO MOMENTUM
LAUNCHES	1978-1984 (8 ON ORDER)
	TIROS-N - 10-13-78 NOAA-6 - 6-27-79 NOAA-7 - 6-23-81
PAYLOAD	AVHRR TOVS - HIRS/2, SSU, MSU SEM DCS

Figure 4-2. TIROS-N/NOAA Series

TABLE 4-1. POWER/THERMAL IMPACT

	AU	$\frac{1}{(AU)^2}$	°C Flat Panel	Cylinder, °C					P <sub>dest</sub> /P <sub>max</sub>				@ P <sub>max</sub> Approximate Average Reduction	V <sub>DD</sub>
				Side Spin	Side Despun	Flat End	Flat Panel	Side Spin	Side Despun	Flat End				
Venus	0.723	1.913	+140	+75	+150	+190	1.052	1.291	1.100	-	+15%	+91%		
Mars	1.524	0.431	+11	-11	+35	+75	0.515	0.476	0.496	0.485	-51%	-57%		
Antares	1.8	0.309	-11	-32	+5	+47	0.403	0.374	0.402	0.391	-61%	-69%		

Earth-Environment Temperatures: Flat Panel +50°C

Cylinder: Side Spinning +10°C  
Side Despun +65°C  
Flat End +100°C

Power Advantage at Destination:  $\frac{1}{(AU)^2} [1 + (T_E - T_D) 0.005]$

T<sub>E</sub> = Earth-Environmental Temperature, °C

T<sub>D</sub> = Temperature at Destination, °C

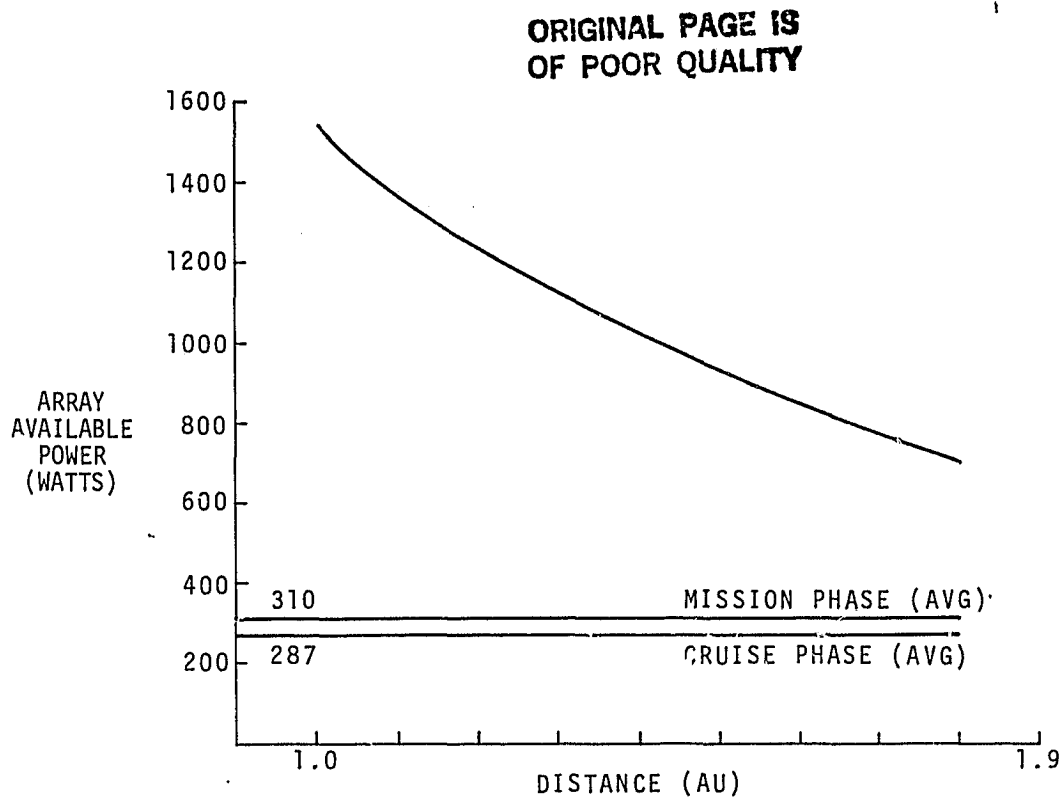


Figure 4-3. Array Power Maximum Power Point Tracker

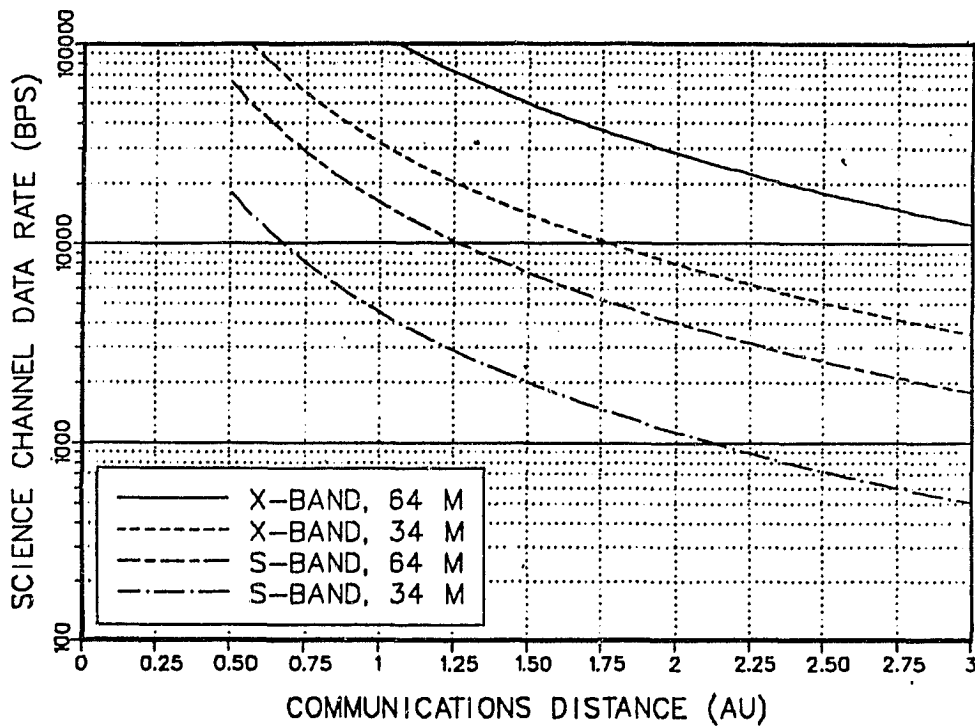


Figure 4-4. Science Channel Capacity

#### 4.4 ASTEROID SPACECRAFT SYSTEM OVERVIEW

Details of each of the subsystems are found in Section 5. The power, thermal, and CDH subsystems are all virtually unmodified. The ADACS is primarily based on DMSP. The propulsion system is that of SAATN, with larger tanks and some thruster layout and sizing modifications. The structure is based on the SAATN analysis. The detailed equipment list may be found in Section 5, and the equipment heritage is as shown in Table 4-2.

The mission targeting options are left essentially open, even though Anteros and Eros were chosen as design base lines. The only real constraints on the target asteroid are the Earth/Sun direction, which would preclude some Earth-crossing asteroids, and the launch of the STS from the Eastern Test Range (ETR), which would preclude some high inclination targets.

Some of the basic tradeoffs made in the course of the study are shown in Figure 4-5. The two most significant changes in the base line system are the partial array deployment for cruise and the decision to go with an all liquid system in place of a solid injection motor. The partial deployment was necessitated by thermal and power requirements during cruise, and the liquid system was dictated by the partial deployment, with the additional advantage of eliminating the concerns of temperature control and degradation of the solid. This same tradeoff was made during the SAATN study for the drift orbit period. The same conclusion was reached, and the SAATN mission uses both a partially deployed array and an all monopropellant system in place of the apogee kick motor (AKM) used in the TIROS/ATN expendable launch vehicle (ELV) configuration.

Table 4-3 shows the operating scenarios resulting from the tradeoffs of Figure 4-5. Table 4-4 summarizes the primary results of the configuration tradeoff studies.

#### 4.5 RELIABILITY AND AUTONOMY

We propose to treat the Asteroid spacecraft in a similar fashion to that of a standard low altitude meteorological satellite. RCA's product assurance (PA) policy and plans already in place are in accordance with the requirements of UHB 5300.4 (1B) and MIL-Q-9858A. They are normally tailored to unique customer requirements. Current TIROS PA documents, as approved by NASA/GSFC, would provide a basis for a JPL project PA plan, which would likewise be tailored.

As shown in the equipment heritage and description table, the spacecraft is fully redundant in all electrical systems. Those mechanical systems that cannot be literally redundant and are mission critical (e.g., the HGA actuator) have effective functional redundancy via alternate operational modes (e.g., the medium gain antenna (MGA) at lower data rates or the HGA pointing via programmed spacecraft maneuvers).

The proper functioning of each system, and automatic switching-on failure or anomaly detection, are handled by the CPU (the RCA SCP-234) which is quadruply redundant, two sides to each CPU and two CPUs. The CPU continually runs self-diagnoses as a background job and monitors the function of all spacecraft systems. The computer itself is single error detecting in its present version

TABLE 4-2. EQUIPMENT HERITAGE AND DESCRIPTION

System/Assembly	Project Heredity	Design Heredity	Qty/ S/C	Redundancy	Spares*	Modifications	Modification Impact
Power PSE	ATN	100%	1	100% electrical	1	Add two level discreet power point voltage levels (modify one board of PC)	Desirable, not required
Batteries	ATN	100%	3	3 for 2	1		
BCX	ATN	100%	1	100% electrical	1		
BCS	ATN	100%	3	100% electrical	1		
SA	ATN	100%	1	5-yr design rgmt	1		
SAD**	ATN	100%	1	100% electrical	1		
ADE**	ATN	100%	1	100% electrical	1		
PC	ATN	90%	1	100% electrical	1		
Data Handling and Command TIP	ATN	75%	1	100% electrical	1	Modify TR readout speed (or buffer output)	Moderate
XSU	ATN	75%	1	100% electrical	1		Minor
SATCU**	ATN	100%	1	Not mission critical	1	Modify instrument interfaces and data acquisition rates to accommodate instrument design, one board each in TIP, CIU, SCU, two boards in CDU	
TR	ATN	100%	3	3 for 2 +100% redundancy	1		
CPU	DMSP	90%	2	100% electrical	1		
CIU	ATN	95%	1	100% electrical	1		
CPC	ATN	100%	1	100% electrical	1		
RXO	ATN	100%	2	100% electrical	1	Rewrite mission control software package	Moderate
SCU	ATN	90%	1	100% electrical	1		
CDU	TIROS	30%	1	100% electrical	1		

\*All vendor units will be spared as complete units; all RCA units will be spared at the box level

\*\*May be added for other missions.

TABLE 4-2. EQUIPMENT HERITAGE AND DESCRIPTION (Continued)

System/Assembly	Project Heredity	Design Heredity	Qty/ S/C	Redundancy	Spares*	Modifications	Modification Impact
<u>Structure</u>							
RSS	ATN/SAATN	50% (ATN)**	1	NA	0	Upper stage interface (IUS or SRM) new	Moderate
ESM	ATN/SAATN	80% (ATN)**	1	NA	0		Minor
SAS	ATN/SAATN	75% (ATN)**	1	NA	0		Moderate
Upper Stage Interface Adapt	New	0%	1	NA	0		Moderate
IMP	Deleted						
<u>Propulsion</u>							
N <sub>2</sub> H <sub>4</sub>	Mod Viking	50%	1	NA	Partial	Tank regualification required for standard Viking tank***	Major
He Tank	Voyager	100%	6	100%	1		
REA	Voyager	100%	4	100%	1		
NEA (2 lbf)	ATN, DMSP	100%	8	33%	2	Control and interface for REA redesign requirement includ- ing bracketry, etc.	Moderate
NEA (0.2 lbf)	Classified	100%	4	100%	1		
<u>Thermal</u>							
ESM Blankets	ATN	95%	1 set	NA-design margin	0	No modification except blanket shape and perhaps some surface finishes	Minor
RSS Blankets	ATN	75%	1 set	NA-design margin	0		
TCEs	ATN	100%	37		2		
Heaters/ Radiators	ATN	100%	1 set	Passive	2		
Louvers							
Pinwheels	ATN	100%	16		1		
Vane	ATN	100%	12		1 set		
Cooling Lines	ATN	100%	1 set	NA-Grd Test	NA		
RCE System	ATN	100%	1 set	NA	0		
*All vendor units will be spared as complete units; all RCA units will be spared at the box level **100% (SAATN)							



TABLE 4-2. EQUIPMENT HERITAGE AND DESCRIPTION (Continued)

System/Assembly	Project Heredity	Design Heredity	Qty/ S/C	Redundancy	Spares*	Modifications	Modification Impact
<u>ADACS</u> IMU	ATN	95%	1	4 for 3 gyros	1	IMU must accept input of star tracker, rather than the DMSP mapper (common to TIROS and DMSP)	Minor
RWA	ATN	75%	4	4 for 3	1		
SSA	ATN	100%	2	100% electrical	1		
PTC	ATN	100%	1	100% electrical	1		
RYC	ATN	100%	1	100% electrical	1		
CSS	ATN/SAATN	0% (ATN**)	2	100% electrical	1		
CSA	Various Options	75%	1	2 for 1	1	ADACS software modifications	Moderate
<b>ORIGINAL PAGE IS OF POOR QUALITY</b>							
<u>Telecommuni- cations***</u> Deep Space XP ON	NASA STD	100%	2	100% electrical	1	Transponder replaced with deep space version	Moderate
HGA	Viking	20%	1	100% electrical	1		
OMA	ATN	60%	1	NA	0		
MGA	Viking	50%	1	NA	0		
STX	ATN	80%	1	NA-backup	1		
Power AMP	Viking	60%	4	100% electrical	2		
Misc RF	Various	50%	1 set	NA-passing elements	0		
<u>Harness</u>	ATN	50%	1	NA	-	Antenna geometry modified	Major
<u>ASE</u> Mechanical	SAATN	0% (ATN)**	1	NA	0	RF hardware modified for different feed paths	Moderate
Electrical	SAATN	0% (ATN)**	1	100% electrical	1		
*All vendor units will be spared as complete units; all RCA units will be spared at the box level. **100% (SAATN)							

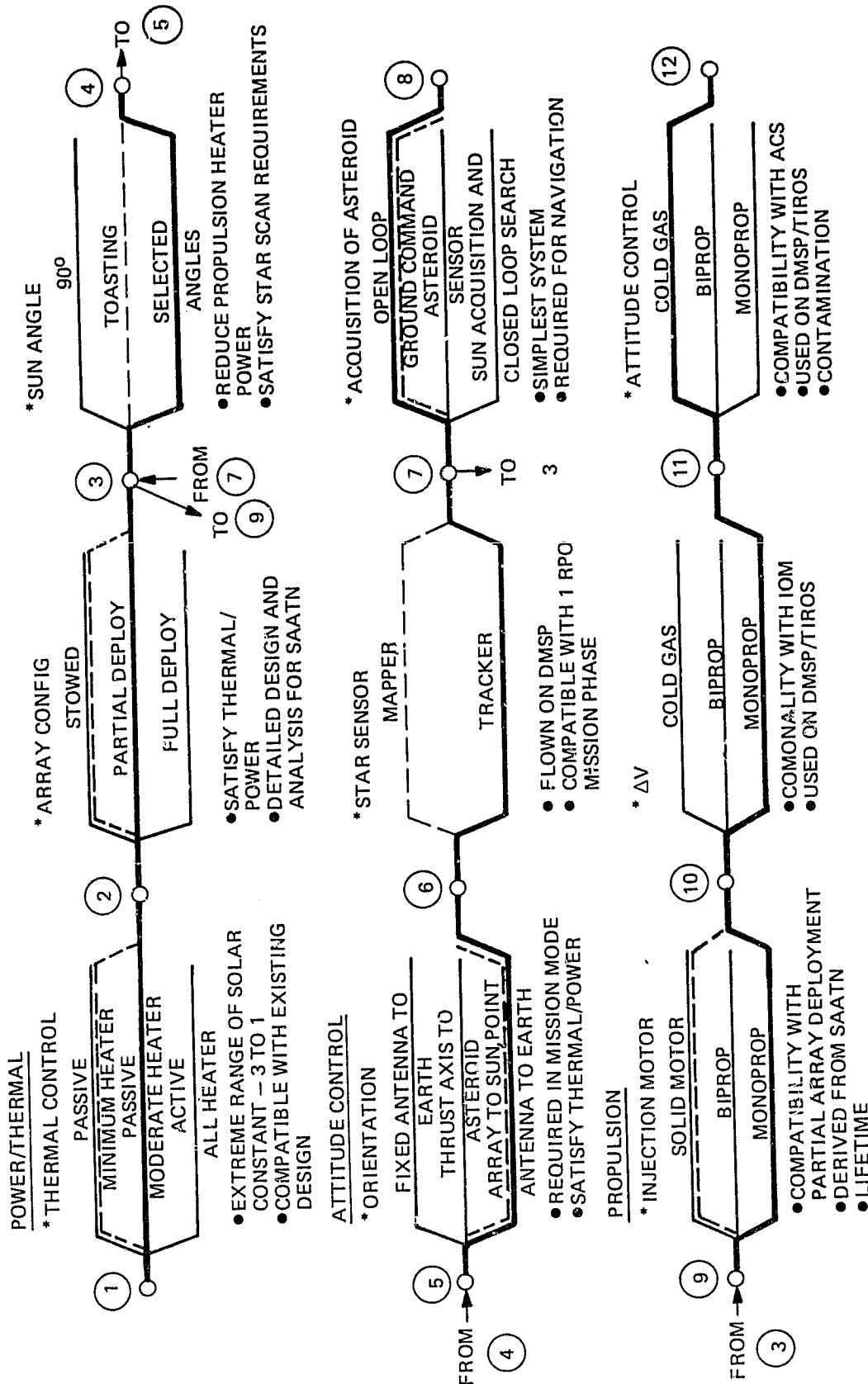


Figure 4-5. Tradeoffs - Cruise and Injection Phase

TABLE 4-3. SELECTED OPERATING SCENARIOS

STS Separation to Cruise Orbit in Injection (90 Minutes)
Spacecraft stowed, using batteries for power, under attitude control of the attached IUS
IUS Separation into Cruise Orbit (1.5 Years)
Inertial control of spacecraft with the vector normal of the partially deployed array pointed toward the Sun, and the long axis of spacecraft oriented to provide convenient communication to Earth through the high gain antenna. Control of high gain antenna pointing is open loop though ground programming. There are some advantages (thermal electric power) to skewing the long axis so that the Sun illuminates the propulsion elements
Rendezvous Maneuver (Asteroid Mission)
The spacecraft long axis is oriented for optimum liquid engine thruster firing while the array normal is maintained as close as possible to the Sun. This is the course rendezvous maneuver. After measurements by the ground and by the imager on the spacecraft, trim maneuvers will be instituted to achieve a variety of orbits (see Section 3)
Mission Operations
The spacecraft solar arrays will be fully deployed and the spacecraft array normal pointed to the Sun. The spacecraft will be controlled at a one-RPO rate to continuously orient at the nadir. The programming of the high gain antenna will be occasionally updated from the ground

and, single error correcting and multiple error detecting in the version to be flown on the next block of DMSP. If a CPU error is detected, the switch to the other side is made automatically.

When a non-CPU error or out-of-limits condition is encountered, a pre-programmed safing sequence is entered, as specified for that condition. This extremely sophisticated system is required for TIROS since, as a low altitude meteorological satellite (METSAT), it is only routinely contacted by two stations and is therefore out of a position where ground contact is possible about 80 percent of the time. This situation forces: 1) the spacecraft to function relatively autonomously with respect to command execution, data gathering, and data transmission; 2) error and fault and isolation to be done on board and communicated to the ground at the beginning of a contact in a way that allows for optimum reaction; and 3) an on-board automatic response to anomalies that leaves the spacecraft in a safe state until the ground can be notified and a response made (e.g., an attitude control subsystem sensor failure would evoke a response that relies on the last good data and the

TABLE 4-4. PRIMARY RESULTS

- The DMSP/TIROS spacecraft is a good fit for the Asteroid (and MGO) missions
- More than 80%, by weight, of the equipment for the mission will be unmodified from TIROS/DMSP or other programs
- Maximum use is made of the work completed on SAATN for NASA/NOAA and block 5D-3 for USAF DMSP to assure STS compatibility
- Major changes will be required in the communications subsystem to be DSN-compatible (use of existing hardware)
- Preliminary analyses indicate a switch from the DMSP star mapper to the NASA standard star tracker (use of existing hardware)
- If a full year of mission operations is required at 100% capacity, the power system will have to be changed from the existing direct energy transfer (DET) type to a maximum power point tracker (MPPT). Recommend that we stay with existing system (solar array cells must be re-laid out) at small penalty of operating time at end of life
- A converter to ternary inputs is required in the command and data handling subsystem to assure DSN command compatibility. Modest modifications to the TIROS data processor and the TIROS tape recorders will be necessary
- Minor modifications (reductions, mainly) in structure are required

inertial measurement unit to provide attitude control, based on extrapolation; this would be adequate until a response could be made from the ground).

The spacecraft requires no modification for the planetary application because of either autonomy (to this level) or redundancy considerations.

#### 4.6 NEW TECHNOLOGY TOOLS

As a base line for the pioneer-class missions, we have assumed no new technology development. No mission-specific new technology requirements have been identified for the Asteroid mission. However, normal next generation state-of-the-art subsystem design updates will take advantage of applicable generic new technology as it becomes available. Specifically, several research and development areas could be of cost-performance benefit to pioneer-class spacecraft and will be used if independently developed. For example:

- A complete X-band system, dropping the S-Band transponder
- A new bipropellant propulsion system
- CCD star sensors (which can also be used for extended objects)

- Improved efficiency nickel hydrogen batteries
- High yield gallium arsenide solar cells
- Bubble memory technology
- Advanced on-board computer design (e.g., the SCP-050)

None of these are mission critical and we have not assumed their availability for the study.

## SECTION 5.0

### SPACECRAFT SUBSYSTEM DESIGN

#### 5.1 MECHANICAL DESIGN

##### 5.1.1 HERITAGE AND COMMONALITY

The Asteroid spacecraft proposed in this study is based on the flight-proven TIROS/DMSF integrated spacecraft system (ISS). Since it is an ISS, the second or final stage of the launch vehicle is an integral part of the satellite. All versions of this design that have flown to date use an expendable launch vehicle (ELV) for the first stage and contain a TE-M-364-15 solid rocket motor as the apogee kick stage. The current spacecraft design has evolved from the initial Thor-compatible DMSF to the current Advanced TIROS-N (ATN), Atlas-compatible design.

A 1980 NASA-funded study identified those modifications to the existing ATN design necessary to produce an STS-compatible spacecraft. The major changes involved: 1) designing the ascent support equipment necessary to electrically interface the spacecraft and the STS, 2) replacing the solid rocket motor upper stage with an all liquid monopropellant system to support drift orbit operations, and 3) the addition of structural mounting points on the spacecraft to support the horizontal mounting of the spacecraft in the newly designed shuttle interface cradle. This spacecraft configuration was known as SAATN.

The overall Asteroid spacecraft family tree, shown in Figure 5.1-1, illustrates the equipment heritage from DMSF, ATN, and SAATN.

##### 5.1.2 GENERAL SPACECRAFT DESCRIPTION

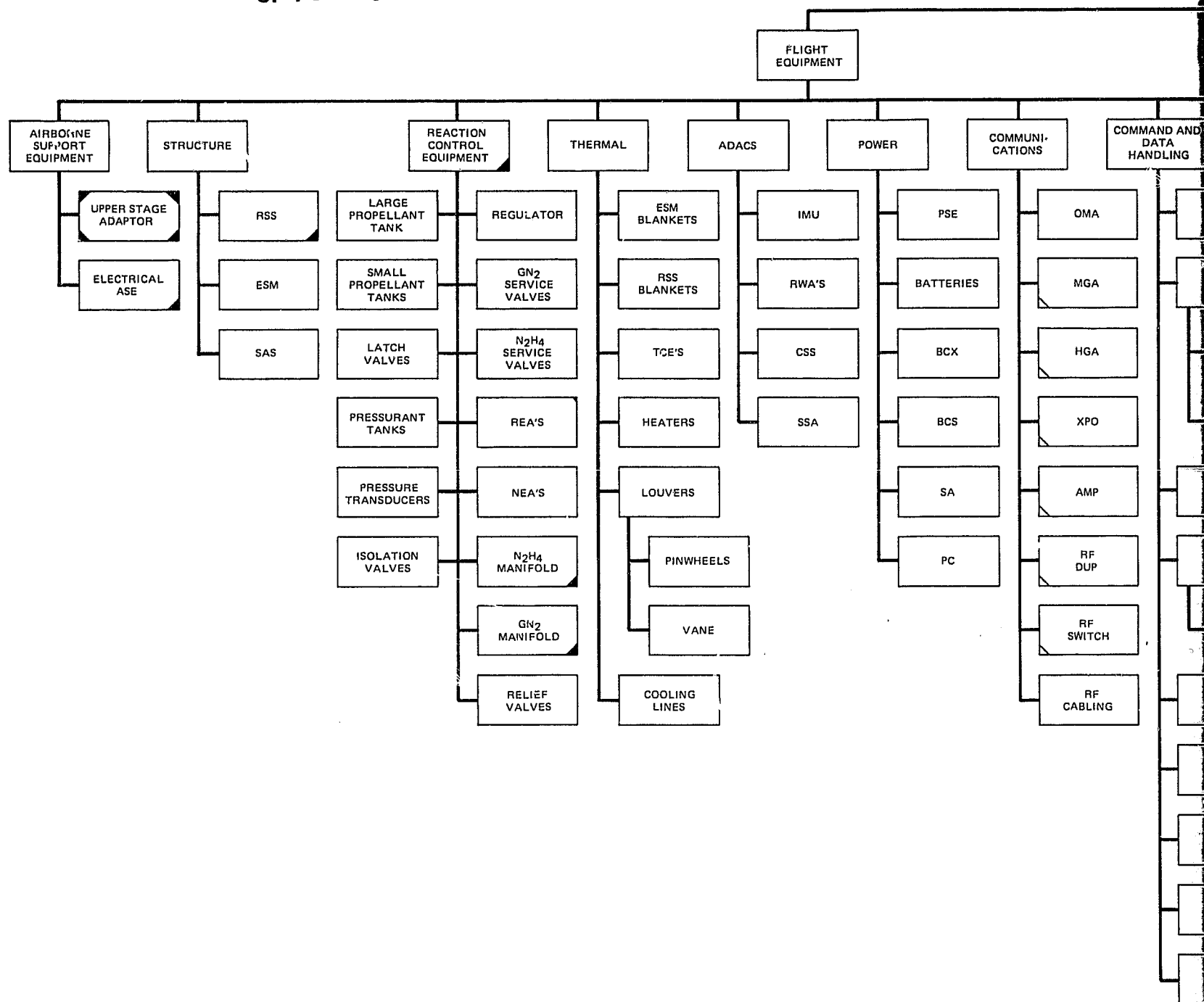
The two Asteroid spacecraft configurations, which will be described later in this section, heavily utilize the design concepts developed in the SAATN study, applying them to both the ATN and TIROS-N spacecraft. An all liquid monopropellant final or rendezvous propulsion system, which is an integral part of the spacecraft, has been selected for the Asteroid spacecraft. This system, with its relatively low thrust level, will permit a partial deployment of the solar arrays during the mission coast phase to support the spacecraft power requirements.

Of the five major mechanical sections that comprise a TIROS structure, 1) the instrument mounting platform (IMP), 2) the equipment support module (ESM), 3) the truss, 4) the reaction control system support structure (RSS), and 5) the solar array support structure (SAS), only the IMP is replaced for the Asteroid spacecraft. This is common when adapting the basic TIROS bus for other than its original meteorological mission since the IMP is unique to the payload complement.

The following paragraphs consist of a general description of the spacecraft-supplied hardware, starting at the inertial upper stage (IUS) and working out.

A new adapter will be designed to interface the aft portion of the RSS to the two-stage IUS which will be used to initiate the cruise phase from the STS orbit. The adapter will be a basic aluminum monocoque strengthened with

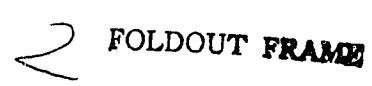
ORIGINAL PAGE IS  
OF POOR QUALITY



**FOLDFOLD**

## EOLDOUT FRAME

ASTEROID  
RENDEZVOUS  
SATELLITE



5-2



longerons, transitioning from the RSS diameter to the IUS interface diameter. The RSS end of the adapter will contain one-half of the separation connectors used to pass commands and telemetry between the spacecraft and Shuttle avionics. This end of the adapter will also contain one-half of the V-Band separation interface.

A Marmon band attachment system will connect the spacecraft to the IUS adapter during the initial phases of the mission. Following the firing of the IUS, the Marmon band will be pyrotechnically fired to separate the spacecraft. A two-bolt system with a cutter on each bolt will provide redundancy.

The next mechanical section, the RSS, is a 39-inch diameter, 32-inch long, cylindrical section comprised of aluminum skin strengthened with five external rings and many vertical internal longerons. All of the reaction control equipment (RCE) and portions of the power subsystem equipment are supported on the RSS. The large monopropellant tank is nested inside the cylinder, while the engines, gas tanks, plumbing, and other components are external to the cylinder. The batteries, battery charge assembly, and array drive electronics (ADE)\* are also located on the RSS. The top of the RSS interfaces with the truss section.

The truss is an 11-element titanium weldment which provides an interface between the symmetric RSS and the asymmetric ESM. Along with providing mechanical torsional stiffness, the truss provides thermal isolation for the ESM.

The ESM is a pentagonal figure generated from a regular hexagon with 20-inch sides and with one apex missing. This generates a fifth, larger side approximately 35 inches wide. The ESM is 77 inches long in Configuration 1 and 58 inches long in Configuration 2. The side, top, and bottom panels are aluminum honeycomb with integral machine-edged members that bolt into an aluminum ESM frame. The inside of the ESM houses the majority of the bus electronic boxes, while a portion of the instrument complement is supported on the outside of the larger ESM panel (Panel 1). During the launch phase, the solar arrays are stowed around the four regular sides of the ESM.

Atop the ESM is a structural element designed to support a portion of the payload or the high gain communications antenna, depending on the configuration.

The final structural element, the SAS, consists of the solar arrays and the attachment hardware to the spacecraft. The eight identical solar arrays utilize aluminum honeycomb substrates with stiffeners on the anti-cell side. The panels are interconnected with hinges and deployment mechanisms. A mast assembly is utilized to interface the two four-pack solar array assemblies with the boom. The boom is attached to the RSS in Configuration 1 and to the top of the ESM in Configuration 2.

---

\*The TIROS/DMSP ADE, solar array drive (SAD) and solar array telemetry commutator unit (SATCU) are not required for the mission considered in this study. Other mission concepts, using other than dawn/dusk Sun-synchronous orbits, would require this equipment.

### 5.1.3 ASTEROID CONFIGURATION

Two spacecraft configurations have been developed during the Asteroid study. Configuration 1, utilizing an ATN-type structure, is shown stowed and deployed in Figures 5.1-2 and 5.1-3, respectively. In this configuration, the gamma ray spectrometer (GRS), the multi-spectral mapper (MSM), the charge coupled device (CCD), the x-ray spectrometer (XRS), the magnetometer (MAG), and the altimeter antenna dish are either mounted on or supported from ESM Panel 1. The high gain antenna dish is mounted off the top of the ESM on a specially designed support structure which permits gimbaling about two axes to obtain Earth pointing. The solar array boom is attached to the IUS adapter end of the RSS in a manner similar to that of the present TIROS program. The mission orientation of this configuration always has the Earth basically along a normal to the ESM top panel (spacecraft -Z axis) and the asteroid along a normal to ESM Panel 1 (spacecraft +X axis). The spacecraft velocity vector is along the +Y spacecraft axis (formed by a right-handed coordinate system with the +X and +Z axes). Because of the Earth/Sun/asteroid geometry for this mission, the Sun will also always be along the spacecraft -Z axis; therefore, once oriented, the solar array does not require routine rotation.

Configuration 2 utilizes a different approach to the mission mode orientation, as well as a different basic bus. The smaller TIROS-N-sized spacecraft is configured as shown in Figure 5.1-4, when stowed, and Figure 5.1-5, when deployed. The MSM, the CCD, the XRS, and the altimeter dish are mounted on ESM Panel 1. A support structure on top of the ESM supports the GRS boom, the magnetometer boom, and the solar array boom. The high gain antenna dish is mounted on the RSS, again permitting two-axis steering. The Earth and Sun in this configuration are always near the spacecraft +Y axis, while the asteroid is still along the spacecraft +X axis. The velocity vector for this configuration is along the +Z axis. Note that either the ATN or the TIROS-N could be configured in either version.

### 5.1.4 WEIGHT SUMMARY

Since the TIROS-N (the smaller of the two) is more than adequate for the mission it was chosen as base line. A weight breakdown summary by subsystem is shown in Table 5.1-1 for the TIROS-N-based spacecraft. The weights for a majority of the components in the structure, the thermal, ADACS, power, data handling, tape recorder, and harness subsystems, are based on currently manufactured boxes for ATN and, consequently, are highly reliable. The tankage and other components for the propulsion system are based on estimates from the SAATN study and are also based on flight-proven components. As can be seen from this summary and the work in Section 4.2, either spacecraft can easily accomplish the mission to Anteros.

### 5.1.5 DEPLOYABLES

There are four deployment mechanisms used on each spacecraft configuration: the solar array panel deployment hinges, the boom deployment mechanism, the GRS mast, and the magnetometer mast. All of these deployment mechanisms are based on previously flown and flight-proven RCA Astro-Electronics designs.

The solar array panels are released from their stowed position along the ESM panels pyrotechnically by the use of redundant cable cutters. The first

ORIGINAL PAGE 13  
OF POOR QUALITY

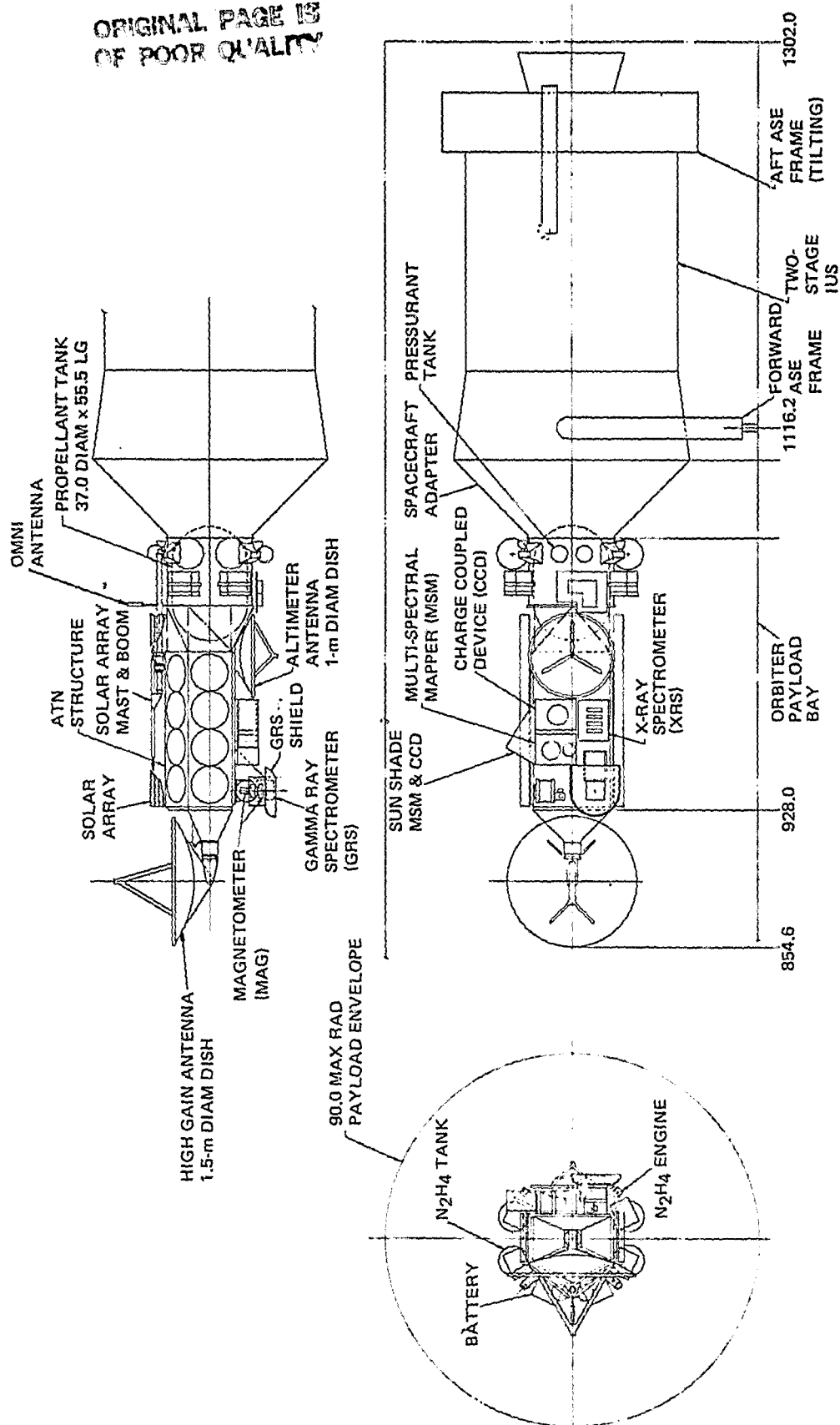


Figure 5.1-2. Configuration 1 - Stowed

ORIGINAL PAGE IS  
OF POOR QUALITY

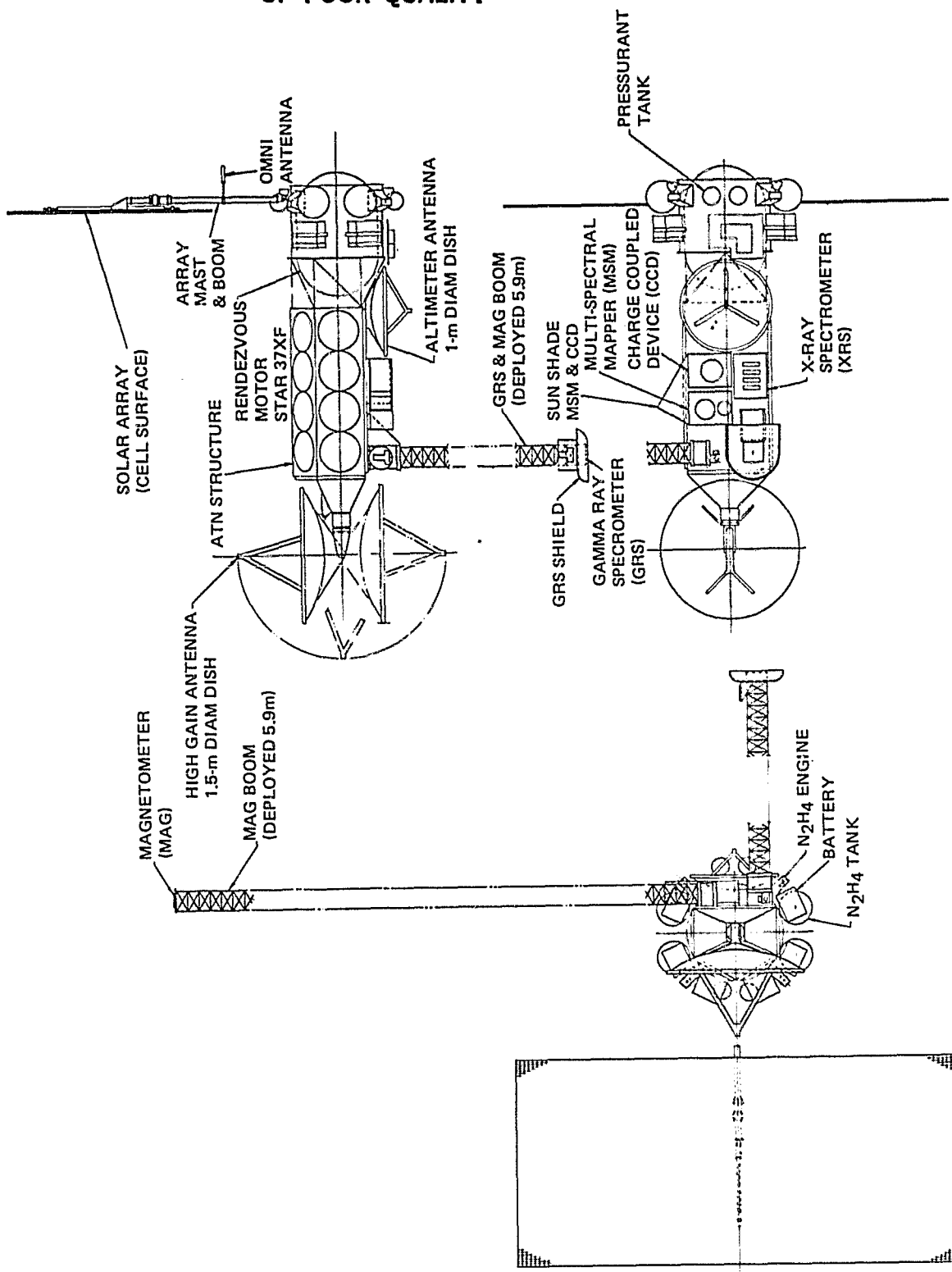


Figure 5.1-3. Configuration 1 - Deployed

ORIGINAL PAGE 19  
OF POOR QUALITY

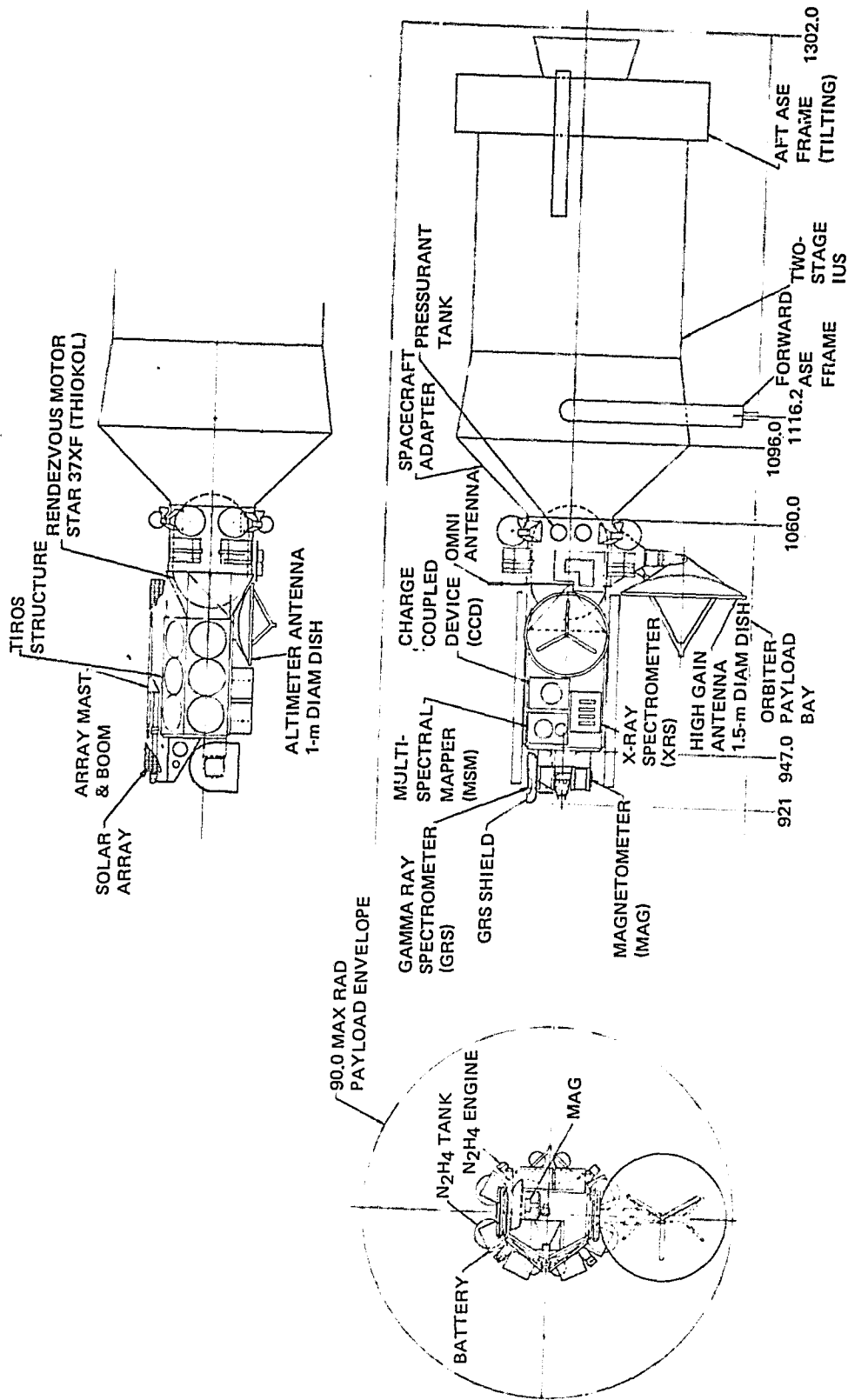


Figure 5.1-4. Configuration 2 - Stowed

ORIGINAL PAGE IS  
OF POOR QUALITY.

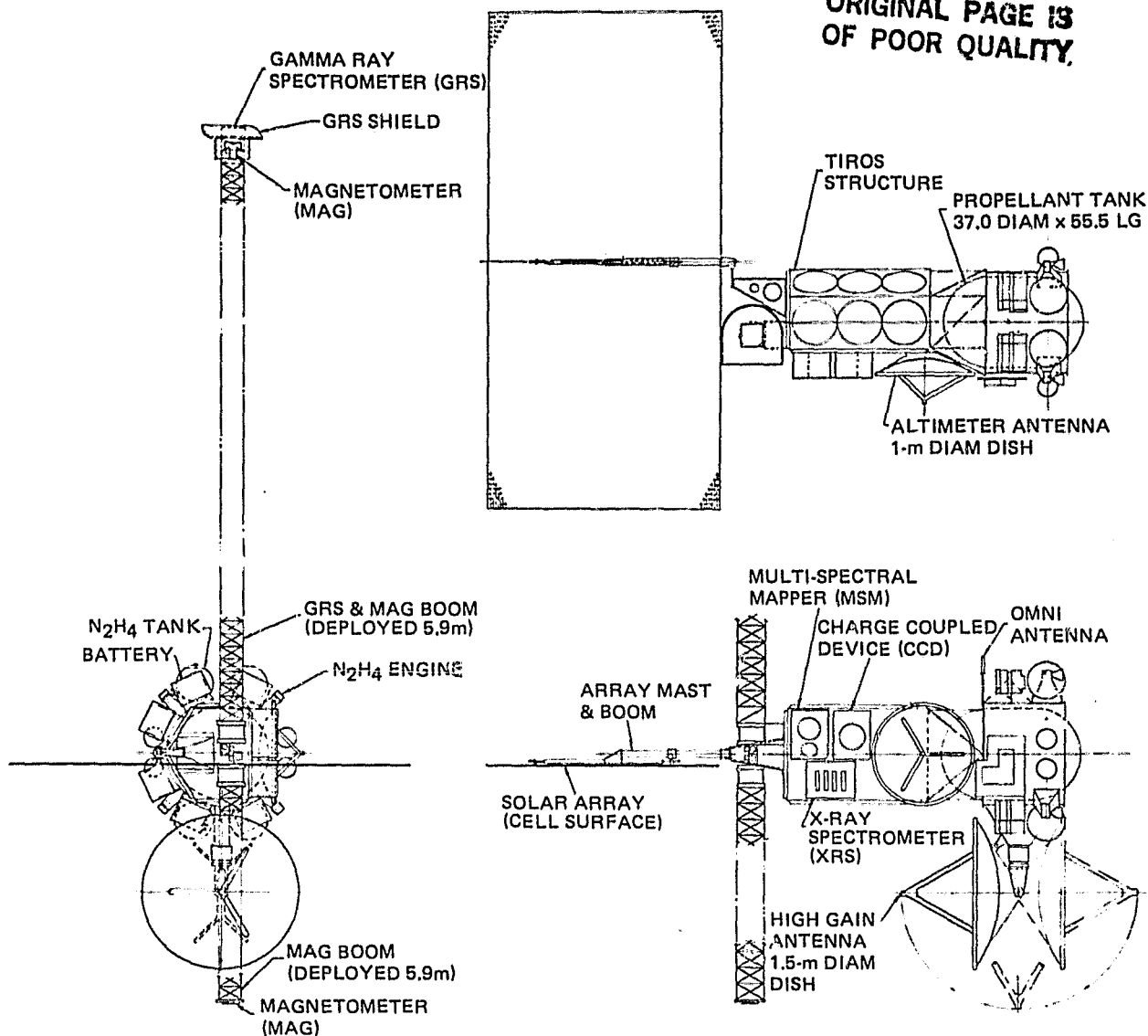


Figure 5.1-5. Configuration 2 - Deployed

deployment phase consists of the spring-energized, liquid damper, rate-controlled unfolding of the eight solar panels into a planar array which remains secured to the ESM apex (shown in Figure 5.1-6). The array remains in this configuration during the cruise phase of the mission. Upon attaining rendezvous with the asteroid, the final array deployment and orientation is initiated. The boom is released from its stowed position on the ESM apex by firing redundant pyrotechnic bolt cutters. This initiates the spring-activated 90° or 180° boom deployment for Configuration 1 or 2. After locking into this position, the array rotates either 180° or 90° about the boom axis to align the solar cell normal and the Sun vector.

The GRS and the magnetometer are deployed away from the spacecraft to prevent instrument data contamination due to the spacecraft. In both configurations, these deployments are affected using Astro booms with pyrotechnic initiators. The solar array hinge lines are similar to those used in the DMSP and TIROS programs, while the Astro booms have been demonstrated on the Atmosphere Explorer (AE) and Dynamics Explorer (DE) programs. Figure 5.1-7 shows the

ORIGINAL PAGE IS  
OF POOR QUALITY

TABLE 5.1-1. NOAA-D WEIGHT REPORT WITH ASTEROID VERSION OPTION

Assembly Name	Proposal 3/75	NOAA-D 3/82	Asteroid
Structure	239.7	290.0	219.5
Thermal	37.2	64.0	51.9
ADACS	114.0	121.3	75.9
RCE	73.0	75.0	*
Power	258.7	286.6	213.6
Communications	34.1	36.5	77.0
Commands & Control	41.4	55.4	55.4
Data Handling	25.3	34.2	66.5**
GFE Payload	382.6	491.6	198.0***
Payload Margin	-	16.4	-
Harness	91.0	110.3	92.7
Balance, Predicted	-	11.2	10.0
Balance, Margin	-	8.8	-
S/C Margin	267.0	-12.3	-
Mass Without Propulsion System	1491.0	1514.1	1060.5 (482 kg)
Propulsion Hardware	105.0	106.0	315.7†
S/C Dry Weight	1596.0	1620.1	1376.2
N <sub>2</sub> H <sub>4</sub>	36.0	37.9	2132.2†
GN <sub>2</sub>	5.0	5.0	150.4†
AKM Expendables	1463.0	1464.0	-
S/C Liftoff	3100.0	3127.0	3658.8 (1663 kg)
*Included in propulsion hardware weight **Includes 2 DTRs, the 5 DTRs on NOAA are in the GFE payload ***Estimated 90 kg †Anteros 1987 Mission, N <sub>2</sub> pressurant			

**ORIGINAL PAGE IS  
OF POOR QUALITY**

TABLE 5.1-1. NOAA-D WEIGHT REPORT WITH ASTEROID VERSION OPTION (Continued)

Structure			
Estimated/Actual Weights			
Assembly Name	Proposal 3/75	NOAA-D 3/82	Asteroid
truss	*	18.3	18.3
ESM	100.5	86.4	86.4
RSS	43.0	50.5	50.5
SAS	9.5	13.3	13.3
IMP	49.4	52.2	-
ESM Brackets	11.2	22.0	22.0
RSS Brackets	26.1	29.2	29.0
IMP Brackets	**	15.3	-
Box Configuration	-	-	-
Coating	-	2.0	-
AKM Nozzle	-	-	-
Shield	-	0.8	-
Structure	239.7	290.0	219.5 (99.0 kg)
*Included in ESM weight **Included in IMP weight			
Thermal			
Estimated/Actual Weights			
Assembly Name	Proposal 3/75	NOAA-D 3/82	Asteroid
TCL Louvers	-	11.7	11.7
THR Heaters & Radiators	-	6.3	6.3
TCE Electronics	-	5.6	5.6
THS Shields & Blankets	-	26.2	26.2



ORIGINAL PAGE IS  
OF POOR QUALITY

TABLE 5.1-1. NOAA-D WEIGHT REPORT WITH ASTEROID VERSION OPTION (Continued)

Thermal (Continued)				
	Estimated/Actual Weights			
Assembly Name	Proposal 3/75	NOAA-D 3/82	Asteroid	
MSU Louvers & Radiators	-	4.3	-	
IMP Sunshade	-	1.0	-	
RSS Sunshade	-	3.7	-	
Misc.	-	2.1	2.1	
RCE Heaters	-	3.1	3.1	
Thermal	37.2	64.0	51.9 (23.6 kg)	
ADACS				
	Estimated/Actual Weights			
Assembly Name	Qty per Equip	Proposal 3/75	NOAA-D 3/82	Asteroid
ESA	1	7.8	10.6	-
SSA	1	3.7*	1.8	-
IMU Assembly	1	22.5	22.2	22.7
RWA	4	33.2	34.0	34.0
PTC	1	1.9	2.2	2.2
RYC	1	4.0	4.2	4.2
CSA**	1	NA	NA	11.0
ADACS (Dry)		73.0	75.0	75.9 (34.4 kg)
*Proposal called for 2 Sun Sensor Assemblies (SSAs) **Celestial Sensor Assembly				

ORIGINAL PAGE IS  
OF POOR QUALITY

TABLE 5.1-1. NOAA-D WEIGHT REPORT WITH ASTEROID VERSION OPTION (Continued)

Power				
		Estimated/Actual Weights		
Assembly Name	Qty per Equip	Proposal 3/75	NOAA-D 3/82	Asteroid
Solar Array	1	87.7	121.9	121.9
SAD	1	8.4	9.6	-
ADE	1	6.0	5.1	-
Batteries:				
8-Cell	2	53.0	53.1	53.1
9-Cell	2	56.6	58.3	-
PSE	1	21.0	26.1	26.1
PC	1	1.1	1.1	1.1
BCA	1	10.6	9.0	9.0
PLR	1	14.3	-	-
BCS	2	2.4	2.4	
Power		58.7	286.6	213.6 (97.1 kg)
Communications				
		Estimated/Actual Weights		
Assembly Name	Qty per Equip	Proposal 3/75	NOAA-D 3/82	Asteroid
STX	3	5.7	5.8	-
VTX	2	4.4	3.6	-
BTX	2	3.0	3.4	-
BCD	1	-	1.7	-
CRD	1	4.5	5.0	-
RFF	6	2.5	8.2	-
Deep Space Transponder	-	-	-	30

ORIGINAL PAGE IS  
OF POOR QUALITY

TABLE 5.1-1. NOAA-D WEIGHT REPORT WITH ASTEROID VERSION OPTION (Continued)

Communications (Continued)				
		Estimated/Actual Weights		
Assembly Name	Qty per Equip	Proposal 3/75	NOAA-D 3/82	Asteroid
RFH	1	1.0	0.1	0.1
RFS	3	*	0.4	0.4
RFT	1	1.0	0.0	-
SBA	3	2.1	0.5	0.5
VRA	1	2.0	3.7	3.7
BDA	1	1.5	1.7	1.7
UDA	1	2.5	2.3	2.3
SOA	2	0.6	0.1	0.1
HGA & Assembly	1	-	-	27.7
Communications		34.1	36.5	66.5 (30.2 kg)
*Proposal had 3 FSAs and 3 SBSs, with a total weight of 3.3 lb				
Command and Control				
		Estimated/Actual Weights		
Assembly Name	Qty per Equip	Proposal 3/75	NOAA-D 3/82	Asteroid
WCU	1	7.0	7.1	7.1
CIU	1	17.2	21.4	21.4
CPU-1	1	7.9	13.3	13.3
CPU-2	1	7.9	11.8	11.8
RXO*	1	1.4	1.8	1.8
Command and Control		41.4	55.4	55.4 (25.2 kg)
*Optional				

ORIGINAL PAGE IS  
OF POOR QUALITY

TABLE 5.1-1. NOAA-D WEIGHT REPORT WITH ASTEROID VERSION OPTION (Continued)

Data Handling				
		Estimated/Actual Weights		
Assembly Name	Qty per Equip	Proposal 3/75	NOAA-D 3/82	Asteroid
TIP	1	10.0	14.1	13.1
MIRP (ADP)	1	9.0	10.6	10.6
XSU	1	6.0	9.1	8.4
SATCU	1	-	0.4	-
Data Handling		145.3	34.2	32.1 (14.6 kg)
DTR	2	*	*	44.9
TOTAL				77.0 (34.9 kg)
*DTR part of payload (GFE) on TIROS				
Harness				
		Estimated/Actual Weights		
Assembly Name		Proposal 3/75	NOAA-D 3/82	Asteroid
IMP		-	8.6	-
ESM:				
Tie-Downs		-	1.4	1.4
SPG		-	0.7	0.7
ESM		-	63.1	63.1
PLG		-	-	-
RSS		-	19.7	19.7
RFC		-	7.8	7.8
SEM		-	9.0	-
Margin		-	-	-
Harness		91.0	110.3	92.7 (42.1 kg)

TABLE 5.1-1. NOAA-D WEIGHT REPORT WITH ASTEROID VERSION OPTION (Continued)

	Center of Gravity				Moments			Products		
	(Pounds)	(Inches)			(Inch-Pound-Second <sup>2</sup> )			(Inch-Pound-Second <sup>2</sup> )		
	Spacecraft	X	Y	Z	I <sub>x</sub>	I <sub>y</sub>	I <sub>z</sub>	I <sub>xz</sub>	I <sub>yz</sub>	I <sub>xy</sub>
Lift-Off	3127.0	0.0	0.0	-54.4	13557.0	13249.0	2109.9	-177.7	-118.9	38.3
AKM Ignition*	3122.4	0.0	0.0	154.4	13523.0	13221.0	2103.0	-77.7	-118.8	36.6
AKM Burnout*	1655.9	0.0	0.0	-74.5	9326.8	9027.7	1551.6	-177.7	-118.7	35.8
Spacecraft in Orbit										
End ΔV Trim*	1640.4	0.0	0.0	-75.1	9117.0	8837.2	1528.1	-177.6	-118.7	29.9
Solar Array Deployed*	1640.1	-1.4	0.0	-62.9	16373.0	15515.0	2523.9	-1458.4	-118.8	29.9
Antennas Deployed*	1640.1	-1.4	0.0	-63.0	16388.0	15550.0	2525.2	-1456.7	-100.9	31.5
Antennas Deployed Less Solar Array	1504.9	0.7	0.0	-74.7	8740.0	8511.7	1336.1	-166.5	-101.0	31.5
*Inertia reports estimated by taking NOAA-C Deltas from NOAA-D liftoff.										
NOTE: This table is for NOAA-D and is presented as typical inertia and CG parameters. Recomputation for the Asteroid mission was considered beyond the scope of the study and would be premature at this time.										

spacecraft in the fully deployed on-orbit configuration with all deployables extended.

## 5.2 PROPULSION SUBSYSTEM

### 5.2.1 INTRODUCTION

After injection and separation from the IUS, the spacecraft propulsion subsystem is required to maintain attitude control and perform various trajectory change maneuvers throughout the coast phase. At asteroid encounter, it will perform all terminal rendezvous and subsequent stationkeeping maneuvers.

ORIGINAL PAGE IS  
OF POOR QUALITY

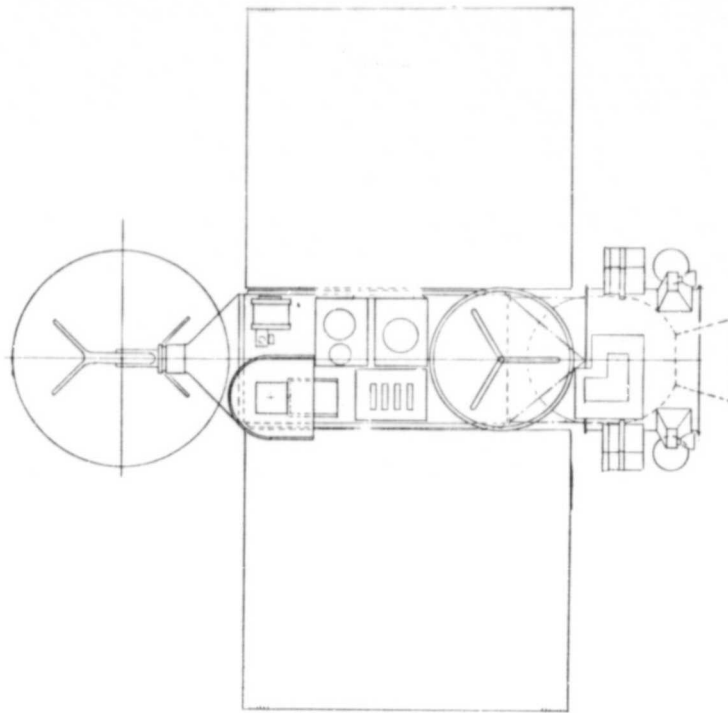


Figure 5.1-6. Configuration 1 - Cruise Mode

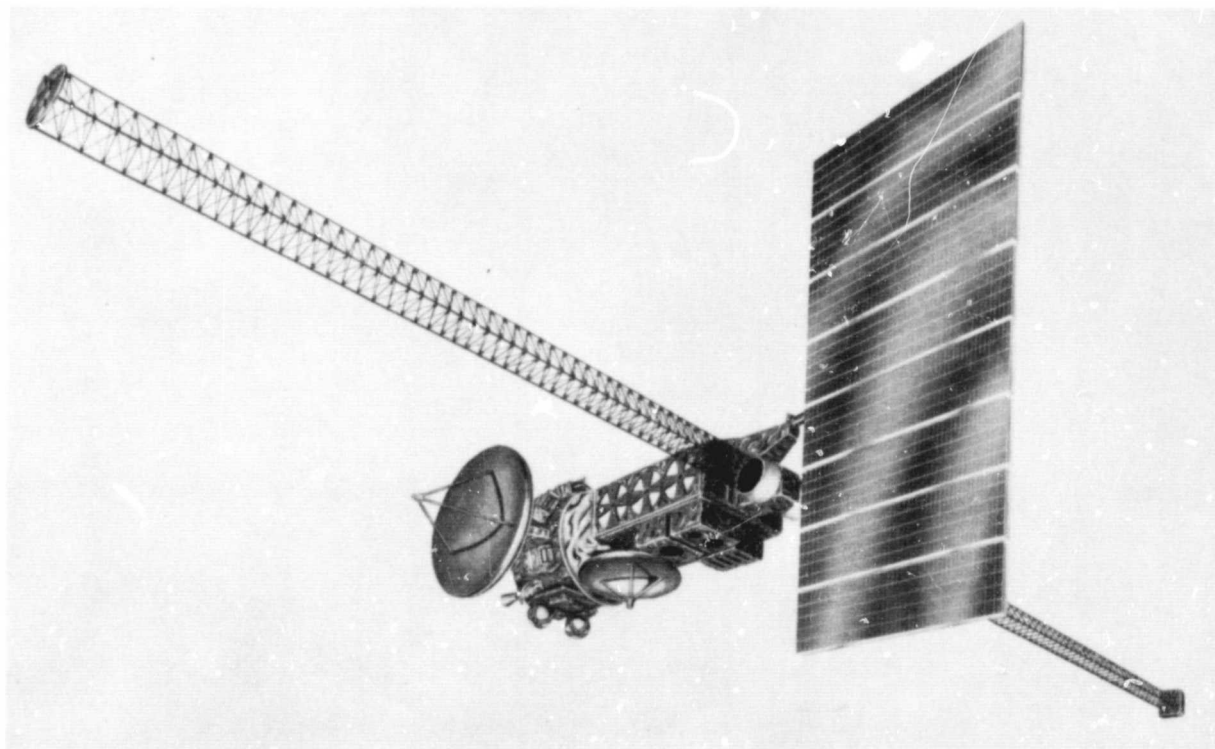


Figure 5.1-7. Fully Deployed On-Orbit Configuration

From the outset, in designing the propulsion subsystem, an attempt has been made to utilize the present TIROS/DMSP design. For the most part, this has been possible; however, some changes have been incorporated. Such changes are a result of design considerations imposed by specific mission requirements and launch vehicle constraints. These are discussed more fully in Section 5.2.2.

### 5.2.2 DETAILED SUBSYSTEM DESIGN

The proposed subsystem design is shown in schematic form in Figure 5.2-1. This differs from the TIROS/DMSP design primarily in three ways. First, the subsystem is configured to meet the safety requirements of NHB 1700.7, imposed as a result of flying on board the STS launch vehicle. A summary of requirements and responses is given in Table 5.2-1. The hardware changes include the addition of four latch valves.

Second, all translation maneuvers are now performed by the four hydrazine monopropellant 100-lbf (445N) engines, without the use of a solid kick motor, to accommodate the terminal rendezvous burn. Therefore, the number of propellant and pressurant tanks has been increased to allow for the greater propellant capacity requirements. The solid motor has been replaced by the hydrazine engines to reduce the maneuver acceleration levels, thereby allowing the solar array to be partially deployed in the transfer orbit. Off-the-shelf propellant tanks are available, namely the 33-inch (84 cm) long, "teardrop," Ti 6Al 4V tanks presently being flown on the LEASAT and SAL programs. To maintain propellant orientation in the low-g environment, a new propellant management device (PMD) is required. This should not have any significant impact on the qualification status of these tanks and RCA has demonstrated on our communications satellites the capability to design such a PMD. The pressurant tank is identical to that proposed to fly on the Intelsat-VI spacecraft. This tank consists of a spherical, Kevlar fiber, structural case with a stainless steel leak barrier. Similar designs have already flown on the STS and on the INSAT spacecraft. As presently envisaged, the propellant tanks will be mounted to the spacecraft exterior using specially designed fixtures. The volume of the propellant tanks will fit in the space vacated by the solid motor.

Since each asteroid target has a different energy requirement and, hence, hydrazine propellant load, the number of tanks (both propellant and pressurant) is mission-specific. It is also dependent on whether helium or nitrogen pressurization is adopted since this decision has a significant impact on initial spacecraft throw-weight and, therefore, propellant load. Table 5.2-2 details the tank configuration as a function of both mission and pressurant. Presently, the base line design assumes the use of nitrogen as the pressurant.

The third change, relative to the TIROS/DMSP design, is the addition of eight more cold-gas attitude control thrusters. Introducing an extra set of gas thrusters removes the possibility of a stuck-open thruster failing the mission by expelling all the pressurant. Should this condition now occur, the failed thruster can be isolated by the latch-valve controlling that branch, and the redundant branch used instead. TIROS/DMSP uses magnetorquers as a backup to the gas engines; however, this option is not available in the greatly reduced magnetic environment of the asteroid belt.

Hardware to be used in the propulsion subsystem is listed in Table 5.2-3.

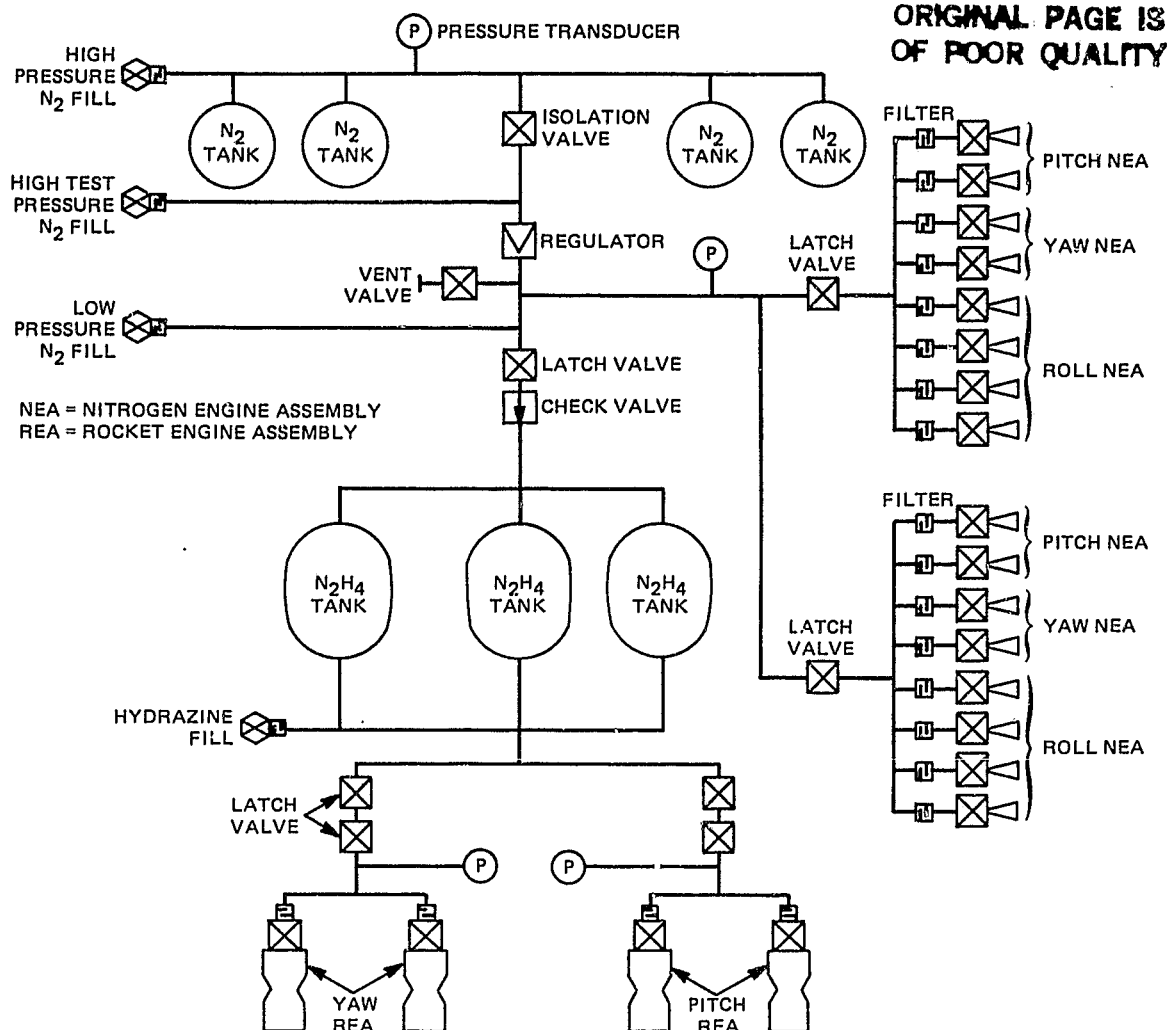


Figure 5.2-1. STS Propulsion Subsystem Configuration Schematic

### 5.2.3 PROPULSION SUBSYSTEM OPERATION

The propulsion subsystem is activated after separation from the STS upper stage. The following paragraphs describe qualitatively the mission sequence and operation. As shown in Figure 5.2-1, high pressure gas is stored in four Kevlar-wrapped tanks at an initial pressure of 4000 pounds-per-square-inch, absolute (psia). This storage manifold is isolated from the regulator and the low pressure, gas distribution manifold by a normally closed, pyrotechnic valve as a safety feature for all pre-launch and STS Orbiter in-bay functions. At launch, the propellant tanks are kept at a low pressure of about 80 psia to ensure propellant stability. Either just prior to, or immediately after upper stage separation, the propellant isolation latch valves are commanded open to prime the propellant lines. This is done before firing the normally closed, pressurant pyro-valve, so that priming is done at the lowest available pressure and thus precluding possible damage to the propulsion hardware. After priming, the isolation valve is fired to the open position, allowing the



ORIGINAL PAGE IS  
OF POOR QUALITY

TABLE 5.2-1. STS SAFETY REQUIREMENTS, NHB 1700.7

Section No.	Requirement	Method of Compliance
202.2	Premature propellant delivery prevented by inclusion of three electrical inhibits and in-flight monitoring and safing by flight crew	(1) Valve actuation is a commanded function (2) Electrical power to valves is from a bus that is timer activated (3) Timer is inhibited until satellite separation Monitoring and overrides of above are provided
202.2B	Three mechanically independent flow control devices; monitoring determined by safety review	Thruster solenoid valves plus two in-series latch valves between tanks and thrusters with dry lines below tank outlet latch valves; latch valves have position monitors
208.4	Pressure vessels have ultimate safety factor of 1.5 and cycle life of twice expected maximum	Qualification demonstration of design levels
208.5	Lines and fittings have ultimate safety factor of 4.0	Qualification demonstration of design levels
210.1 210.2 210.3	Pyrotechnic devices meet MIL-STD-1412	NSI or equivalent initiators will be used
202.2	Catastrophic hazard function (namely, premature firing of pyrotechnic isolation valve followed by regulator failure) must be controlled by three inhibitors	(1) Valve actuation is a commanded function (2) Bus power is activated by a timer (3) Timer is inhibited prior to separation
206	Design shall preclude failure propagation from the payload to the environment outside the payload	The pyrovalve isolation of the high-pressure supply prevents tank failure due to a regulator failure

TABLE 5.2-2. ASTEROID PROPULSION SYSTEM REQUIREMENTS

Mission Objective	Anteros								Eros	
	5/27/87		6/6/87		5/22/90		5/25/92		1/25/89	
Launch Date	1888		2011		1525		1312		1936	
Mission $\Delta V$ (m/s)	1888		2011		1525		1312		1936	
Pressurant	He	N <sub>2</sub>	He	N <sub>2</sub>	He	N <sub>2</sub>	He	N <sub>2</sub>	He	N <sub>2</sub>
Pressurant Wt (kg)	10.6	68.2	13.1	69.5	7.9	51.6	7.7	36.7	10.6	68.7
Propellant Wt (kg)	856	967	970	1115	585	634	460	490	899	1022
System Wt (kg)	132.4	143.2	164.0	143.2	100.6	111.5	100.6	79.7	132.4	143.2
Full-Up Propulsion Weight (kg)	999	1178	1147	1328	694	797	568	606	1042	1234
No. of N <sub>2</sub> H <sub>4</sub> Tanks										
33" Teardrop (Ti 6Al 4V)	3	4	4	4	2	3	2	2	3	4
No. of Pressurant Tanks, 21.2" Spheres (Kevlar)	4	4	5	4	3	3	3	2	4	4

**ORIGINAL PAGE IS  
OF POOR QUALITY**

TABLE 5.2-3. BASE LINE FEED SYSTEM COMPONENTS SUMMARY

Component	Vendor	Heritage
Hydrazine Thruster	Rocket Research	Voyager
Propellant Tank	PSM Fansteel	LEASAT, SAL
Pressurant Tank	ARDE	Proposed I-VI Tank
Pressure Regulator	Marotta	TIROS-N, DMSP
Latch Valve, GN <sub>2</sub>	Hydraulic Research	TIROS-N, DMSP
Latch Valve, N <sub>2</sub> H <sub>4</sub>	Consolidated Controls	Skylab
Isolation Valve, GN <sub>2</sub>	Pyronetics	TIROS-N, DMSP
Vent Valve	Carleton Controls	TIROS-N, DMSP
Pressure Transducer	Statham	TIROS-N, DMSP, Satcom, NOVA
Check Valve	Carleton Controls	Satcom
N <sub>2</sub> H <sub>4</sub> Service Valve	Pyronetics	TIROS-N, DMSP, Satcom
GN <sub>2</sub> Service Valve	Pyronetics	TIROS-N, DMSP, Satcom
Nitrogen Thrusters	Wright Components	TIROS-N, DMSP

pressurant to flow through the single-stage regulator, which reduces the outlet pressure to 360 psia.

The low pressure manifold is protected from regulator failure (overpressure) by an overboard vent through a pressure-actuated relief valve. The regulated pressure supply is used for pressurizing the hydrazine propellant tank and for thrusting through the cold-gas thruster assemblies. The gas thruster halfsets are manifolded through latch valves; these are used to provide isolation and a redundant seal to the thruster valves to reduce on-orbit leakage potential. The pressurization line to the hydrazine propellant tanks contains a latch valve and a check valve to prevent reverse flow of the propellant into the nitrogen manifold. Three pressurant fill valves are included in the manifold to provide entry points for pressurization and acceptance testing. Two pressure transducers are located in the gas manifold; one provides monitoring of the high pressure storage system, while the other monitors the regulator outlet pressure.

The hydrazine monopropellant is stored in multiple titanium propellant tanks. A surface-tension propellant management device is located over the outlet to provide gas-free flow to the hydrazine thrusters during zero or adverse gravity-start operations.

The tank-outlet manifold splits into two branches, with each supplying propellant to two thrusters. One branch feeds the two yaw torque thrusters, and the other feeds the two pitch thrusters. Each branch also contains two latch valves in series to meet the STS safety requirements. A hydrazine fill valve is included upstream of the latch valves to permit propellant loading in the tank while the manifold remains dry below the valves. The dry manifold is required to meet STS safety requirements. Pressure transducers are located in the manifold branch lines downstream of the latch valves to verify the line-priming event and monitor the feed pressure to the engines.

All four hydrazine engines are operated simultaneously to provide the transfer orbit and rendezvous velocity increments. The parallel arrangement of the thrusters permits a failure-mode velocity capability with either of the two sets of engines operational. The same total impulse could still be obtained from the system. Steering during velocity thrusting periods is accomplished by off-pulsing the appropriate hydrazine engine, with roll control about the thrust axis being achieved by pulsing the gas thrusters. Three-axis reaction forces during coast periods and in the final operational orbit are provided by pulsing the gas thrusters. Momentum wheel dumping is also accomplished by pulsing the cold-gas engines. All of these hydrazine and cold gas maneuvers have been demonstrated on TIROS-N and DMSP.

### 5.3 ATTITUDE CONTROL SUBSYSTEM

#### 5.3.1 ATTITUDE CONTROL SYSTEM (ACS) OVERVIEW

The attitude determination and control subsystem (ADACS) is a zero-momentum, four reaction wheel system using as a base line pressurized nitrogen ( $\text{GN}_2$ ) thrusters for momentum desaturation. Attitude reference measurements are provided by a star tracker, a nadir sensor, a Sun sensor, and gyros. The ADACS orients the spacecraft inertially during the cruise phase to provide illumination of the solar array and a secure communications link with the Earth. The spacecraft is nadir-oriented during the terminal navigation phase and during the on-orbit science phase. An autonomous solar reacquisition capability to a safe-hold mode is provided to insure the safety of the spacecraft in the event that attitude lock is ever lost. The primary differences in hardware between the ADACS for the Asteroid mission and the DMSP system are that they use different star and nadir sensors. Otherwise the two systems are functionally equivalent.

The most stringent attitude control system requirements are those imposed by the multispectral mapper (MSM) during the operations orbit phase. The preliminary requirements derived from the Galileo near infrared mapping spectrometer (NIMS) are as follows:

Knowledge of attitude with respect to an orbital reference frame	1 mR
Absolute pointing error including control errors and knowledge uncertainty	2 mR
Pointing stability	20 $\mu\text{R}/\text{sec}$

### 5.3.2 BASE LINE DESIGN SUMMARY

Table 5.3-1 shows a summary of the ADACS requirements for the various phases of the Asteriod mission as derived from interpretation of the specified requirements. Table 5.3-2 shows a comparison of the key elements of the ADACS design required to meet the specifications of the Asteroid missions along with the demonstrated capability of the DMSP spacecraft. This table clearly indicates the fundamental suitability of the DMSP system for the Asteroid mission. A nadir orientation of the spacecraft is a natural selection for the on-orbit phase of the mission because it is the simplest method of accommodating the science requirements. A base line dawn-dusk orbit provides full solar array illumination without active tracking of the Sun. This orbit also results in a simple conical high gain antenna (HGA) earth track, at once per orbit, with a cone angle of less than  $35^\circ$ . Other orientations of the orbit plane with respect to the Sun line can be accommodated by using techniques that are routinely employed on the DMSP and TIROS spacecraft. These techniques include: 1) actively driving the solar array about the pitch axis; 2) deploying the array to a preselected, fixed cant angle from the drive axis; and 3) performing commanded yaw maneuvers to keep the Sun on a desired side of the spacecraft. Figure 5.3-1 shows a block diagram of the basic ADAC subsystem.

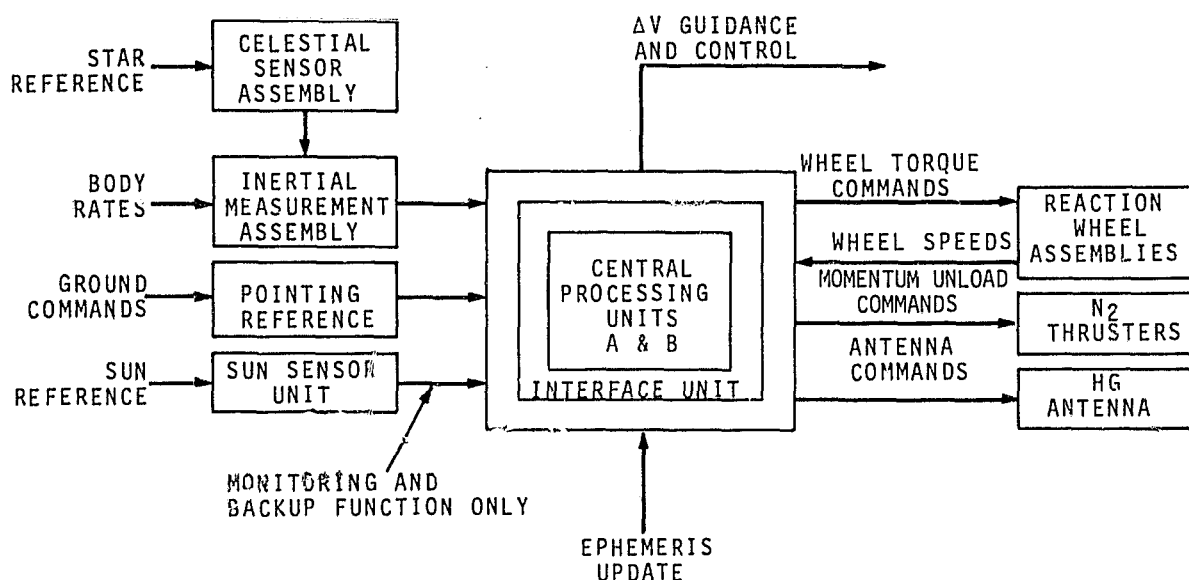


Figure 5.3-1. Simplified Block Diagram of the Attitude Determination and Control Subsystem (ADACS)

There would be some design changes to the spacecraft if it became necessary to accommodate a continuously changing, arbitrary orientation of the orbit plane with respect to the Sun line. For example, a two-axis solar array drive would be required, and the angular freedom of the HGA gimbals would have to be greatly increased. For these reasons it is desirable to design the science mission, perhaps by extending its duration, to take greater advantage of periods of favorable Earth-asteroid-Sun geometry.

ORIGINAL PAGE IS  
OF POOR QUALITY

TABLE 5.3-1. ADACS REQUIREMENTS FOR ASTEROID MISSION

Boost Phase:	All functions provided by STS/IUS
Cruise Phase:	Control orientation of spacecraft to satisfy power/thermal constraints; periodical control orientation of high gain antenna
Initial Rendezvous Phase:	Orient for $N_2H_4$ motor firing; inertial orientation commanded from ground
Terminal Rendezvous Phase:	Orientation and firing time, and firing sequence, commanded from ground - requirements determined from imager (per JPL approach)
Mission Phase:	Slowly varying inertial orientation, or IRPO orientation; solar array oriented normal to Sun; high gain antenna oriented to Earth

TABLE 5.3-2. ADACS DESIGN FOR ASTEROID MISSION AS COMPARED TO DMSP

All functions for all phases demonstrated on DMSP*	
Functional Comparison	
Asteroid Mission	DMSP Mission
IRPO mission phase	IRPO (one revolution/100 minutes) within $0.01^\circ$ pointing accuracy with inertial/celestial reference
Inertial orientation (motor firing and $\Delta V$ maneuvers)	Inertial orientation (motors firing and $\Delta V$ maneuver)
Control during large disturbance (motor firing)	Control during large disturbance (motor firing)
Maintenance of body-fixed axis to slowly rotating inertial reference (Sun)	Maintenance of body-fixed axis to slowly rotating inertial reference (Sun-synchronous orbit normal)
Open loop pointing of appendage (high gain antenna)	Open loop pointing of appendage (solar array)
Momentum dumping ( $GN_2$ system)	Momentum dumping (MAG system with $GN_2$ back-up)
*One exception - acquisition on DMSP done closed loop through horizon sensor; on Asteroid mission through open loop commands based on imager	

C-2

### 5.3.3 ATTITUDE CONTROL SUBSYSTEM BASE LINE DESIGN

#### 5.3.3.1 Cruise Injection and Cruise Control

It has been assumed for the purpose of this study that the two-stage IUS is the basic launch vehicle. Thus, the spacecraft is virtually inert from the time of the STS launch to the post-IUS separation and no guidance control or attitude control functions are required until this separation occurs. The cruise navigation requirements on the ACS are essentially a subset of the on-orbit requirements and will be accomplished with the star trackers and ground determined mid-course maneuvering. The key to simplified control during this mission phase is the ability to save the spacecraft in the case of attitude reference loss. The basic philosophy used to cope with this occurrence is described in Section 5.3.4. The base line attitude control system is shown in Figure 5.3-1.

#### 5.3.3.2 Asteroid Orbit Injection Control

The injection attitude control system is functionally equivalent to the hydrazine trim burn attitude control system design employed on TIROS-N/ATN. The system must: 1) orient the thrust axis for the orbit adjust burns, 2) maintain the orientation during the burns, and 3) provide coarse inertial pointing at other times. During the hydrazine burns, motion about the thrust axis is controlled by the gas thrusters, and motion about the two transverse axes is controlled by off-pulsing the hydrazine engines. In the event of a single failure of a hydrazine engine, the opposite hydrazine thruster will be deactivated and gas thrusters will be used for control about that transverse axis. All three axes are controlled by the gas thrusters during reorientation maneuvers and attitude hold prior to transfer to reaction wheel control. The system design goals, based upon the results of the guidance system analysis, are to provide control to within  $1.0^\circ$  about the thrust axis and to within  $0.2^\circ$  about the transverse axes. The target attitude, desired velocity change, and hydrazine engine burn duration are commanded from the Earth. Hydrazine engine shutdown will occur when either the commanded burn duration is reached or the output of an integrating accelerometer mounted along the thrust axis equals the commanded change in velocity.

#### 5.3.3.3 On-Orbit Control

A functional block diagram of the primary ADACS is shown in Figure 5.3-2.

The on-orbit attitude control system uses the reaction wheels to provide control torques and the gas thrusters to provide desaturation torques. The system is functionally equivalent to the TIROS-N back-up attitude control system which uses gas thrusters rather than magnetic torquers for desaturation. One of two different modes of operation of the system is employed, depending on the mission phase. During the cruise phase, the system tracks a commanded inertial orientation. After acquisition of the asteroid, the control system follows a commanded nadir orientation that is computed on-board from the inertial attitude and the ephemeris. This second mode is identical to the normal on-orbit mode of the DMSP control system, except that the star tracker provides continuous attitude measurements for the Asteroid mission whereas the DMSP star scanner provides intermittent attitude updates to the gyros.

ORIGINAL PAGE IS  
OF POOR QUALITY

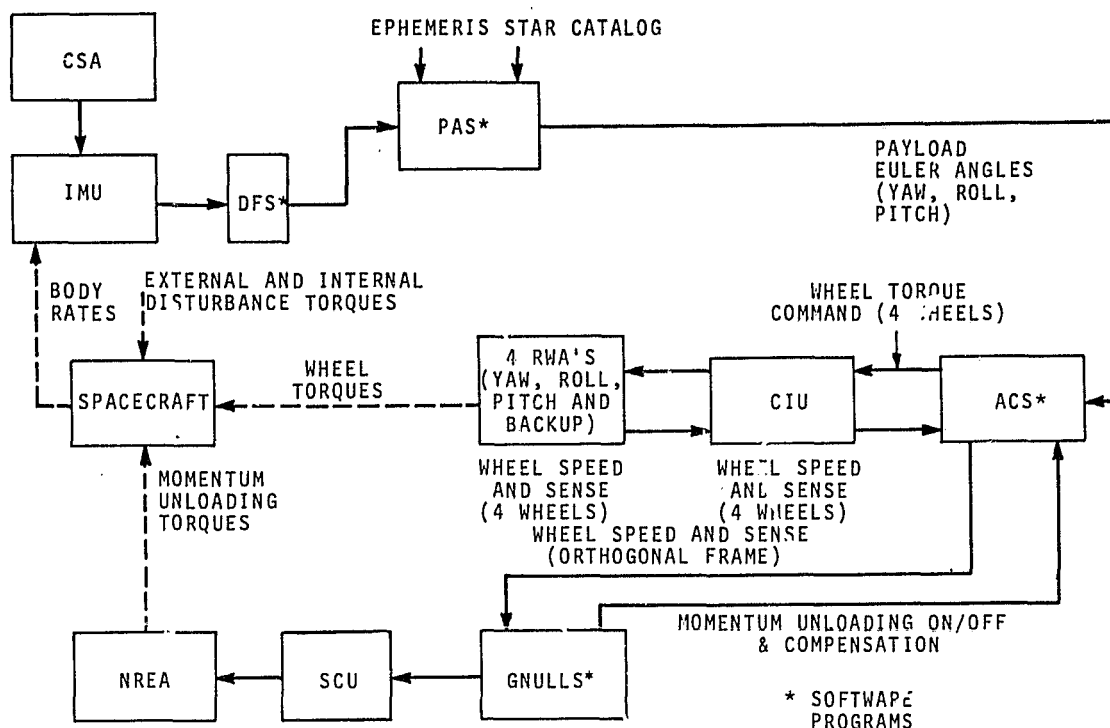


Figure 5.3-2. Primary ADACS Functional Block Diagram

The star tracker has been chosen to replace the DMSP star scanner for two reasons. First, the star scanner is totally inappropriate for missions involving extended periods of inertial reference tracking such as during the cruise phase of the Asteroid mission. Second, the DMSP system is designed for the relatively rapid orbit-rate scan of the star field provided by a low altitude planetary orbit. The orbital rate around an asteroid is likely to be 20 times slower to insure a stable orbit. Consequently, the attitude update rate will be 20 times slower, and gyro drift would seriously degrade the accuracy of a star scanner type system.

A nadir sensor is required in order to establish the relative orientation of the spacecraft and asteroid during the terminal navigation phase of the mission. The Galileo-derived CCD imager with 200 mm optics and 50 x 50 milliradian field of view can provide a suitable nadir reference during most of this mission phase. The dynamic range of the instrument as a nadir sensor is from less than 100 km to more than 100,000 km for most Earth-approaching asteroids. Ground control utilizing CCD telemetry will be sufficiently accurate to maintain the asteroid in the center of the field of view of the imager throughout this altitude range. However, accurate open loop nadir pointing control based on imager telemetry is not feasible for spacecraft-asteroid ranges on the order of 10 km. The difficulties encountered at this altitude stem from the higher rates of change of the relative orientation and the large apparent diameter of the asteroid compared to the field of view of the imager.



#### 5.3.4 SAFE-HOLD CONTROL SYSTEM

The safe-hold control system is provided to ensure the safety of the spacecraft in a powered-up state in the event of a loss of attitude lock from one of the other control modes. The safe-hold mode is entered automatically whenever the on-board computer detects either loss of attitude reference or excessively large attitude errors or body rates. The system inhibits the firing of the hydrazine engines and removes power from the reaction wheels. The gyros are used to fire the gas thrusters so that an appropriate body rate is established to bring the Sun into the field-of-view of the Sun acquisition sensor. This attitude is then held while ground controllers determine corrective measures to restore the spacecraft to an acceptable configuration.

No hardware changes are required to the ADAC subsystem driven by these considerations. A large number of the basic software algorithms can be applied directly and/or derived from the existing architecture of the TIROS/DMSP software.

#### 5.4 POWER SUBSYSTEM

An asteroid rendezvous with a TIROS/DMSP satellite poses three distinct problems for the power subsystem design. Energy balance must be met during three phases of the satellite mission: 1) the launch and drift phase associated with a Shuttle launch, 2) the cruise phase, and 3) the mission phase. The crucial phase is the one that requires the satellite to operate at 1.8 AU. When traveling from 1 AU to 1.8 AU, the solar array is required to operate at cold temperatures and low solar intensity input. The power available for mission loads is affected by the power subsystem design. There are two design options under consideration for the Asteroid satellite, the present SAATN power subsystem design and a maximum power point tracking system.

Adopting the SAATN power subsystem implies the use of a boost discharge direct energy transfer (DET) power subsystem. A block diagram of this power subsystem is shown in Figure 5.4-1. The primary source is a single-axis-oriented solar array with a secondary source of three nickel cadmium batteries. The power subsystem output consists of a regulated +28-Vdc bus and a +5-Vdc bus. The major components are the solar array, batteries, power supply electronics (PSE), battery charge assembly (BCA), and power converter (PC). (The solar array drive (SAD), and array drive electronics (ADE) may be required for alternate missions.)

During the cruise and mission phases, the ADAC system maintains the solar array for normal Sun incidence. The solar array supplies current to the PSE during normal daytime operation. Power above that required by satellite loads and battery charging is dissipated by partial shunts located on the array so that the excess power is dissipated outside the main modules of the satellite.

The three batteries (each having a capacity of 26.5 ampere hours) supply power through the boost regulator when required. Each battery consists of two battery packs. A mode controller senses the +28-Vdc bus voltage and operates the partial shunts and/or charge regulator to maintain regulation. The power converter derives +5-Vdc regulated power (which is used to power interface circuits) from the +28-Vdc regulated power.

ORIGINAL PAGE IS  
OF POOR QUALITY

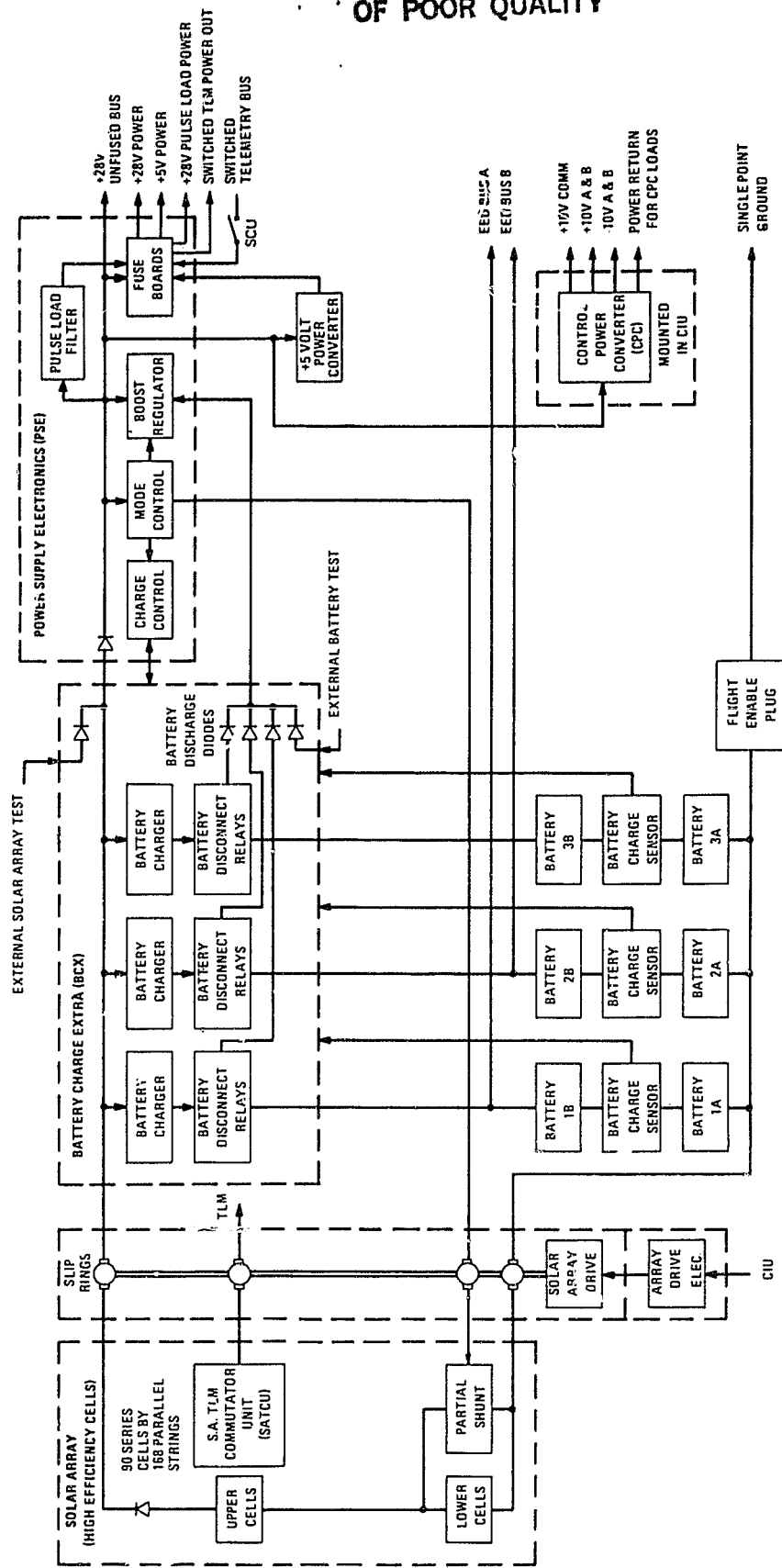


Figure 5.4-1. SAATN Power Subsystem Block Diagram

Automatic switchover occurs from primary to back-up circuitry for the boost regulator, charge regulator, and mode controller in response to signals from failure-detection circuits. Either primary or back-up circuits may be selected by ground command. Commandable battery charge-and-discharge disconnect relays are provided. Full circuit redundancy also exists in the PC, ADE, and partial shunts. The hardware elements of the SAATN power subsystem are summarized in Table 5.4-1.

During the parking orbit the solar array will not be deployed. Therefore, the satellite will be on battery power for 90 minutes. A detailed power requirement study for separation from orbiter to injection remains to be done. However, the three 26.5 A-H batteries are capable of supporting 320 watts for 90 minutes. This will well exceed the spacecraft housekeeping requirements for the parking orbit.

The power required for the cruise and mission phases of the Asteroid satellite is shown in Table 5.4-2 and the power profile is shown in Figure 5.4-2. The average cruise and mission power requirements are 197 watts and 311 watts, respectively. The peak load demand for both phases is 383 watts. The duration of the peak load is eight hours during cruise phase and one hour during mission phase. There is an additional battery recharge requirement whenever the battery is discharged or in continuous overcharge. The battery requires a minimum continuous overcharge current of 0.5 ampere per battery in order to maintain the battery at a 100 percent state of charge.

The power available at the 28-Vdc bus for a DET power subsystem is shown in Figure 5.4-3, which includes the effects of temperature, solar intensity variations, and a conservative radiation environment. Also included are the diode and harness losses from the solar array to the 28-Vdc bus. The time required for the Asteroid satellite to reach 1.8 AU will depend on the asteroid selected for rendezvous.

As indicated in Figure 5.4-3, the SAATN power subsystem cannot support more than 260 watts. This available power is sufficient to support the average load requirements of the cruise phase, but it is not sufficient to support the peak requirement of 383 watts. During the peak load, the battery would be required to supply 87 watts for eight hours. This would result in 49 percent depth of discharge (DOD) on the battery. The feasibility of using the DET system will depend on the particular mission selected.

Figure 5.4-4 shows the power available from the solar array as a function of operating voltage. Because the DET solar array is forced to operate at 31V, not all available power is usable power. At 1.8 AU, if the array were operating at 53V, the available power would be 533 watts.

Figure 5.4-5 is a simple block diagram of a maximum power point tracker (MPT). The system has a tracking unit which senses the maximum power available from the array when the load demand requires it. When the load demand is less than the maximum power, the array will operate to the right of the maximum power point, supplying only the power required. The MPT system has only one regulator (buck), which reduces the high input voltage to a regulated output voltage of +28V.

TABLE 5.4-1. EPS COMPONENT CHARACTERISTICS (SAATN)

Parameter	Value
<b>Solar Array (SA)</b>	
Panels per Spacecraft	8
Panel Area Dimension	109.5 x 24.2 in <sup>2</sup>
Panel Weight	16.8 lb
Total Array Area	147.2 ft <sup>2</sup>
Total Array Weight	134.4 lb
<b>Solar Cell Characteristics</b>	
Type	High Efficiency
Area	2 x 4 cm (oversized)
Base Resistivity	1-3 ohm-cm
Thickness	0.010 in
<b>Coverglass</b>	
Type	Fixed Silica
Thickness	0.006 in
<b>Array Solar Cell Layout</b>	
Number of Series Cells	90
Number of Parallel Strings	168
<b>Partial Shunt Configuration</b>	
Number of Partial Shunt Circuits	48 (6 per panel)
Number of Series Solar Cells across Each Shunt	58
<b>Solar Array Drive Unit (SAD)*</b>	
Motor Type	DC Brushless Torque Motor
Number of Power Sliprings Used	24
Number of Signal Sliprings	7
Weight	9.9 lb
<b>Solar Array Drive Electronics (ADE)*</b>	
Weight	6.0 lb
Size	5.4 x 7.6 x 9.5 in
<b>Battery (BAT)</b>	
Number per Spacecraft	3
Number of Series Cells	17
Number of Assemblies	
9-Cell Pack	3
8-Cell Pack	3
*May be required for alternate missions.	

TABLE 5.4-1. EPS COMPONENT CHARACTERISTICS (SAATN) (Continued)

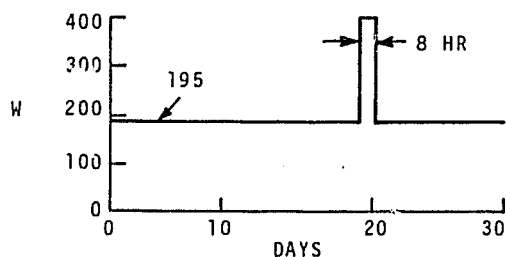
Batteries (Continued)	
Weight of Assemblies	
9-Cell Pack	28.8 lb
8-Cell Pack	25.9 lb
Total Battery Weight	164.1 lb
Pack Size (both packs identical)	14 x 9.1 x 5.5 in
Charge Control System	
Current Limiting Selectable by Command	10, 7.5, or 0.5 amp
Voltage Limiting (Temperature Dependent)	4 Levels by Command
Power Supply Electronics (PSE)	
Weight	26.2 lb
Size	16.9 x 9.2 x 10.8 in
+28V Bus Characteristics	
1) Regulation	±2%
2) Ripple	Less than 50 millivolts (into a resistive load)
3) Transient Response	0.2 volt (output) for load change of 6 amps at a rate of 20 mA/μs
Boost Regulator Efficiency	87% minimum at full load
Battery Charge Assembly (BCX)	
Weight	
Radiator Plate	17.1 lb
Size	25.0 x 18.0 x 3.0 in
Charge Current Range per Battery	0.5 to 10.0 amp
Power Converter (PC)	
Weight	1.1 lb
Size	4.0 x 4.0 x 2.5 in
+5V Bus Characteristics	
1) Regulation	5%
2) Ripple Voltage	Less than 50 millivolts into a resistive load
Converter Efficiency	77% minimum at full load
Battery Current Sensors (BCS)	
Number per Spacecraft	3
Weight (each)	1.0 lb
Size (each)	4 x 7.3 x 1.7 in

ORIGINAL PAGE IS  
OF POOR QUALITY

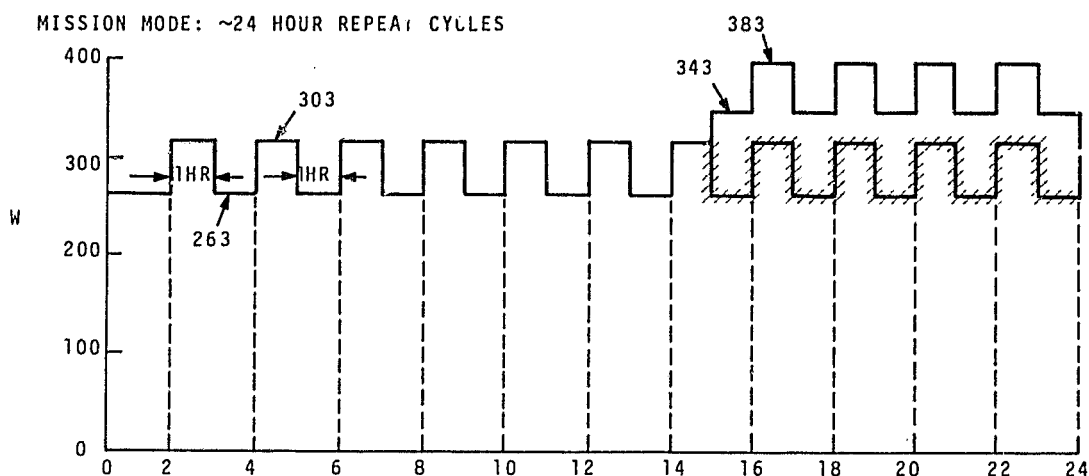
TABLE 5.4-2. ASTEROID POWER REQUIREMENTS

<u>Cruise Phase</u>	Heaters	S/C	Instr	Comm	Total
Cruise Quiescent	109	86	*	0	195
Instrument Calibration (Real Time)	96	122	85	80	383
<u>Mission Phase</u>					
Quiescent	125	86	*	0	211
Data Acquisition	96	122	65	0	283
Data Transmission	96	122	65	80	363
*In heaters budget Note: S-Band beacon included in S/C column (5W)					

CRUISE PHASE: MAINTAIN QUIESCENT, GO TO CAL FOR ~8 HOURS  
ONCE EVERY MONTH.



MISSION MODE: ~24 HOUR REPEAT CYCLES



- 1) NO ECLIPSE
- 2) 67%\* OF THE TIME 263W+303W STEPS (2 HOUR TOTAL CYCLE)
- 3) 33%\*\* OF THE TIME 343W+383W STEPS (2 HOUR TOTAL CYCLE)

Figure 5.4-2. Asteroid Load Profile for Cruise and Mission Phases

ORIGINAL PAGE 15  
OF POOR QUALITY

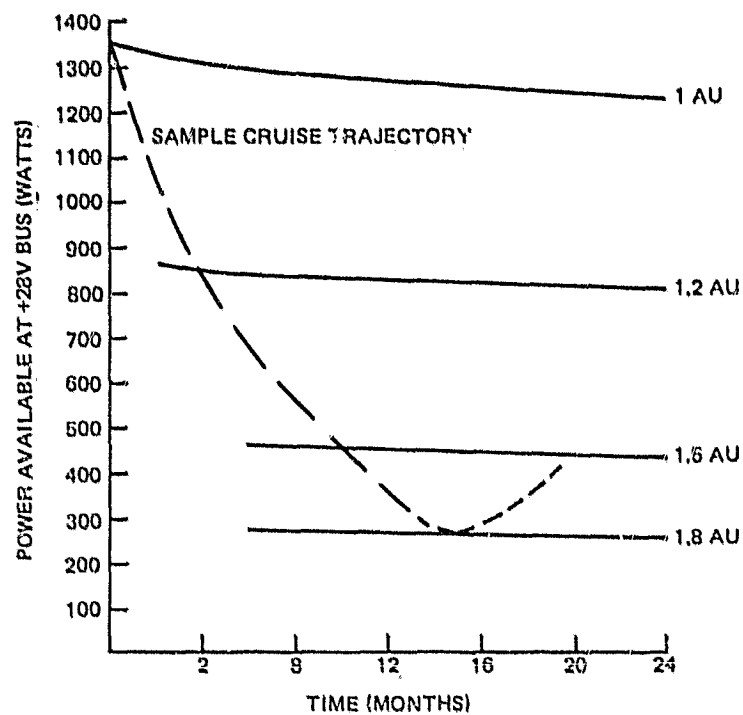


Figure 5.4-3. Power Available for DET Power Subsystem

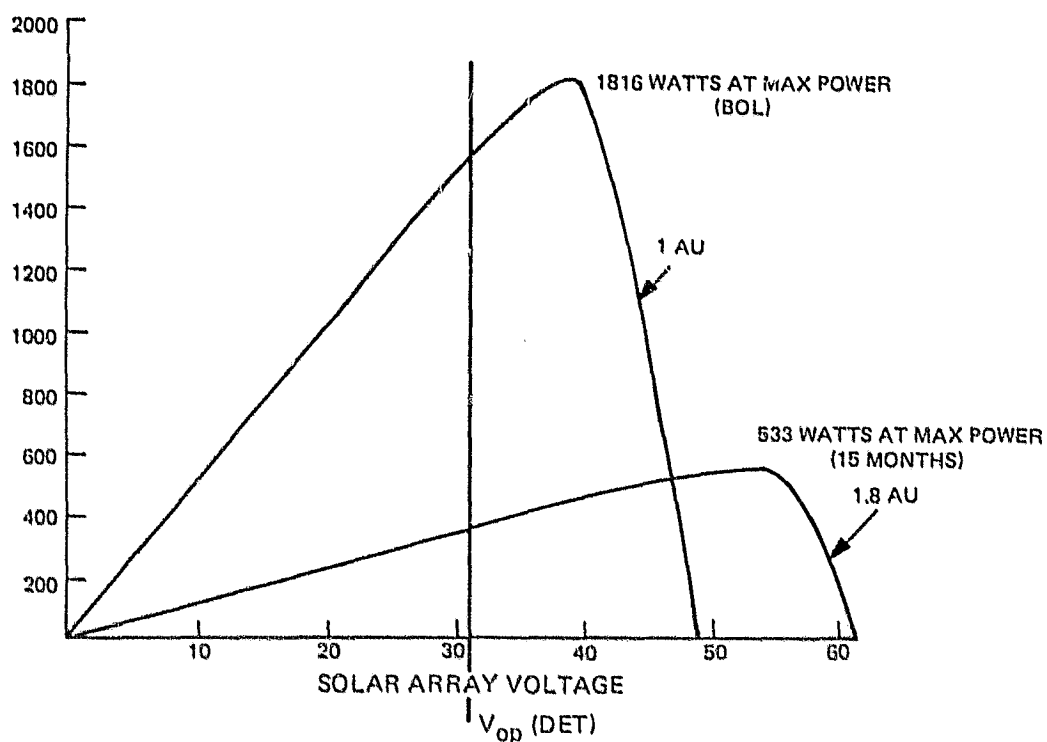


Figure 5.4-4. Solar Array Output Power for DET Power Subsystem

ORIGINAL PAGE IS  
OF POOR QUALITY

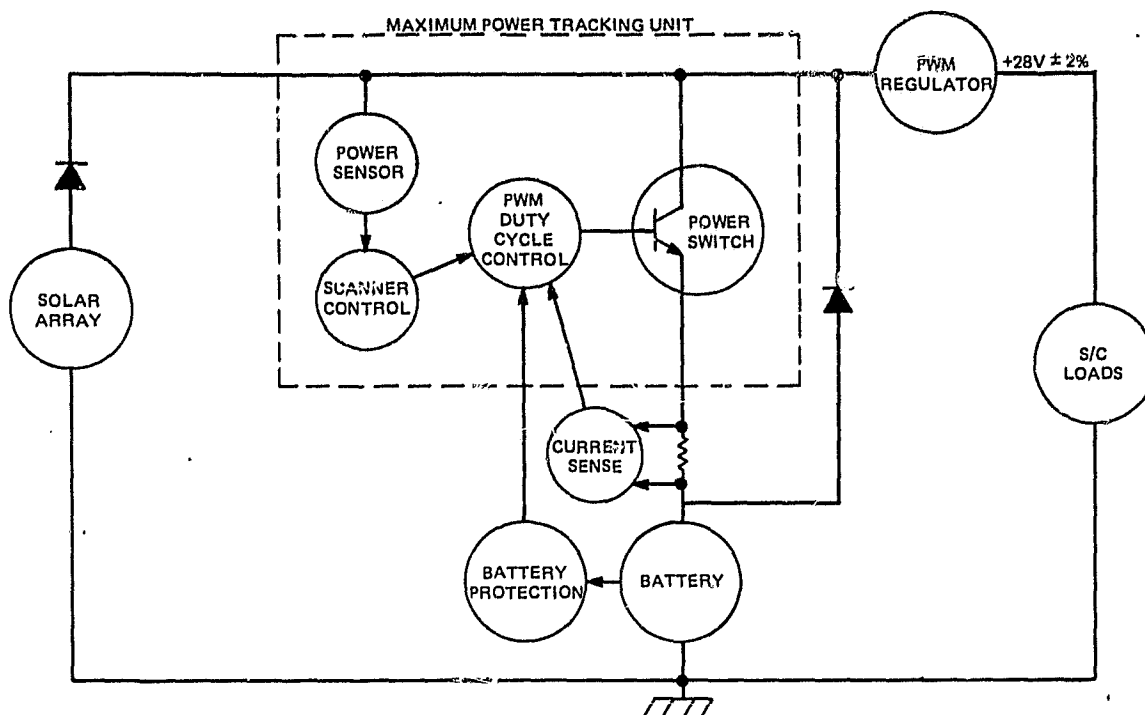


Figure 5.4-5. Maximum Power Tracker (MPT) Block Diagram

Figure 5.4-6 shows the power available at the 28-V bus if the array were to operate at the maximum power point. As shown in the figure, sufficient power would be available to support the cruise and mission phases of the Asteroid rendezvous out to 1.8 AU if the MPT system were used. However, there are advantages and disadvantages in using an MPT system (see Table 5.4-3).

A third option is a two-voltage option, commandable between a voltage optimum near 1 AU and one optimum near 1.6 AU, to be chosen as a function of mission phase.

## 5.5 TELECOMMUNICATIONS

A block diagram of the base line telecommunications subsystem is shown in Figure 5.5-1, and the characteristics are described in the following paragraphs. The primary elements of the telecommunications subsystem will be the transponders, radio frequency (RF) amplifiers, RF diplexers, RF switch, and the antennas - a fan beam, an omni, and a two-axis steerable 1.5 meter dish.

At any time, one transponder will be connected to the high gain antenna and the other transponder will be connected to the omni via a "failsafe" RF switch. Commands received by either transponder will be routed to the command and data handling subsystem via the command reformatting unit (refer to Section 5.7.1.7). Real-time or recorded data from the command and data handling subsystem will be received from the cross strap unit (XSU) by one or both transponders. The transponder output will be further amplified to 20 watts of spacecraft transmitter output power and routed to the steerable high gain dish or to the omni antenna by the RF switch.



ORIGINAL PAGE IS  
OF POOR QUALITY

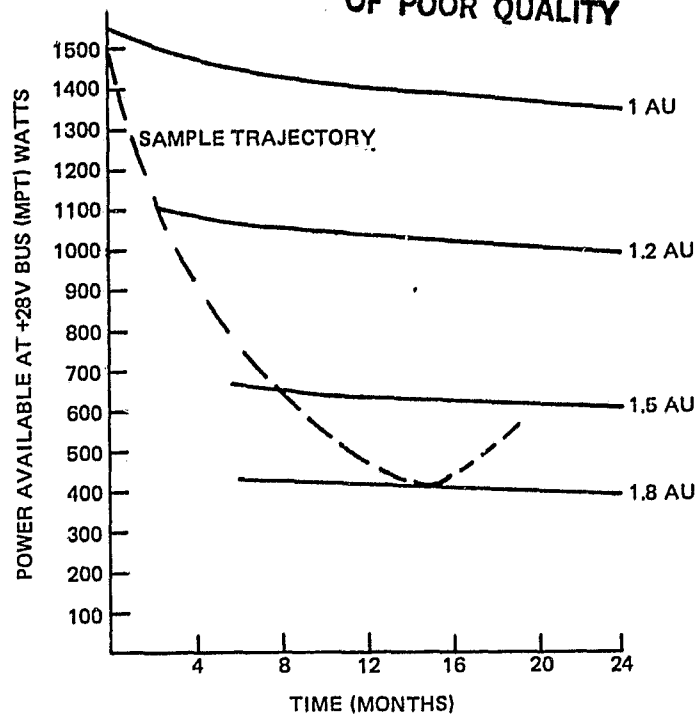


Figure 5.4-6. Power Availability for MPT Power Subsystem

TABLE 5.4-3. ADVANTAGES AND DISADVANTAGES OF THE DET AND MPT SYSTEMS

Advantages		Disadvantages
DET	Significant flight experience	Solar array operates at fixed voltage
	High transfer efficiency	
	17 series cells in battery	
	Partial shunt regulation usable	
MPT	Prototype built and tested	Large thermal dissipation in EPS elements
	Utilizes all array power	
	Excess array capability not dissipated	
	Load bus performance determined by regulator	
	Requires less array	Interaction and control of three separate regulatory elements affects load bus performance characteristics
		No flight experience
		High input voltage to EPS elements
		27 series cells in battery
		Maximum power tracking operative only when array capability greater than load
		Charge current limiting can reduce tracking advantage

A detailed tradeoff remains to be done in using either a DET, MPT, or selectable power point system.

ORIGINAL PAGE IS  
OF POOR QUALITY.

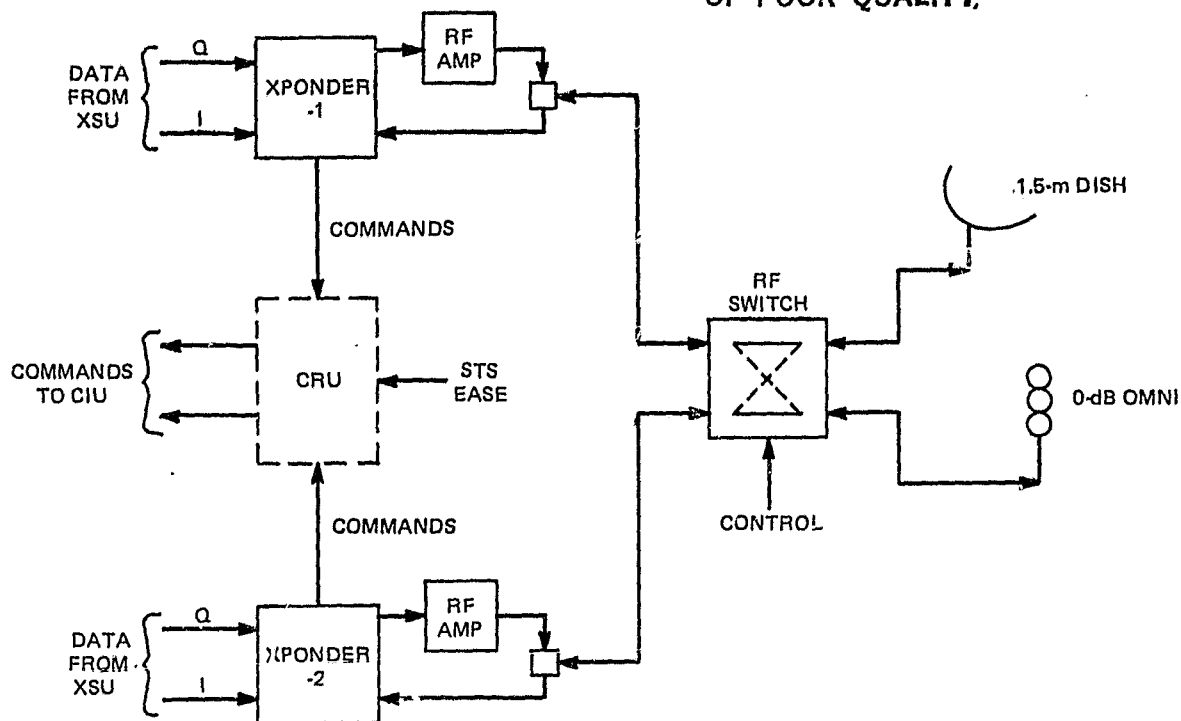


Figure 5.5-1. Communications Subsystem

Figures 5.5-2 through 5.5-5 illustrate communications performance capability over typical asteroid distances of 0.5 to 3.0 AU. The assumptions of Table 5.5-1 apply to the above figures and to Tables 5.5-2 through 5.5-6 which present typical link summaries at a distance of 1 AU. When transmitting engineering data via the omni to the 34-meter ground antenna, the signal-to-noise ratio (S/N) in the ground station carrier loop bandwidth (assumed to be 1 Hz) is not adequate to support communications all the way to 3 AU. This can be seen in Figure 5.5-4 by the fact that the curves terminate between 1.5 AU and 2.2 AU. Similarly, inadequate S/N in the spacecraft carrier loop bandwidth (assumed to be 20 Hz) prevents use of the spacecraft omni in conjunction with the 34-meter ground transmitting antenna at distances above 2.25 AU.

Forward and return communications will normally be conducted via the two-axis steerable, high gain dish antenna. Pointing of this antenna will be controlled by the spacecraft computers. During any period that the high gain antenna is not properly oriented, engineering data can be transmitted and commands received via the omni antenna. Coherent turnaround will be provided for tracking purposes. During the cruise phase of the mission, a minimum of two hours per day contact will be used. During the mission phase, a minimum of eight hours contact per day will be used to transmit the recorded science data.

The key point here is that this is only a base line system designed to demonstrate feasibility; a detailed tradeoff will be required when a specific payload and mission is selected. In addition, new technology developments, such as an advanced X-band system, would be of significant advantage if developed by JPL prior to project initiation.

ORIGINAL PAGE 13  
OF POOR QUALITY

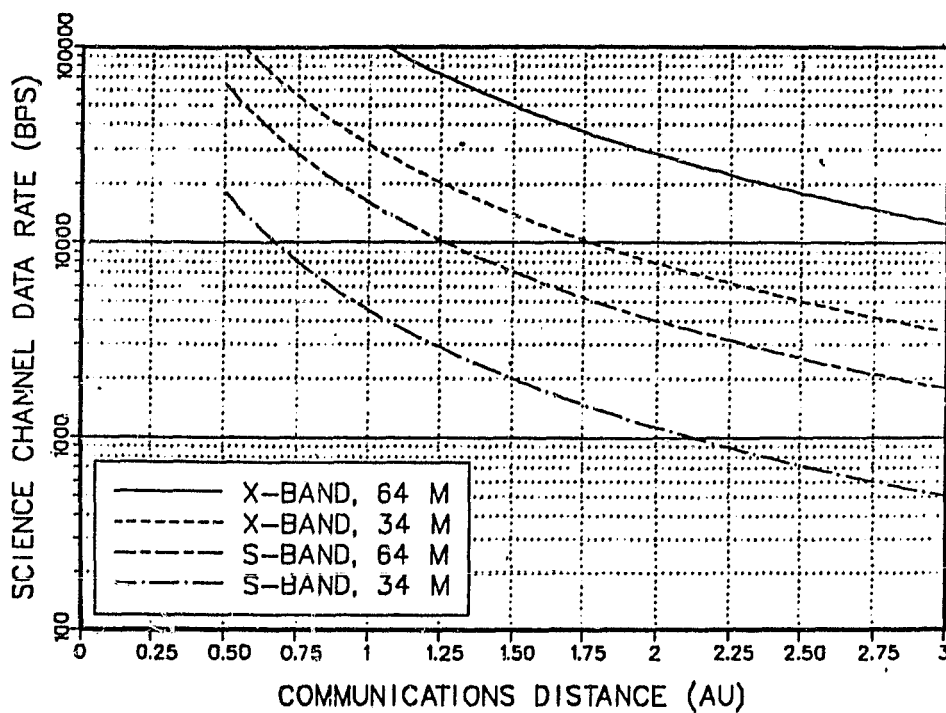


Figure 5.5-2. Science Channel Capacity

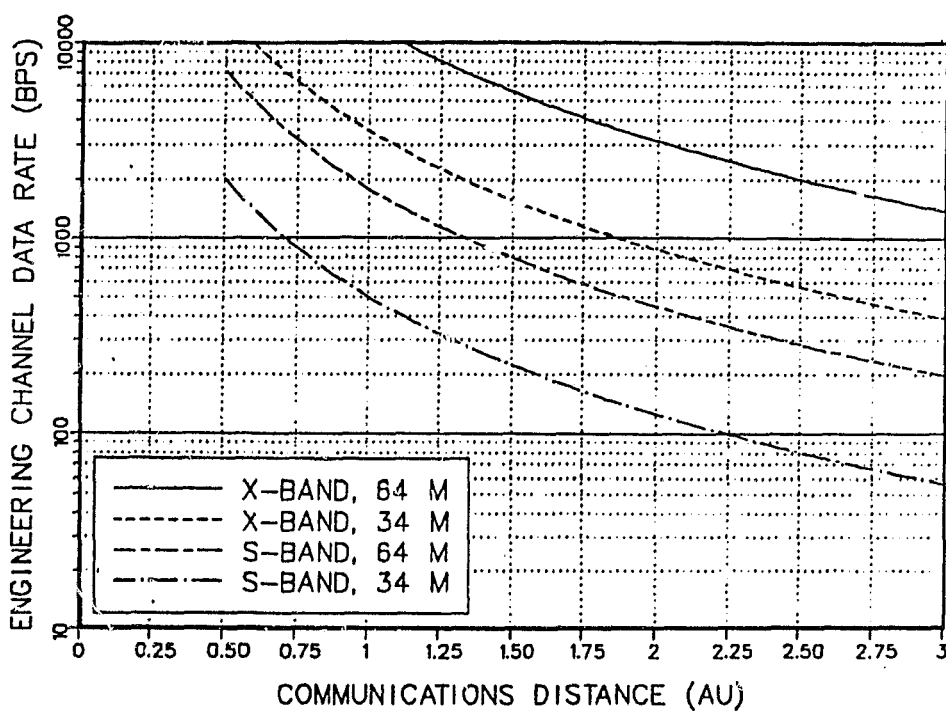


Figure 5.5-3. Engineering Channel Capacity

ORIGINAL PAGE IS  
OF POOR QUALITY

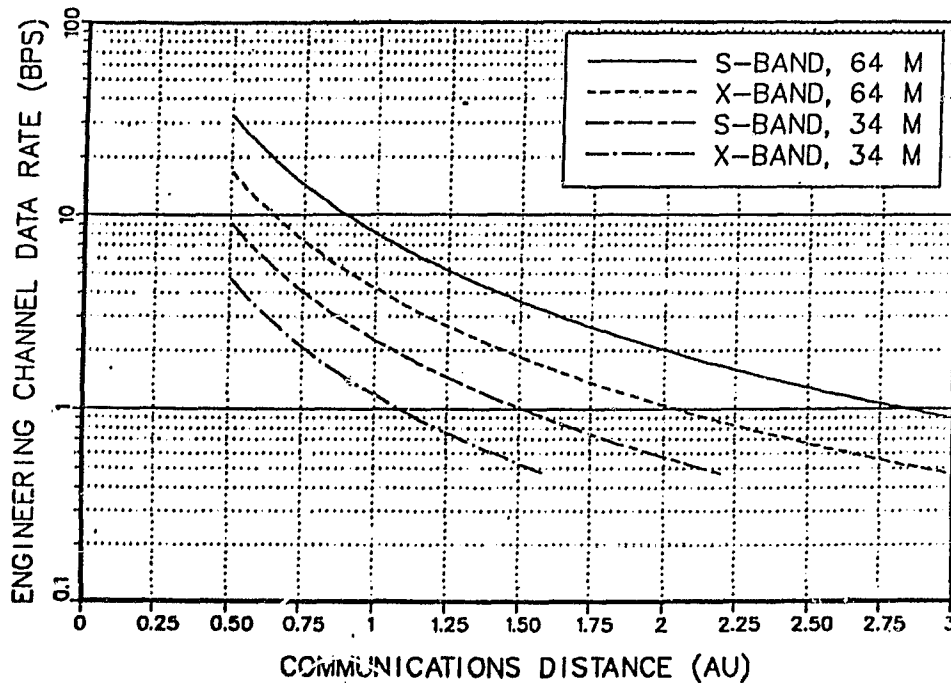


Figure 5.5-4. Engineering Channel Capacity (S/C LGA)

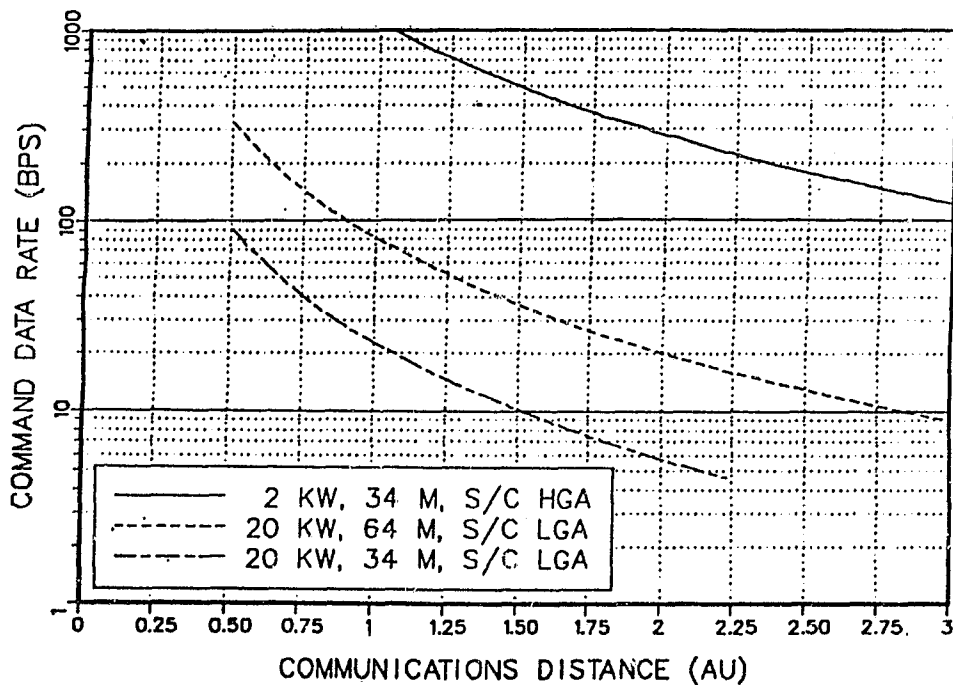


Figure 5.5-5. Command Channel Capacity

TABLE 5.5-1. COMMUNICATIONS LINK ASSUMPTIONS

Parameter	Figure Number			
	5.5-2	5.5-3	5.5-4	5.5-5
Data Type	Science	Engineering	Engineering	Command
Simultaneous Science/Engineering	Yes	Yes	No	-
Band	X, S	X, S	X, S	S
S/C Antenna	1.5-m Dish	1.5-m Dish	Omni	1.5-m/Omni
S/C Transmit Power	20W	20W	20W	-
Subcarrier	Square Wave	Square Wave	Square Wave	Sine Wave
Modulation Index	0.8 rad $\pm 12\%$	0.45 rad $\pm 12\%$	0.45 rad $\pm 12\%$	1.0 rad $\pm 5\%$
Error Coding	32,6 Bi-orthogonal	None	None	-
Error Rate	$1 \times 10^{-2}$ (word)	$5 \times 10^{-3}$ (bit)	$5 \times 10^{-3}$ (bit)	$1 \times 10^{-5}$ (bit)

Table 5.5-2. SCIENCE/ENGINEERING X-BAND LINKS WITH HIGH GAIN ANTENNA

ORIGINAL PAGE IS  
OF POOR QUALITY

Deep Space Downlink: RF Parameters				
Frequency = 8415.0				
No.	Parameter (Units)	64-m Ant Value	34-m Ant Value	Remarks
1	S/C Transmit Power (dBW)	13.01	13.01	Power = 20W
2	S/C Transmit Circuit Loss (dB)	-2.00	-1.00	
3	S/C Antenna Gain (dBi)	39.83	39.83	Dia = 1.5m; Eff = 0.550
4	S/C Antenna Pointing Loss (dB)	-1.00	-1.00	
5	Free Space Loss (dB)	-274.47	-274.47	Range = 150 million km
6	Atmospheric and Rain Loss (dB)	-0.20	-0.20	
7	Polarization Loss (dB)	-0.20	-0.20	
8	G/S Antenna Gain (dBi)	71.16	65.67	Dia = 64m/34m Eff = 0.410
9	G/S Antenna Pointing Loss (dB)	0.00	0.00	
10	G/S Receive Circuit Loss (dB)	0.00	0.00	
11	G/S Receive Input Power (dBW)	-152.87	-158.36	Sum of 1 through 10
12	G/S System Noise Density (dBW/Hz)	-212.37	-212.37	Sys Temp = 42°K
13	Rcvd Pwr/Noise Density (dB/Hz)	59.50	54.00	11 - 12
Deep Space Downlink: Carrier Performance				
No.	Parameter (Units)	64-m Ant Value	34-m Ant Value	Remarks
14	Carrier Modulation Loss (dB)	-5.24	-5.24	
15	Carrier Loop Noise BW (db-Hz)	10.79	10.79	Loop BW = 12 Hz
16	C/N in Carrier Loop (dB)	43.47	37.97	13+14-15
17	Required C/N (dB)	10.00	10.00	
18	Margin (dB)	33.47	27.97	16 - 17

TABLE 5.5-2. SCIENCE/ENGINEERING X-BAND LINKS WITH HIGH GAIN ANTENNA (Continued)

Deep Space Downlink: Science Data Channel Performance				
No.	Parameter (Units)	64-m Ant Value	34-m Ant Value	Remarks
19	Sci Chan Modulation Loss (dB)	-4.93	-4.93	, Index = 0.80 rad +/-12.0%
20	Waveform Distortion Loss (dB)	-0.50	-0.50	
21	Radio Loss (dB)	-0.30	-0.30	
22	Subcarrier Demod Loss (dB)	-0.20	-0.20	
23	Bit Sync/Detection Loss (dB)	-0.10	-0.10	
24	Sci Chan Data Rate (dB/Hz)	50.47	44.97	
25	Bit Energy/Noise Density (dB)	3.00	3.00	
26	Reqd Bit Energy/Noise Density (dB)	3.00	3.00	Rate = 111350/31426 bps 13+19+20+21+23-24
27	Margin (dB)	0.00	0.00	25 - 26
Deep Space Downlink: Telemetry Channel Performance				
No.	Parameter (Units)	64-m Ant Value	34-m Ant Value	Remarks
28	TLM Chan Modulation Loss (dB)	-12.36	-12.36	Index = 0.45 rad +/-12.0%
29	Waveform Distortion Loss (dB)	0.00	0.00	
30	Radio Loss (dB)	-0.70	-0.70	
31	Subcarrier Demod Loss (dB)	-0.20	-0.20	
32	Bit Sync/Detection Loss (dB)	-0.10	-0.10	
33	TLM Chan Data Rate (dB/Hz)	40.94	35.44	
34	Bit Energy/Noise Density (dB)	5.20	5.20	
35	Reqd Bit Energy/Noise Density (dB)	5.20	5.20	Rate = 12411/3503 bps 13+28+29+30+32-33
36	Margin (dB)	0.00	-0.00	34 - 35

TABLE 5.5-3. SCIENCE/ENGINEERING S-BAND LINKS WITH HIGH GAIN ANTENNA

Deep Space Downlink: RF Parameters				
Frequency = 2295.0				
No.	Parameter (Units)	64-m Ant Value	34-m Ant Value	Remarks
1	S/C Transmit Power (dBw)	13.01	13.01	Power = 20W
2	S/C Transmit Circuit Loss (dB)	-0.60	-0.60	
3	S/C Antenna Gain (dBi)	28.55	28.55	Dia = 1.5m; Eff = 0.550
4	S/C Antenna Pointing Loss (dB)	-1.00	-1.00	
5	Free Space Loss (dB)	-263.19	-263.19	Range = 150 million km
6	Atmospheric and Rain Loss (dB)	0.00	0.00	
7	Polarization Loss (dB)	-0.20	-0.20	
8	G/S Antenna Gain (dBi)	60.95	55.45	Dia = 64m/34m; Eff = 0.525
9	G/S Antenna Pointing Loss (dB)	0.00	0.00	
10	G/S Receive Circuit Loss (dB)	0.00	0.00	
11	G/S Receiver Input Power (dBw)	-164.48	-167.97	Sum of 1 through 10
12	G/S System Noise Density (dBW/Hz)	-213.55	-213.55	Sys Temp = 320K
13	Rcvd Pwr/Noise Density (dB/Hz)	51.07	45.57	11 ... 12
Deep Space Downlink: Carrier Performance				
No.	Parameter (Units)	64-m Ant Value	34-m Ant Value	Remarks
14	Carrier Modulation Loss (dB)	-5.24	-5.24	
15	Carrier Loop Noise BW (dB/Hz)	10.79	10.79	Loop BW = 12 Hz
16	C/N in Carrier Loop (dB)	35.04	29.54	13+14-15
17	Required C/N (dB)	10.00	10.00	
18	Margin (dB)	25.04	19.54	16 - 17

ORIGINAL PAGE 13  
OF POOR QUALITY



TABLE 5.5-3. SCIENCE/ENGINEERING S-BAND LINKS WITH HIGH GRAIN ANTENNA (CONTINUED)

Deep Space Downlink: Science Data Channel Performance				
No.	Parameter (Units)	64-m Ant Value	34-m Ant Value	Remarks
19	Sci Chan Modulation Loss (dB)	-4.93	-4.93	Index = 0.80 rad +/-12.0%
20	Waveform Distortion Loss (dB)	-0.50	-0.50	
21	Radio Loss (dB)	-0.30	-0.30	
22	Subcarrier Demod Loss (dB)	-0.20	-0.20	
23	Bit Sync/Detection Loss (dB)	-0.10	-0.10	
24	Sci Chan Data Rate (dB/Hz)	42.04	36.54	Rate = 159824510 bps 13+19+20+21+22+23-24
25	Bit Energy/Noise Density (dB)	3.00	3.00	
26	Reqd Bit Energy/Noise Density (dB)	3.00	3.00	
27	Margin (dB)	-0.00	0.00	25 - 26
Deep Space Downlink: Telemetry Channel Performance				
No.	Parameter (Units)	64-m Ant Value	34-m Ant Value	Remarks
28	TLM Chan Modulation Loss (dB)	-12.36	-12.36	Index = 0.45 rad +/-12.0%
29	Waveform Distortion Loss (dB)	0.00	0.00	
30	Radio Loss (dB)	-0.70	-0.70	
31	Subcarrier Demod Loss (dB)	-0.20	-0.20	
32	Bit Sync/Detection Loss (dB)	-0.10	-0.10	
33	TLM Chan Data Rate (dB/Hz)	32.51	27.02	Rate = 1781/503 bps 13+28+29+30+31+32-33
34	Bit Energy/Noise Density (dB)	5.20	5.20	
35	Reqd Bit Energy/Noise Density (dB)	5.20	5.20	
36	Margin (dB)	0.00	0.00	34 - 35

TABLE 5.5-4. ENGINEERING DATA S-BAND LINKS WITH OMNI ANTENNA

Deep Space Downlink: RF Parameters				
Frequency = 2295.0				
No.	Parameter (Units)	64-m Ant Value	34-m Ant Value	Remarks
1	S/C Transmit Power (dBW)	13.0	13.01	Power = 200W
2	S/C Transmit Circuit Loss (dB)	-0.60	-0.60	
3	S/C Antenna Gain (dBi)	0.00	0.00	
4	S/C Antenna Pointing Loss (dB)	0.00	0.00	
5	Free Space Loss (dB)	-263.19	-263.19	Range = 150 million km
6	Atmospheric and Rain Loss (dB)	0.00	0.00	
7	Polarization Loss (dB)	-0.20	-0.20	
8	G/S Antenna Gain (dBi)	60.95	55.45	Dia = 64m/34m; Eff = 0.525
9	G/S Antenna Pointing Loss (dB)	0.00	0.00	
10	G/S Receive Circuit Loss (dB)	0.00	0.00	
11	G/S Receiver Input Power (dBW)	-190.03	-195.52	Sum of 1 through 10
12	G/S System Noise Density (dBW/Hz)	-213.55	-213.55	Sys Temp = 320K
13	Rcvd Pwr/Noise Density (dB/Hz)	23.52	18.03	11 - 12
Deep Space Downlink: Carrier Performance				
No.	Parameter (Units)	64-m Ant Value	34-m Ant Value	Remarks
14	Carrier Modulation Loss (dB)	-1.15	-1.15	
15	Carrier Loop Noise BW (dB/Hz)	0.00	0.00	Loop BW = 1 Hz
16	C/N in Carrier Loop (dB)	22.37	16.87	13+14-15
17	Required C/N (dB)	10.00	10.00	
18	Margin (dB)	12.37	6.87	16 - 17

ORIGINAL PAGE IS  
OF POOR QUALITY

TABLE 5.5-4. ENGINEERING DATA S-BAND LINKS WITH OMNI ANTENNA (Continued)

Deep Space Downlink: Telemetry Channel Performance					
No.	Parameter (Units)	64-m Ant Value	34-m Ant Value	Remarks	
28	TLM Chan Modulation Loss (dB)	-8.27	-8.27	Index = 0.45 rad +/-12.0%	
29	Waveform Distortion Loss (db)	0.00	0.00		
30	Radio Loss (dB)	-0.70	-0.70		
31	Subcarrier Demod Loss (dB)	-0.20	-0.20		
32	Bit Sync/Detection Loss (dB)	-0.10	-0.10		
33	TLM Chan Data Rate (dB/Hz)	9.03	3.01		
34	Bit Energy/Noise Density (dB)	5.21	5.74		
35	Reqd Bit Energy/Noise Density (dB)	5.20	5.20		
36	Margin (dB)	0.01	0.54		
				Rate = 8/2 bps 13+28+29+30+31+32-33 34 - 35	

TABLE 5.5-5. ENGINEERING DATA K-BAND LINKS WITH OMNI ANTENNA

Deep Space Downlink: RF Parameters				
Frequency = 8415.0				
No.	Parameter (Units)	64-m Ant Value	34-m Ant Value	Remarks
1	S/C Transmit Power (dBW)	13.01	13.01	Power = 20W
2	S/C Transmit Circuit Loss (dB)	-1.00	-1.00	
3	S/C Antenna Gain (dBi)	0.00	0.00	
4	S/C Antenna Pointing Loss (dB)	0.00	0.00	
5	Free Space Loss (dB)	-274.47	-274.47	Range = 150 million km
6	Atmospheric and Rain Loss (dB)	-0.20	-0.20	
7	Polarization Loss (dB)	-0.20	-0.20	
8	G/S Antenna Gain (dBi)	71.16	65.67	Dia = 64m/34m; Eff = 0.410
9	G/S Antenna Pointing Loss (dB)	0.00	0.00	
10	G/S Receive Circuit Loss (dB)	0.00	0.00	Sum of 1 through 10 Sys Temp = 420K 11 - 12
11	G/S Receiver Input Power (dBW)	-191.70	-197.19	
12	G/S System Noise Density (dBW/Hz)	-212.37	-212.37	
13	Rcvd Pwr/Noise Density (dB/Hz)	20.67	15.17	
Deep Space Downlink: Carrier Performance				
No.	Parameter (Units)	64-m Ant Value	34-m Ant Value	Remarks
14	Carrier Modulation Loss (dB)	-1.15	-1.15	Loop BW = 1 Hz 13+14-15 16 - 17
15	Carrier Loop Noise BW (dB/Hz)	0.00	0.00	
16	C/N in Carrier Loop (dB)	19.51	14.02	
17	Required C/N (dB)	10.00	10.00	
18	Margin (dB)	9.51	4.02	

ORIGINAL PAGE IS  
OF POOR QUALITY

ORIGINAL PAGE IS  
OF POOR QUALITY

TABLE 5.5-5. ENGINEERING DATA K-BAND LINKS WITH OMNI ANTENNA (CONTINUED)

Deep Space Downlink: Telemetry Channel Performance					
No.	Parameter (Units)	64-m Ant Value	34-m Ant Value	Remarks	
28	TLM Chan Modulation Loss (dB)	-8.27	-8.27	Index = 0.45 rad +/-12.0%	
29	Waveform Distortion Loss (dB)		0.00		
30	Radio Loss (dB)	-0.70	-0.70		
31	Subcarrier Demod Loss (dB)	-0.20	-0.20		
32	Bit Sync/Detection Loss (dB)	-0.10	-0.10		
33	TLM Chan Data Rate (dB/Hz)	6.02	0.00		
34	Bit Energy/Noise Density (dB)	5.37	5.90		
35	Reqd Bit Energy/Noise Density (dB)	5.20	5.20		
36	Margin (dB)	0.17	0.70		
				Rate = 4/1 bps 13+28+29+30+31+32-33 34 - 35	

TABLE 5.5-6. S-BAND COMMAND LINK SUMMARY

Deep Space Uplink: RF Parameters Frequency = 2113.3 MHz					
No.	Parameter (Units)	34-m Ant Value	64-m Ant Value	34-m Ant Value	Remarks
1	G/S Transmit Power (dBW)	33.01	43.01	43.01	Power = 2 kW/20 kW/20 kW
2	G/S Transmit Circuit Loss (dB)	0.00	0.00	0.00	Dia = 34m; Eff = 0.525
3	G/S Antenna Gain (dBi)	54.74	60.23	54.74	Range = 150 million km
4	G/S Antenna Pointing Loss (dB)	0.00	0.00	0.00	
5	Free Space Loss (dB)	-262.47	-262.47	-262.47	
6	Atmospheric and Rain Loss (dB)	0.00	0.00	0.00	
7	Polarization Loss (dB)	-0.50	-0.50	-0.50	
8	S/C Antenna Gain (dBi)	27.83	0.00	0.00	1.5m Eff 0.55/zero dB/zero dB
9	S/C Antenna Pointing Loss (dB)	-1.00	0.00	0.00	
10	S/C Receive Circuit Loss (dB)	-1.50	-1.50	-1.50	Sum of 1 through 10
11	S/C Receiver Input Power (dBW)	-149.89	-166.72	-166.72	TA = 1000K; NF = 6.5 dB
12	S/C System Noise Density (dBW/Hz)	-197.95	-197.95	-197.95	11 - 12
13	Rcvd Pwr/Noise Density (dB/Hz)	48.06	36.72	31.23	
Deep Space Uplink: Carrier Performance					
No.	Parameter (Units)	34-m Ant Value	64-m Ant Value	34-m Ant Value	Remarks
14	Carrier Modulation Loss (dB)	2.58	-2.58	-2.58	Loop BW = 20 Hz
15	Carrier Loop Noise BW (dB/Hz)	13.01	13.01	13.01	13+14-15
16	C/N in Carrier Loop (dB)	32.47	21.13	15.64	
17	Required C/N (dB)	8.65	8.65	8.65	
18	Margin (dB)	23.82	12.48	6.99	16 - 17

ORIGINAL PAGE IS  
OF POOR QUALITY

TABLE 5.5-6. S-BAND COMMAND LINK SUMMARY (Continued)

Deep Space Uplink: RF Parameters					
Frequency = 2113.3 MHz					
No.	Parameter (Units)	34-m Ant Value	64-m Ant Value	34-m Ant Value	Remarks
19	CMD Chan Modulation Loss (dB)	-4.45	-4.45	-4.45	Index = 1.00 rad +/-5.0%
20	Waveform Distortion Loss (dB)	0.00	0.00	0.00	
21	Radio Loss (dB)	-1.70	-1.70	-1.70	
22	Subcarrier Demod Loss (dB)	0.00	0.00	0.00	
23	Bit Sync/Detection Loss (dB)	0.00	0.00	0.00	
24	CMD Chan Data Rate (dB/Hz)	30.41	19.03	13.42	
25	Bit Energy/Noise Density (dB)	11.50	11.54	11.65	
26	Reqd Bit Energy/Noise Density (dB)	11.50	11.50	11.50	
27	Margin (dB)	0.00	0.04	0.15	
					Rate = 1098/80/22 bps 13+19+20+21+22+23-24 25 - 26

Rate = 1098/80/22 bps  
13+19+20+21+22+23-24  
25 - 26

## 5.6 THERMAL DESIGN CONSIDERATIONS

The thermal design considerations for the Asteroid mission focus on minimizing the thermal control heater power required by instrument and support equipment, especially at a distance of 1.8 AU, while at the same time maintaining a high temperature thermal margin in the near-Earth and cruise-phase portions of the mission. Thermal requirements in terms of operating, non-operating, and survival or "safe state" temperatures are shown in Table 5.6-1.

TABLE 5.6-1. ASTEROID MISSION EQUIPMENT TEMPERATURE REQUIREMENTS

	Allowable Temperatures (°C)			
	Operating		Non-Operating	
Equipment	Max	Min	Max	Min
Instruments	30	10	40	0*
Housekeeping Electronics	45	-5	45	-5
Batteries	30	0	35	0
Propulsion Elements				
• AKM (if solid)	40	0	45	-5
• N <sub>2</sub> H <sub>4</sub>	100	5	100	5
• MMH/N <sub>2</sub> O <sub>3</sub> (if bipropellant)	50	5	50	5
*Minimum safe state instrument temperatures are 15°C lower.				

The overall thermal control configuration shown in Figure 5.6-1 is derived from the ATN design. It employs passive finishes and insulation blankets, augmented by heaters and louvers driven by solid-state electronic controllers. The controllers perform a dual function by activating either a heater on the louver drive bi-metal element (which opens the louver to allow heat rejection for hot cases) or a make-up heater for "cold cases."

For the Asteroid mission, the combination of reduced solar constant, and loss of Earth infrared (IR) and albedo, results in a substantially colder environment than the current ATN environment. Therefore, special measures (namely, instrument covers and black insulation blankets) must be incorporated to minimize heater demands. Covers on the S-band receiver (SRX), and the MSM, UCD, and GRS instruments result in an estimated heater requirement of 4 watts, as compared with 23 watts if they were not covered. Although enough power may be available to allow uncovered instruments, covers may still be required to protect against the contamination potential of the STS and cruise-phase portions of the mission. The use of insulation blankets having a black outer layer,



ORIGINAL PAGE IS  
OF POOR QUALITY

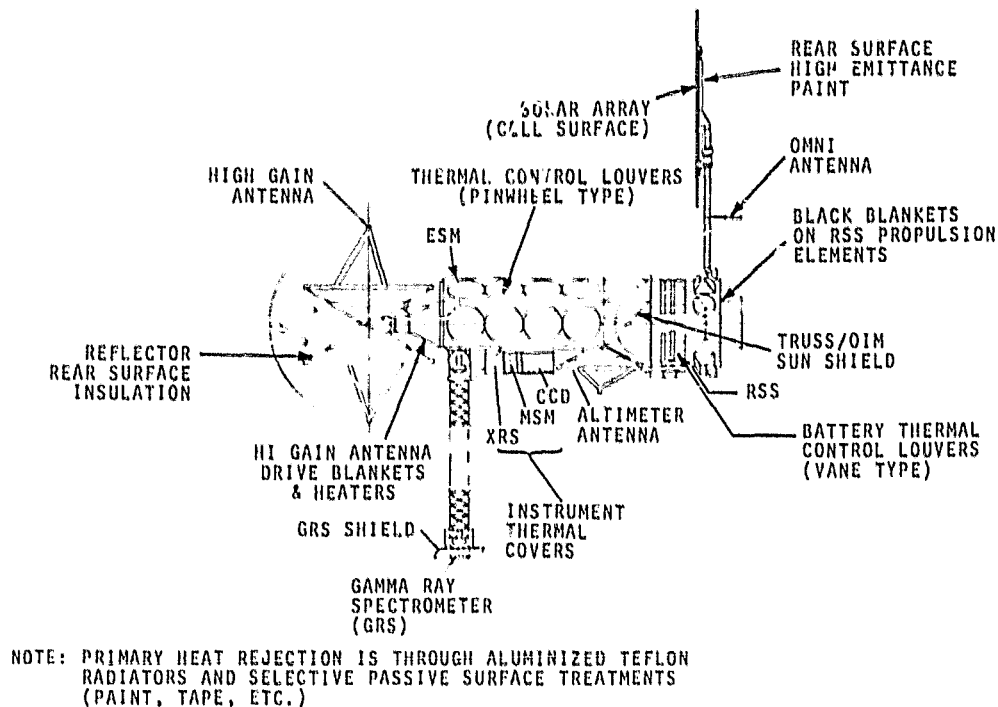


Figure 5.6-1. Thermal Control Configuration

combined with selected spacecraft orientation with respect to the Sun, results in satisfactory thermal control during the near-Earth phase of the mission. During the cruise phase, heater requirements continually increase, reaching the maximum values shown in Table 5.6-2 at 1.8 AU. In addition to the heater requirements shown in the table, thermal control of the radar altimeter antenna will require approximately 5-10 watts of additional heater power.

A large portion of the required heater power (~60 watts) is used to maintain the propulsion system elements above 10°C. Higher  $\alpha/\epsilon$  coatings, such as aluminized Kapton ( $\alpha/\epsilon \sim 3.0$ ), were considered for the outer blanket layer to further reduce heater requirements, at 1.8 AU. However, these coatings result in unacceptably high propulsion element temperatures in the near-Earth vicinity unless the orientation of the spacecraft is severely constrained. Additional optimization using a mix of  $\alpha/\epsilon$  materials could further reduce heater requirements but is somewhat less predictable; therefore, it was not considered in this phase of the study. A black Kapton outer layer is the selected approach.

Thermal control during pre-launch, launch and ascent, and STS drift phases of the mission has been analyzed for the SAATN spacecraft and is applicable to the Asteroid mission. Since the ESM and the REA support structure (RSS) are thermally configured to accommodate these environments for the ATN spacecraft, attention was directed to the externally mounted equipment unique to the Asteroid mission. Since all instruments will be off (except for brief calibration periods) during this phase of the mission, heater requirements and contamination control become the prime concerns. Heater requirements (coldest STS orientation) will be similar to those shown in Table 5.6-2. Contamination control, as well as prevention of direct solar impingement down optical trains, can be achieved through the use of covers.

TABLE 5.6-2. THERMAL CONTROL HEATER REQUIREMENTS AT 1.8 AU

Section	Heater Power (watts)	
	Safe State Temperatures	Minimum Non-Operating Temperatures
High Gain Antenna Drive	10	10
ESM	0	0
Instruments	23 (4 with covers)	39
Dampers	6	6
Subtotal ESM	39	55
Batteries	10	10
Propulsion	60	60
Subtotal RSS	70	70
Total	109	125

Thermal transients that occur as a result of deployment from the STS, reorientation during the cruise phase, or eclipsing during the mission phase are accommodated within the system thermal time constraints; therefore, no special thermal constraints are anticipated.

## 5.7 DATA HANDLING AND COMMAND

### 5.7.1 COMMAND

A block diagram of the command subsystem is shown in Figure 5.7-1, and the characteristics are described in the following paragraphs. Table 5.7-1 shows a summary of the command and data system requirements and characteristics.

#### 5.7.1.1 Controls Power Converter (CPC)

This unit, although physically located within the controls interface unit (CIU), is generally considered a part of the power subsystem. It provides 10-volt power to the CIU and to the CPUs, and +10-volt power to spacecraft bus units and instruments for use in powering interface circuits.

#### 5.7.1.2 Central Processing Units (CPUs)

The computers are redundant in that either CPU can perform the entire mission. The CPUs will be based on the DMSP design, with each containing a 32K read/write memory with single-error-correction/multiple-error-detection capability for fault tolerant processing. The computers are loaded prior to lift-off in either the STS or expendable launch vehicle configuration and can be

ORIGINAL PAGE IS  
OF POOR QUALITY

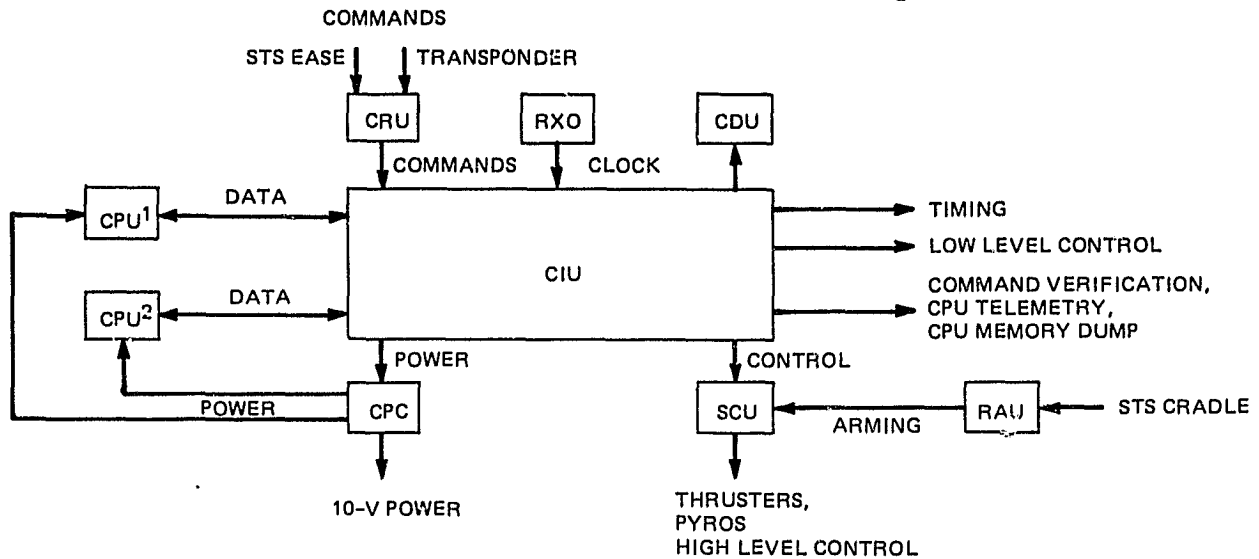


Figure 5.7-1. Command Subsystem Block Diagram

reloaded in-orbit if reprogramming is desired. Memory size is such that the initial load contains all required codes for STS ascent, STS parking orbit, cruise phase, and final mission operation.

#### 5.7.1.3 Redundant Crystal Oscillator (RXO)

The RXO will be a dual, oven-controlled crystal oscillator which meets the Asteroid mission stability requirements. The TIROS RXO is specified at 1 part in  $10^8$  per day, and NOVA RXOs have been selectively measured to 1 part in  $10^{10}$  per day. The RXO provides the timing for the command and data handling subsystems, as well as for the instruments. The spacecraft bus utilizes binary divisions of a 5.12-MHz source to provide timing in multiples and fractions of seconds. For this reason, the command and data handling subsystem components require a 5.12-MHz master clock. If the Asteroid mission instruments require frequencies presently not available, they will be provided through frequency synthesis in the cross-strap unit in a manner similar to that currently used on TIROS spacecraft to provide data recording and playback blocks. Except for phase-locked loop jitter, these clocks have the same stability as the RXO, from which the input to the synthesizer is obtained.

#### 5.7.1.4 Signal Conditioning Unit (SCU)

The SCU provides high level control signals for activating thrusters, pyrotechnics, propulsion latch valves and heaters. For the Asteroid mission, the SCU will also perform the remote arming unit (RAU) functions described below, as was proposed for the SAATN program.

#### 5.7.1.5 Command Distribution Unit (CDU)

If instrument command requirements are for switched relay contacts and for relay drivers, then a CDU will be added to include the necessary relays and drivers, activated by low level control signals from the CIU.

TABLE 5.7-1. COMMAND AND DATA HANDLING

<p>Requirement</p> <p>Provide command, telemetry, and science data processing</p>
<p>Command Uplink</p> <p>Add a command reformatting unit to convert DSN uplink to ternary form required by spacecraft command distribution unit  Command rates up to 2 kbps determined by uplink data rate  Can handle high rate on or near-Earth and low rates in deep space</p>
<p>Control Signals</p> <p>Add a remote arming unit to meet STS safety requirements  86 10-volt and 45 5-volt level command control lines available for instruments  Auxiliary distribution unit can provide 192 additional 10-volt logic level control lines  Control lines are static bi-level or pulsed  Any relay drive or switched power requirements would mean addition of a conversion unit</p>
<p>Computer Capability</p> <p>Redundant on-board computers  Each computer has 32K read-write memory with single-error-correction/multiple-error-detection capability  Computers loaded prior to liftoff</p>
<p>Clock and Sync Signals</p> <p>Anteros clock stability requirements unknown  TIROS 5.12-MHz master clock 1 part in <math>10^8</math>/day, 2 parts in <math>10^6</math>/year  NOVA oscillators selectable to 1 part in <math>10^{10}</math> per day  Clock sync signals readily available from existing TIROS design:  1 second, 32 seconds, 128 seconds, 256 seconds sync, 1.248-MHz clock</p>
<p>Recording Capacity</p> <p>3 recorders removed from TIROS configuration  2 remaining recorders have combined capacity of <math>4.5 \times 10^8</math> to <math>18 \times 10^8</math> bits depending on record mode  Recorders will be examined for applicability to high-rate-record low-rate-playback operation</p>
<p>Data Processing</p> <p>Instrument data processing requirements unknown  TIROS high rate processor - 665.4 kbps, inputs data from one instrument  Extent of changes required depends on instrument data frame size  Two data formats: engineering data only; combined engineering and science data  Output data rates determined by communications subsystem</p>

#### 5.7.1.6 Remote Arming Unit (RAU)

The RAU is basically a timer which provides the necessary inhibitors to meet STS safety requirements. An external programming plug inhibits the RAU functions for a non-STS launch. Independent control of the SCU, pyro, and hydrazine functions is possible from the STS electrical airborne support equipment (EASE) and from ground test equipment. In normal operation, the SCU and pyro functions will be enabled by the RAU when the spacecraft separation from the STS exceeds the distance required for safety. Similarly, at a second distance, the hydrazine system will be enabled.

#### 5.7.1.7 Command Reformatting Unit (CRU)

The TIROS/DMSF controls interface unit (described below) is built to accept commands demodulated from a ternary bit stream from a command and data acquisition (CDA) station. To be compatible with the binary deep space network (DSN) command stream, the CRU is used to transform the demodulated DSN signal to the three lines ("1", "0", "S") used by the CIU. The CRU will be a modification of that proposed for SAATN. In addition to the reformatting function, the CRU will provide a selection of uplink sources between the on-board transponder and the STS EASE.

The cross-strapping approach proposed for the Asteroid mission is a modification of the CRU cross strapping designed for SAATN. The proposed cross strapping is shown in Figure 5.7-2.

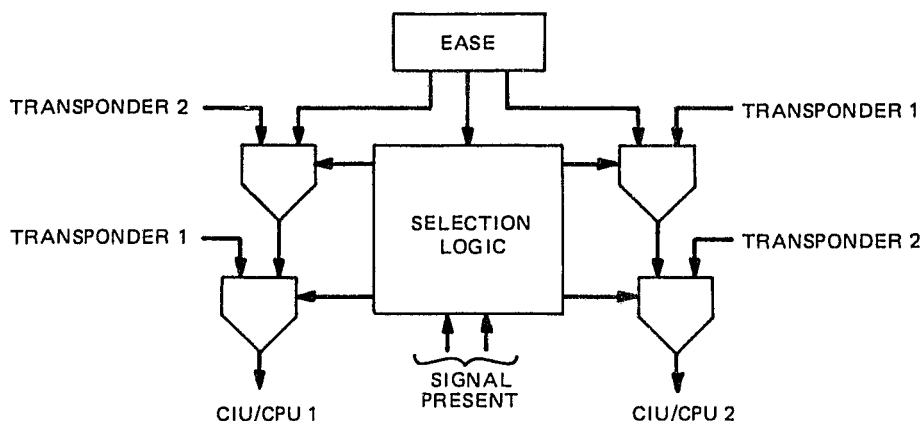


Figure 5.7-2. Cross Strapping Proposed for Asteroid

The selection logic works as follows. Use the EASE if the EASE is connected; otherwise select either transponder 1 or 2, according to the following tabulation:

Transponder 1 Active	Yes	No	No	Yes
Transponder 2 Active	No	Yes	No	Yes
CPU 1 uses Transponder No.	1	2	2	1
CPU 2 uses Transponder No.	1	2	1	2

If a transponder somehow fails while active, one CPU is lost. However, if a transponder fails while inactive, the remaining transponder can be used with either CPU or both.

#### 5.7.1.8 Controls Interface Unit (CIU)

The CIU provides the interface between the CPUs and the rest of the satellite, distributing data, low level control signals, and timing, and inputting data for processing by the CPUs. The present CIU will be modified, as proposed for SAATN satellites, to function as required during phases of the mission prior to the final operational phase of the mission. The present CIU has over 120 low level discrete control bits available for use directly by instruments, or indirectly, through SCU and CDU relays and drivers. The total number of commands required by Asteroid sensors is not known but presumably will not exceed 120. If it does, an annex to the CIU (and existing design) can provide 96 bi-level control lines and 96 hardware-controlled-pulse-duration pulse control lines. CIU pulse commands have a duration that is under software control and can range from one-half to one and one-half seconds. If Asteroid instruments are designed to accept logic level command signals at  $1 \pm 0.5$  second pulse duration, the TIROS CIU will require no change for commands. If a 100-millisecond relay drive or relay contact closure is required, the CIU and SCU changes described above will be made. The CIU can process commands at up to 2 kilobits per second, depending on the clock received from the CRU.

#### 5.7.2 DATA HANDLING

A block diagram of the data handling subsystem is shown in Figure 5.7-3, and the characteristics are described in the following paragraphs.

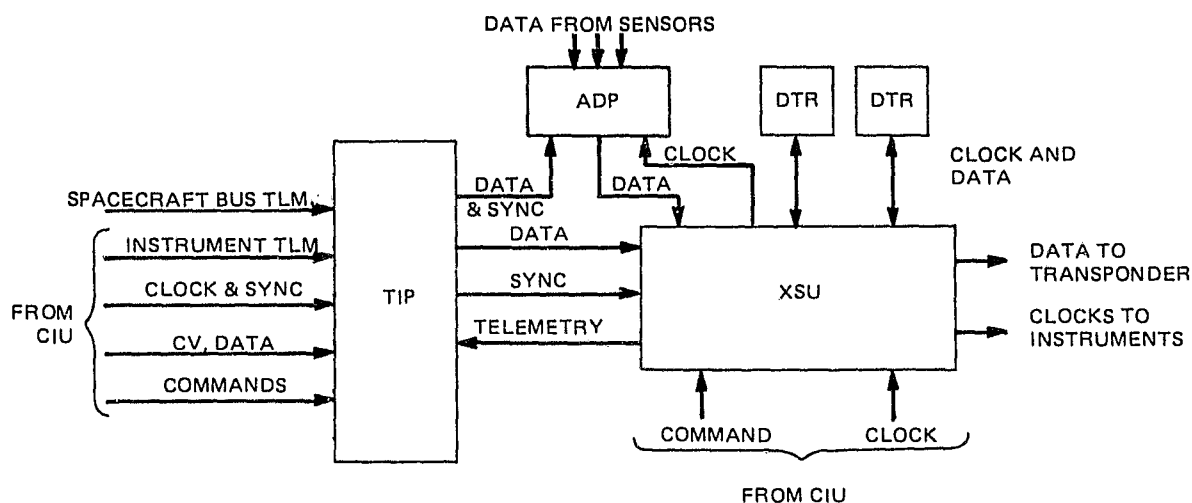


Figure 5.7-3. Data Handling Subsystem

#### 5.7.2.1 Tape Recorders (TR)

The tape recorders allow instrument and spacecraft bus data to be recorded and played back at optimum times. The TIROS digital tape recorders (DTRs) each consist of two independent transports and a common electronics section. The DTRs record in one of two modes. In the low data rate mode, one track is used for a capacity of  $1.125 \times 10^8$  bits per transport ( $2.25 \times 10^8$  bits per DTR). A second mode is used for high rate recording. In this mode, four tracks are used, for a total of  $4.5 \times 10^8$  bits per transport. For TIROS, data is recorded in either the low or high rate mode on any given transport and then played back over a ground station at a 4 to 1 or 40 to 1 speed up, depending on data type. For the Asteroid mission, the requirements are reversed, and data must be recorded at high rates for short periods of time and then played back at much lower rates for long periods.

#### 5.7.2.2 Cross Strap Unit (XSU)

The XSU will provide the required clock signals to the instruments and tape recorders. The instrument clocks readily available from an unmodified TIROS XSU are at a frequency of 1.248 MHz. The XSU provides all data path steering required to record TIROS information processor (TIP) data, record Asteroid data processor (ADP) data, play back recorded data, and transmit data in real time.

#### 5.7.2.3 TIROS Information Processor (TIP)

The TIP gathers housekeeping telemetry, computer telemetry, memory dumps, and command verification. It formats the data into a low rate data stream, which also includes TIP overhead such as time code and frame counter. The data stream will consist of approximately 2-kbps housekeeping data. The present TIP operates at either 8.32 kbps or 16.64 kbps, so some changes will be required in the formatting logic. Readily available sync signals from a TIROS TIP are 1 second, 32 seconds, 128 seconds, and 256 seconds.

#### 5.7.2.4 Asteroid Data Processor (ADP)

The ADP will provide a function similar to that performed by the TIROS manipulated information rate processor (MIRP). This function is to input sensor data (high and low rate for the Asteroid mission) and format the sensor data, time code, and ancillary data into a science data channel which is subsequently sent to the XSU to be recorded and played back through a transponder.

## SECTION 6.0

### AEROSPACE GROUND EQUIPMENT AND GROUND DATA SYSTEM

#### 6.1 AIRBORNE SUPPORT EQUIPMENT (ASE)

The major item of ASE is the space shuttle vehicle (SSV) cradle and its interface with the internal upper stage (IUS). The electronics to interface with IUS checkout systems, checkout software, and the harness for the cradle are all required and based on RCA's SAATN work (and are included in the cost estimates). On the other hand, the cradle, which can be a major cost driver to the program, has certain options that should be considered. There is at present a high probability that TIROS or DMSP will be launched by the SSV before the Asteroid mission. If this happens, all SSV interface problems will be solved, and all cradle and other interface hardware will be available for use, subject to modifications for interfacing with the IUS/ASE. However, it is not certain that any of this hardware will be available within the necessary time frame. Therefore, as a worst case scenario, we have assumed that the Asteroid project will be responsible for providing all of the ASE for the mission.

In this case, there are two further options: 1) to use the existing (or slightly modified) ASE from some other project (or the IUS), or 2) to build a new version of the ASE. At the onset of the SAATN study, a tradeoff was made between using a modified version of the PAM-D cradle/cocoon, the basic cradle in a "stretch" version, and designing a TIROS-unique cradle. McDonnell Douglas Astronautics Corporation (MDAC) was to be used as a major subcontractor in both cases and, based on in-house and MDAC analysis, it was determined that the costs for the two were equivalent; therefore, the decision was made to opt for the new version.

During the Asteroid study, this decision was re-evaluated briefly for two reasons. First, we thought there might be some advantage if we could find a cradle that could be used with less modification, given the availability of the IUS/ASE. Second, although the TIROS spacecraft requires a cocoon for the SSV launch for contamination controls, it is not clear that the Asteroid instrument complement requires the same degree of cleanliness since critical instruments will be sealed. This is important because the cocoon is expensive.

We briefly contacted the TDRS project management office (PMO) at Goddard Space Flight Center (GSFC) to inquire as to how they are solving the SSV accommodation problem. They are also using the two-stage IUS, and all of their SSV interface problems are being handled by Boeing as part of the IUS. In essence, this resolves their problem by elimination of this area as a PMO responsibility, at least from an accounting standpoint if not from a technical one. This is a significant point for us in that the same philosophy may apply. As our base line we are proposing, like TDRS, to use the IUS cradle with a unique adapter between the IUS adapter fitting and the spacecraft. This looks viable; however, we did not address the problem of landing loads in the cantilevered position, and a more detailed study would be required to do so. We do know that this is the configuration that TDRS will fly in on the IUS, cantilevered on an extremely large stack (at least 15 to 20 feet longer than the Asteroid stack); therefore, it is not unreasonable to assume that this problem has been addressed. Finally, TDRS has opted not to use a cocoon



in the SSV, and access to the environmental analysis that led to this decision would be helpful in determining our requirements.

The primary conclusion that can be drawn at this time is that the best approach to the SSV ASE for the Asteroid mission is to use the IUS/ASE developed for TDRS, but further study is needed before the tradeoffs can be clearly evaluated and priorities established. Further, the primary driver of the tradeoff will be cost since a variety of alternatives are technically feasible.

## 6.2 ASTEROID AEROSPACE GROUND EQUIPMENT (AAGE)

The ground support equipment (GSE) comprises all of the mechanical and electrical equipment required for handling and testing the satellite from bus assembly through launch. The GSE will consist of a modified Advanced TIROS-N AGE (ATNAGE), launch-site support equipment, and assorted handling and support fixtures. A photograph of the existing ATNAGE is presented in Figure 6-1. The ATNAGE hardware and software configurations, including the changes required for the Asteroid spacecraft, are described herein. Descriptions of the fixtures and launch-site equipment requirements are also presented.



Figure 6-1. TIROS-N Aerospace Ground Equipment

### 6.2.1 SYSTEM CONFIGURATION

The base line AAGE system will consist of three Data General (DG) computers and associated peripherals. Although the existing ATNAGE may be available for use, depending on the state of the TIROS project requirements at that time, we expect that this is unlikely and would recommend an updated computer to replace the old DG S/200 systems. We would, however, retain the same basic system structure and data flow. Note that the TIROS data stream is significantly

more complex than that of the Asteroid spacecraft because of the number of telemetry streams, the type of data, and the rates. Significant simplification may be possible. To illustrate this, we show the ATNAGE configuration in Figure 6-2. The three computers are designated as Computers A, B, and C and are used as follows:

- Computer A is a DG S/200 dedicated to running high rate information (HRI) software analysis. All control comes from, and all analysis results go to Computer B.
- Computer B is also a DG S/200. The satellite bus and system control software reside in the foreground of Computer B. All telemetry assimilation, TIP telemetry limit checking, command verification, and command generation take place in this computer. Computer B also sends low rate data to Computer C and receives messages from Computer A. All operator control inputs go through Computer B. The Atlas run-time system is used in the performance of all Atlas-controlled test procedures and resides in the background of Computer B.
- Computer C is a DG S/230. All low rate instrument software analyses are performed in Computer C.

Above each computer in the figure is shown its primary function in the Asteroid system. Computer A will act as a buffer for data acquisition at high rates and for data archiving; this permits the collection of data to proceed independent of the load on the rest of the system. Computer B will be able to interface directly with the spacecraft to acquire low rate data (1 to 2 kbps), definitely, and the 16-kbps data, depending on computer load) to process in real time. This computer will be real time only, and if it cannot keep up with the data stream while performing certain functions, it will buffer itself via Computer A and acquire the data from A as it becomes ready to process it. Computer C will be the prime machine for data analysis and evaluation for the spacecraft and will interface with the instrument AGE systems. Finally, it should be noted that, if the DG machines are replaced, we will evaluate the possibility of combining two or even all three of the computers into a somewhat larger machine. However, even in this case, the three conceptual functions described above will be maintained, and the interface will be via internal software rather than hardware links between machines.

#### 6.2.2 HARDWARE CONFIGURATION

The ATNAGE configuration as modified for the Asteroid mission is shown in Figure 6-3. The ATNAGE computer hardware currently consists of a series of DG Eclipse S/200 and Eclipse S/230 computer systems, with general purpose input-output (I/O) boards to handle TIP and HRI processing and other special purpose processing. These general purpose boards were designed and developed at RCA for use in the DG computers. There are two identical computer systems used in the testing of satellites at RCA Astro-Electronics. One of the computers is shipped to ETR and used in the monitoring and commanding of the satellites prior to the launch. There are two additional computers in the ATNAGE system; one is used as a satellite simulator, and the second is the software development facility (SDF). The simulator is an Eclipse S/200, used primarily in testing the software. The SDF is used for the compilation and basic module

ORIGINAL PAGE IS  
OF POOR QUALITY

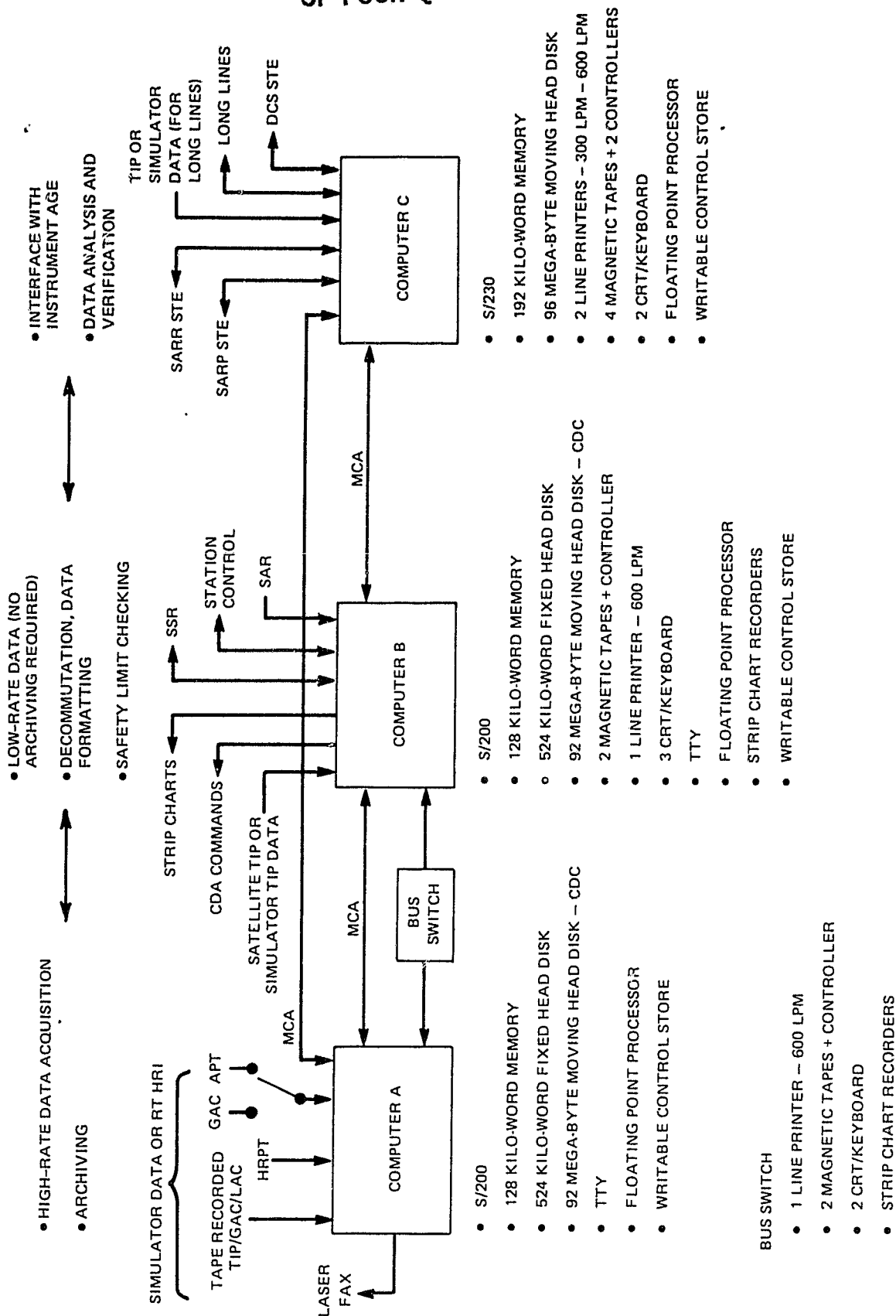


Figure 6-2. ATNAGE System Configuration with Asteroid Mission Modifications

DELETED FOR THE ASTEROID MISSION



### Figure 6-3. ATNAGE Hardware Configuration

testing of the software, for data base maintenance, and for maintenance of the Atlas test procedures.

The ATNAGE hardware complement also includes the following:

- The satellite support rack (SSR) and remote power switch (RPS), shown in Figure 6-4, incorporate all hardware required to excite and monitor satellite hard line test input, including power, and to monitor non-mission-data hard line test output
- RF processing equipment includes all receivers, RF switches, bit synchronizers, frame synchronizers, command transmitters, command generators (both computer-controlled and manually controlled), and recording and monitoring equipment necessary to test the satellite. The RF section of the ATNAGE is shown in Figure 6-5
- The ordnance device simulator (ODS) is a portable, manually operated unit (see Figure 6-6) built to meet safety requirements for operation with the satellite on the booster and is capable of interfacing directly with the satellite during testing

#### 6.2.3 SPECIAL TOOLS AND FIXTURES

Much of the fixturing developed during the TIROS and Advanced TIROS programs will remain usable for the Asteroid program. The new fixturing that is required is necessitated, in general, by: box additions and/or changes in the ESM and the deletion of the IMP, changes to the propulsion system, and a Shuttle-mounting arrangement totally different from the ELV.

The new fixtures are required for box changes and/or additions, and for a generally heavier satellite. In particular, the following new fixtures will be required:

- ESM panel rearrangement will require new honeycomb panel routing templates and drill jigs
- Manufacturing tooling will be needed to wind and form the new front panel torquing coil
- Modification to the satellite thermal vacuum fixture will be required to provide the Earth sensors (for STS launch options) with cold targets
- Because of the weight increase of the overall satellite, a change in the cross-section and profile of the V-band separation rig is anticipated. New RSS interface adapters (used during RCE buildup, boom deployment, and mass properties measurements) will be required

Fixtures required because of the new propulsion system (for STS launch options) are as follows:

- The ATN RCE mockup will be upgraded to represent STS/Atlas. This fixture is used during development of manifolds and bracketry for the propulsion system

ORIGINAL PAGE  
BLACK AND WHITE PHOTOGRAPH

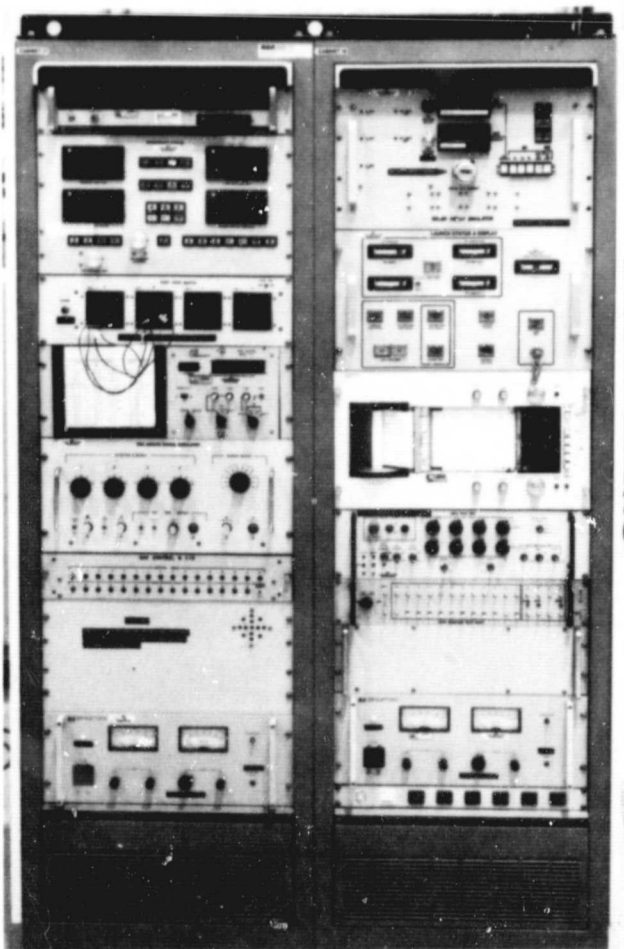
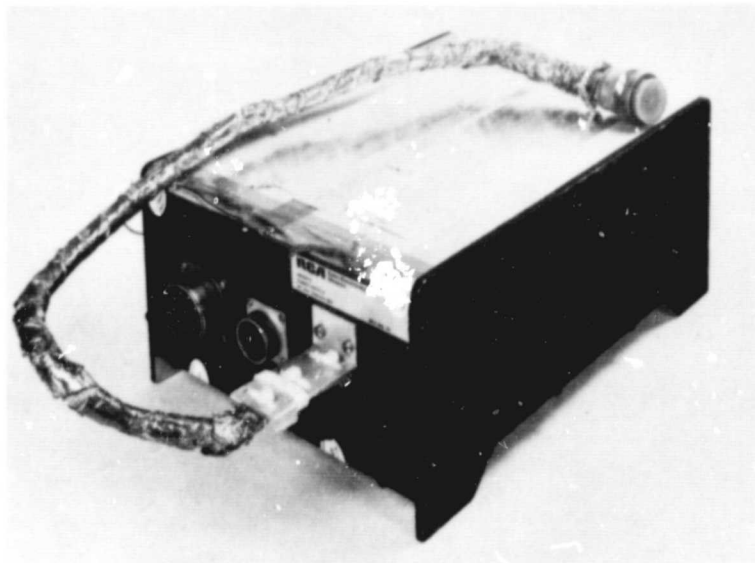


Figure 6-4. Satellite Support Rack and Remote Power Switch

ORIGINAL PAGE  
BLACK AND WHITE PHOTOGRAPH

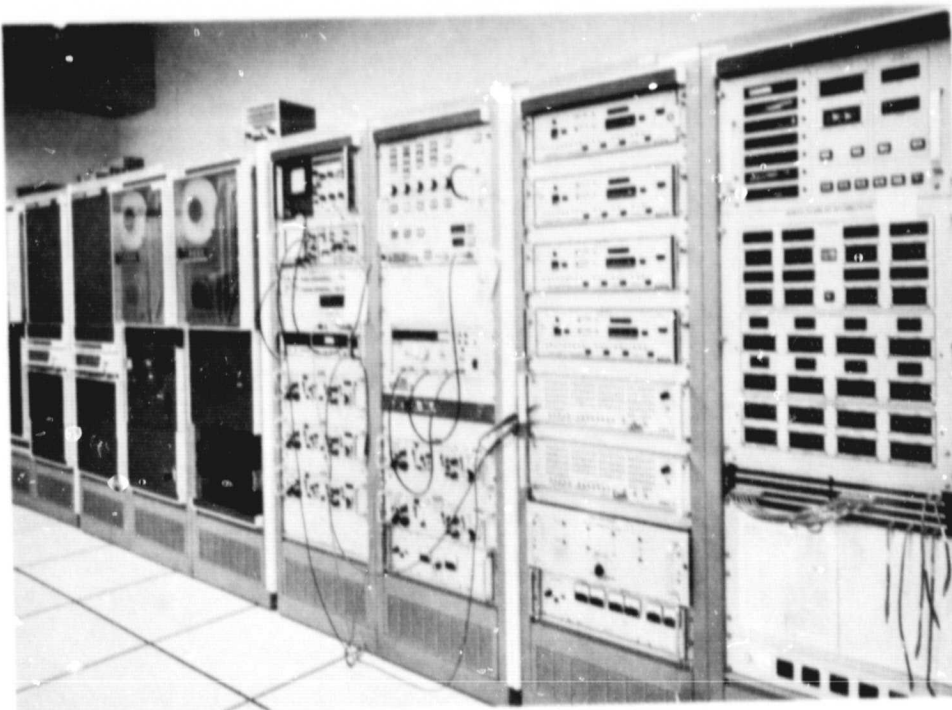


Figure 6-5. RF Section of ATNAGE

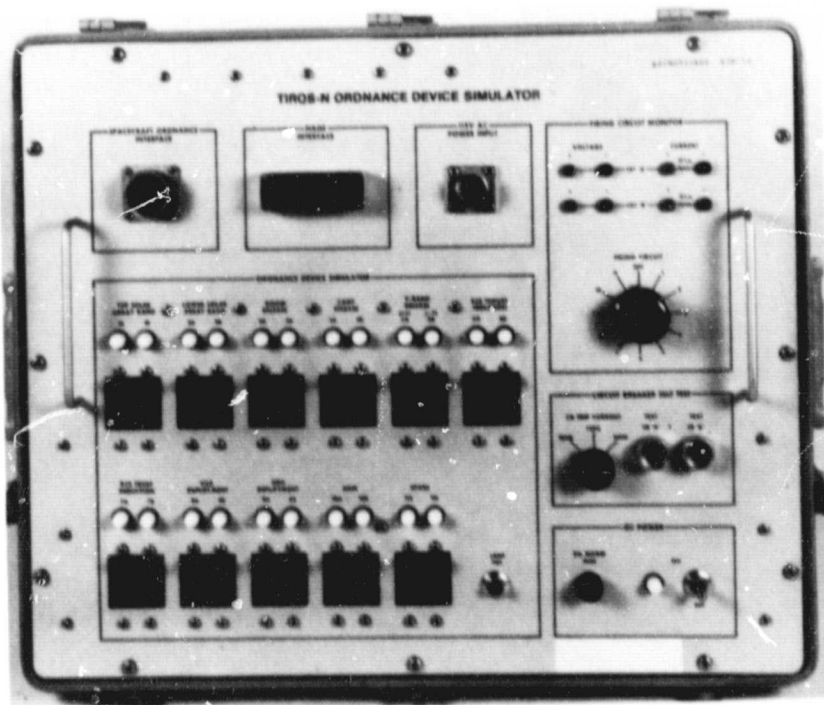


Figure 6-6. Ordnance Device Simulator

- A tank handling and transport fixture will be built for storing, transporting, and installing the new hydrazine tank

New fixtures (for STS launch options) required because of the mounting arrangement in the Shuttle, a three-point pick-up along X (satellite coordinates), are as follows:

- Interface fixtures, two types, representing the intermediate-cradle-to-cradle interface and the satellite-to-intermediate-cradle interface
- Dummy separation bolts
- A horizontal lifting fixture for lifting the satellite in the +X up attitude
- A spring caging tool, used for compressing the separation springs before mating and demating the satellite from the intermediate cradle
- A modified shipping container capable of interfacing with the intermediate cradle



## SECTION 7.0

### PROGRAM MANAGEMENT

#### 7.1 ASTEROID PROGRAM PHILOSOPHY

One of the most significant factors in a successful low cost program is the organization and control of the project management office (PMO). For the Asteroid mission we will maintain the TIROS PMO philosophy and use a similar top-down PMO organization. Figure 7-1 shows a summary of the tools available to the RCA program manager and a rough time-phasing of when they can be applied. The three key areas are the work breakdown structure (WBS), the project schedule, and the defense electronic products integrated control technique (DEPICT).

The project schedule is the ultimate base line against which all performance and cost data must be measured. An actual schedule, as planned in 1978 for the DE project, is shown in Figure 7-2. This schedule was, in fact, executed as planned, and the spacecraft were successfully launched 3 August 1981. Since schedule control and cost control are intimately related, this type of performance is essential for maintaining a low cost program. Note that we would anticipate the schedule to be similar to that of Figure 7-2.

The application of the TIROS PMO organization will provide a substantial "corporate memory" for the project by virtue of the wealth of information already available on the basic design. A large part of this experience will allow us to have confidence in design margins (thereby minimizing additional testing), will provide existing design analysis (thereby minimizing "re-invention of the wheel"), and will provide a solid, flight-power, hardware demonstration which will allow use of the prototype concept for development and testing.

#### 7.2 PMO ORGANIZATION

As is the case with all RCA Astro-Electronics programs, the PMO will be organized as a core of key individuals with matrix-type assignments from skill groups within Astro-Electronics, as required. The project manager will have access to management at the required levels to deal with problems as they arise. The WBS really provides the key to PMO organization, and it will be used by the program manager early in the hardware phase to define his organization. The preliminary WBS will, therefore, be a key output of the program study phase.

#### 7.3 COST SCHEDULE MANAGEMENT

Based on the WBS, specific elements of work are identified at the box level, and shop orders and schedules are identified at that level. A specific individual is identified as responsible for schedule reporting at that level. The DEPICT system keeps track of expenditures at that level and generates monthly a cost schedule output. This output allows the program manager to determine earned value and to monitor the progress of his program at a level that identifies cost and/or schedule problems early enough to evaluate and implement solutions before the problem has overall program impact.

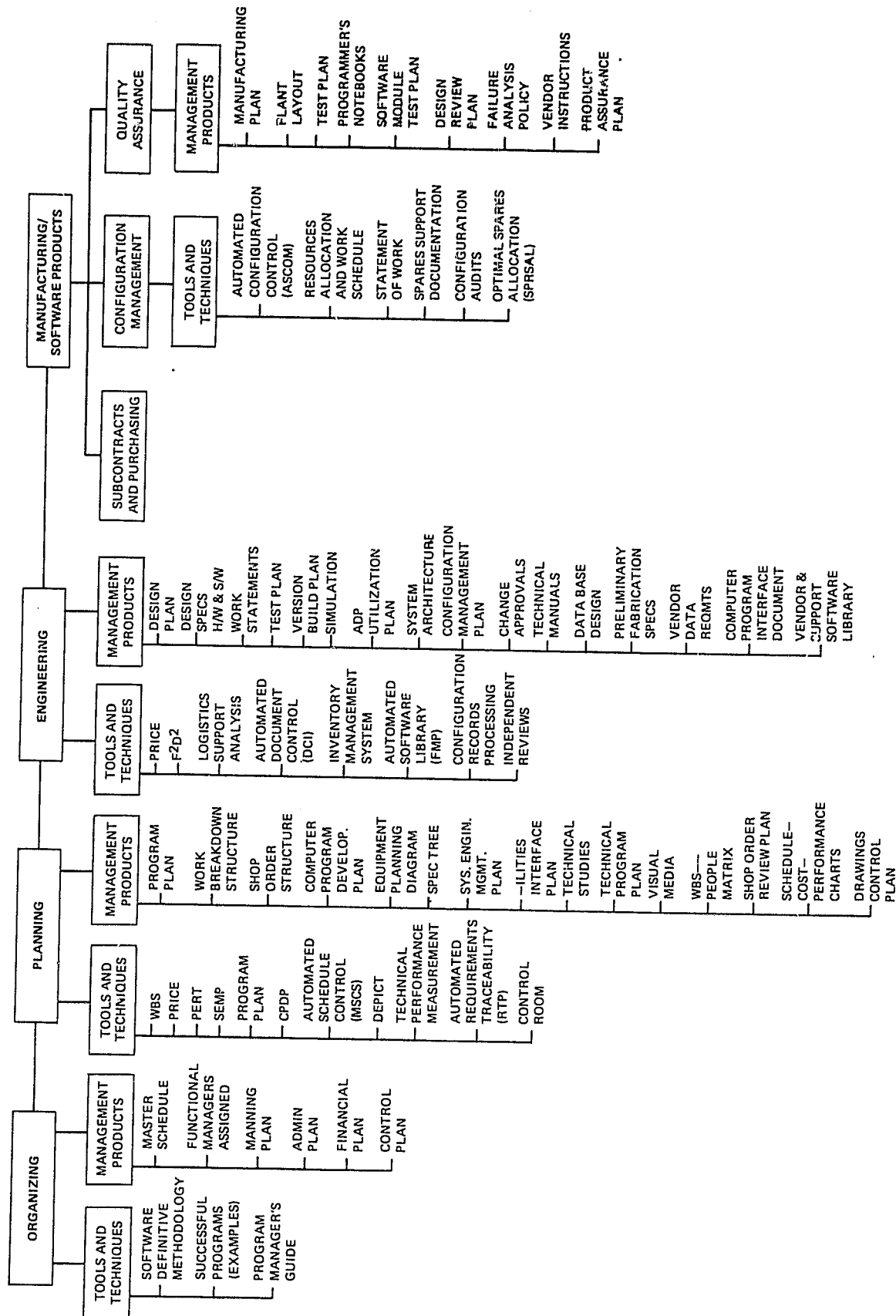


Figure 7-1. RCA Management Tools

ORIGINAL PAGE IS  
OF POOR QUALITY

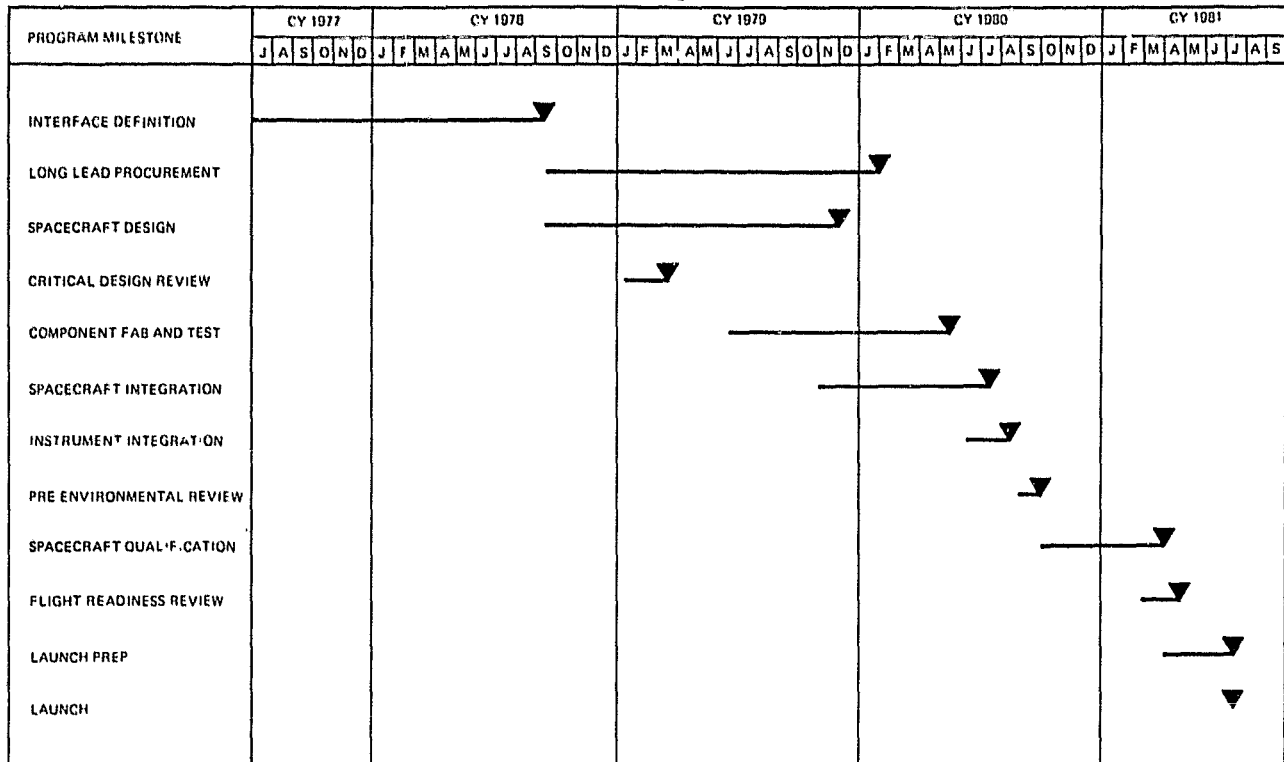


Figure 7-2. Dynamics Explorer Overall Program Schedule

#### 7.4 QUALITY CONTROL PLAN

It is RCA's position that the disciplines of quality assurance and reliability must be considered at the study level and must be an inherent part of design tradeoffs early in any spacecraft program. An active quality assurance program with strict controls, as described below, is essential. However, there is no substitute for designing reliability into a subsystem by the proper choice of components (using designs that keep all components as far away from limiting specifications as possible) and by ensuring that layouts and interconnections between boards and boxes are manufacturable and easy to inspect for workmanship. The PMO reliability and quality assurance (R&QA) program will be based on the DE Reliability Program Plan, RCA 2295106, as approved by NASA/GSFC. The major components of the plan are:

- Reliability analysis including failure mode, effects, and criticality analysis (FMECA), design reviews, parts application reviews, parts design tolerances (worst case) reviews
- Design reviews; subsystem design reviews, spacecraft-level design reviews
- Parts and materials; program-approved parts MIL-STD-975, GSFC PPL-13, RCA PPL 1971202 (Atmosphere Explorer Program Non-Standard Parts List)

- Quality control inspection (incoming in-process)
- Fabrication control

Further details of the plan may be found in the Dynamics Explorer Baseline Definition Document.

#### 7.5 RELIABILITY AND QUALITY ASSURANCE LABORATORY FACILITIES

The Reliability and Quality Assurance Laboratory performs detailed investigations related to the reliability and quality assurance aspects of equipment. Investigation capabilities include electrical, bench, and thermal testing, and mechanical, dimensional, and destructive pull tests to 136 kg (300 lb). This laboratory also performs detailed examinations, including visual microscopic to 2000X, photographic to 2000X, 100-kV, 3-mA, x-ray, and plotted cross-section analysis. It also conducts chemical analyses of plating solutions and printed circuit board etching baths.

#### 7.6 USE OF EXISTING HARDWARE

The possibility of using residual hardware (primarily from flight stores at JPL) has been considered. Based on our analysis, we have concluded that:

- Component level surplus is certainly usable
- Use of assemblies such as thrusters, hydrazine tanks, and handling equipment with designs constrained to availability may be cost effective
- Electronic assemblies at the box level are of limited, if any, value due to complexities in modification, interface requirements, and test definition
- Use of residual booms, appendages, and/or antennas (high cost, primarily mechanical items) may be cost-effective even given the necessity of designing unique interfaces

A more detailed analysis must await the specific design of the system, and these conclusions will be kept in mind as the design evolves.

## SECTION 8.0

### REFERENCES

1. M. L. Stancati and J. K. Soldner, "Near-Earth Asteroids: A Survey of Ballistic Rendezvous and Sample Return Missions," AAS Paper 81-185, August 1981
2. N. D. Hulkower, "Missions to Rendezvous with Near-Earth Asteroids Launching in 1988 to 1990," JPL Interoffice Memorandum 312/82.3-1933, 1982
3. N. D. Hulkower, "Missions to Rendezvous with Near-Earth Asteroids Launching in 1991 to 1996," JPL Interoffice Memorandum 312/82.3-1958, 1982
4. N. D. Hulkower and D. J. Ross, "Missions to the Asteroid Anteros and the Space of True Anomalies," Journal of Guidance and Control, 1982
5. N. D. Hulkower, "Opportunities for Rendezvous and Round Trip Missions to 1982 DB Based on Updated Elements," JPL Interoffice Memorandum 312/82.3-2046, 1982
6. W. B. Gray, "Calculation of Upper Stage Plane Change Penalty," JPL Interoffice Memorandum 312/82.8-682, 1982
7. A. L. Friedlander, W. C. Wells, D. R. Davis, K. Housen, and L. K. Wilkening, "Asteroid Mission Study," Report No. SAI 1-120-839-M11, 1979
8. S. H. Ottke, "Orbits About Asymmetrical Bodies," JPL Interoffice Memorandum 312/80.2-342, 1980
9. A. Schwalb, "The TIROS-N/NOAA A-G Satellite Series," NOAA TM NESS 95, March 1978